Intrinsic and Extrinsic Roles of T-type Calcium Channels in Brain Tumors

Collin Joseph Dube
Charlottesville, VA

B.S. Biochemistry, Rowan University, 2012
M.S. Biotechnology, Johns Hopkins University 2016

A Dissertation presented to the Graduate Faculty of the
University of Virginia in Candidacy for the
Degree of Doctor of Philosophy

Department of Microbiology, Immunology & Cancer Biology

University of Virginia
April 2025

Abstract

Brain tumors represent a diverse group of neoplasms with distinct genetic, molecular, and cellular characteristics that drive their pathogenesis and therapeutic resistance. Glioblastoma (GBM) is the most common and most deadly primary malignant brain tumor. GBM is associated with a dismal prognosis and an average life expectancy of ~15 months despite optimal therapy consisting of surgery, chemotherapy and radiation. Medulloblastoma (MB) is the most common pediatric brain tumor. Medulloblastoma is a CNS tumor that arises from the cerebellum, primarily in pediatric patients. The 5-year survival rate for pediatric MB patients is ~ 70%. However, patients treated with radiation therapy frequently experience permanent neurological deficits such as reduced motor and cognitive functions. T-type calcium channels are low-voltage-activated calcium channels with established roles in neuronal excitability, neuronal plasticity, proliferation, and differentiation.

In Chapter 2 we elucidate the role of microenvironmental and intrinsic T-type calcium channels in glioblastoma (GBM) progression. We demonstrate that Cav3.2 deletion in the tumor microenvironment significantly reduces tumor growth and prolongs survival. Using syngeneic GBM models in the Cav3.2 knockout (KO) mice and single-cell RNA sequencing (scRNA-seq), we show that microenvironmental Cav3.2 modulates neuronal and glial processes, downregulating genes critical for maintaining the oligodendrocyte progenitor cell (OPC) state, including *SOX10* and *Olig2*. Additionally, neuronal Cav3.2 enhances neuron-GBM stem cell (GSC) synaptic interactions, promoting GSC proliferation. Pharmacological inhibition of Cav3 with mibefradil suppresses neuronal gene expression in GSCs and synergizes with temozolomide (TMZ) and radiation to further reduce tumor burden and improve survival. These findings underscore the significance of Cav3.2 in both the tumor and microenvironment, supporting mibefradil as a potential therapeutic adjunct to standard GBM treatments.

In Chapter 3 we investigate the role of T-type calcium channels in medulloblastoma. We analyzed publicly available bulk and single-cell RNA-seq datasets showing that T-type calcium channels are upregulated in over 30% of medulloblastomas, with high expression correlating with poor prognosis. Expression levels vary across molecular subgroups, highlighting their heterogeneous role in tumor biology. Functional assays demonstrate that pharmacological inhibition with mibefradil or siRNA-mediated silencing reduces tumor cell proliferation, viability, and invasion. We performed. proteomic screenings (RPPA) and single-cell co-expression analyses to identify key cancer signaling pathways modulated by T-type calcium channel inhibition. In vivo, oral administration of mibefradil suppresses tumor growth and extends survival in orthotopic xenograft models. This study provides the first comprehensive multi-omic characterization of T-type calcium channels in medulloblastoma and supports repurposing mibefradil as a potential therapeutic strategy for these aggressive pediatric brain tumors.

This dissertation establishes T-type calcium channels as critical regulators of brain tumor progression, influencing both tumor-intrinsic and microenvironmental processes. In glioblastoma, Cav3.2 in the tumor microenvironment promotes neuronal and glial signaling, facilitating tumor growth. In medulloblastoma, T-type calcium channels drive tumor proliferation, invasion, and survival. Pharmacological inhibition with mibefradil effectively disrupts these oncogenic processes, demonstrating therapeutic potential in both tumor types. These findings underscore the translational relevance of targeting T-type calcium channels and support further investigation into mibefradil as a viable therapeutic strategy for aggressive brain tumors.

Acknowledgements

I would first and foremost like to thank my advisor, Dr. Roger Abounader. You were the first person at UVA to believe in me and fight for me to get into grad school as a non-traditional candidate. You have been one of the kindest and caring people that I have ever met and always made sure everyone knew that the science was important but being a good person and helping others was important. You set a great example in how to help other achieve their goals.

Next, I would like to thank my thesis committee: Dr. Andrew Dudley, Dr. Hui Zong, Dr. Swapnil Sokusare, and Dr. Janet Cross. Thank you for your support and feedback through this process as well as advocating for me at the tail end. I'd like to give a special thank you to Dr. Janet Cross for all she does for the program and having the ability to work with her as GBS president to help give the students the best experience and always taking the time out of her busy schedule to check in on me and allow several venting sessions.

I would like to thank the Abounader Lab members. It has been many years together with numerous faces coming and going along the journey. I'd like to extend appreciation to former postdocs in the lab Dr. Elizabeth Xu, Dr. Nichola Cruickshanks and Dr. Baomin Wang for providing experimental guidance and help in those early years. I'd like to extend thanks to the current members: Ying, Shekhar, Myron, Kadie and Yunan. You all have really helped make a great lab environment over the past few years as well as really helped me grow as a scientist. I'd also like to thank my former undergraduate students: Michelle Lai, Esther Xu, Aditya Sorot. Thank you for your help with our work, and for the opportunity to teach and have fun at the same time. A special shoutout to

Pawel Marcinkiewicz and Lily Dell'Olio for keeping me company in the lab every weekend over the past two years which was a lot of fun.

Next I need to thank all of the people who have kept me sane all the years here in Charlottesville during this PhD. First goes out to all the soccer teams I played for FC Beercelona, Nerds Immunity and Furious George with special shoutout to Phil and Dr. Tori for getting me on Beercelona. Also shoutout to Clint for sticking around in Cville to play with me after everyone else left as well as becoming my cycling partner. Thank you to the members of those teams for giving me non science outlets every week look forward to and get all my aggression out at the same time. Next is Doris who kept me company in lab every weekend for numerous years and really pushed me to be scientist I am today. I'd like to thank my training partners Brady and Matteo for keeping me sane during the pandemic and carrying 95lbs of weight to Penn Park everyday for lifting together. Lastly but certainly not least is the boys Mark, Justin and Nick. Thank you boys for always being there for me especially over the last two years when I really needed support.

Lastly are the ones who helped me get to graduate school. Shoutout to the OG crew from home (Cannone, Pat, Q, Jackie, Marie, Zullo) and the SOS crew (Luke, Tom, Anthony, Ashley, Danny, Kaitlyn). I would not be here without the support of you all during those dark years. I'd like to acknowledge those who aren't with us anymore Nick, Rusty, Zach, Aunt Jayne and Grandpa Don. The loss of you all happened at significant times in my life that really shaped the person I am today and led me to pursuing my PhD at UVA. Next is my rocks Sobo and Dr. Al. The two of you have always been there for me through all the highs and lows and I wouldn't be here without you boys. The last and most important thank you goes to my family Mom, Dad, Frank, Kristin. I couldn't do this

without the love and support of all of you. You have seen me at the lowest and helped bring me up to my highest.

Table of contents

List of Figures

List of Abbreviations

- GBM-Glioblastoma
- TCGA- The Cancer Genome Atlas
- EGFR- Epidermal Growth Factor
- NF1- Neurofibromin 1
- PDGFR- Platelet-derived growth factor receptor
- NPC-like- Neural precursor like
- OPC-like- oligodendrocyte precursor-like
- AC-like- Astrocyte like
- MES-like- mesenchymal-like
- DIPG- Diffuse intrinsic pontine glioma
- DMG- Diffuse midline glioma
- MB- Medulloblastoma
- SHH- Sonic Hedgehog medulloblastoma
- WNT- Wnt medulloblastoma
- GP3- Group 3 medulloblastoma
- GP4- Group 4 medulloblastoma
- Cav3- T-type calcium channels
- TMZ- Temozolomide
- Mib- Mibefradil
- GSC- Glioma stem cells
- OPC- Oligodendrocyte precursor-like cells
- NPC- Neural precursor-like cells
- RCAS- Replication-competent avian leukosis virus
- XFM- *Ntv-a Ink4a-Arf-/- LPTEN* mouse model
- hdWGCNA- High dimensional weighted gene co-expression network analysis
- WT- Wild type C57/Bl6 mice
- Cav3.2 KO- $Cacna1h^{-/-}$ whole body knockout mouse
- MRI- magnetic resonance imaging
- GFP-Green fluorescent protein
- scRNA-single-cell RNA sequencing
- GO BP- Gene ontology biological pathways
- GO CC- Gene ontology cellular compartment
- GO MF- Gene ontology molecular function
- RPPA-Reverse Phase Protein Arrays
- PBTA-Pediatric Brain Tumor Atlas
- DME- Differential Module Eigengene analysis
- TPM- Transcripts per million
- siRNA- small interfering RNA
- shRNA- short hairpin RNA

Chapter 1- Introduction

1.1.0 Introduction Overview

This dissertation focuses on elucidating the role of T-type calcium channels in brain tumors. T-type calcium channels are voltage-gated calcium channels expressed in normal cells such as neurons and overexpressed in cancer cells. We focus on the intrinsic role of calcium channels in glioblastoma and medulloblastoma. Additionally, we examine the extrinsic role of T-type calcium channels in the tumor microenvironment, specifically neuronal Cav3.2 in promoting glioblastoma progression.

1.2.0 Brain Tumors

Brain tumors represent a diverse group of neoplasms with distinct genetic, molecular, and cellular characteristics that drive their pathogenesis and therapeutic resistance. Among these, glioblastoma (GBM), medulloblastoma (MB), and diffuse intrinsic pontine glioma (DIPG) are among the most aggressive and clinically challenging malignancies, each arising in different regions of the central nervous system and exhibiting unique molecular landscapes. GBM, the most common and lethal primary brain tumor in adults, originates in the cerebral hemispheres, particularly the frontal and temporal lobes, and is characterized by extensive intratumoral heterogeneity, diffuse infiltration, and resistance to conventional therapies, with a median survival of approximately 15 months despite maximal treatment[1]. Medulloblastoma is the most prevalent malignant pediatric brain tumor, arising in the cerebellum and frequently disseminating via cerebrospinal fluid (CSF) pathways, with four molecular subgroups—WNT, SHH, Group 3, and Group 4—that dictate prognosis and therapeutic response[2]. DIPG, a fatal pediatric glioma, is localized to the pons, a critical brainstem structure responsible for motor and autonomic functions, making surgical resection impossible. It

is driven by hallmark histone H3K27M mutations that reprogram epigenetic landscapes and confer profound resistance to current treatment modalities, resulting in a median survival of less than one year[3]. The distinct anatomical locations, molecular features, and treatment challenges of these tumors underscore the urgent need for innovative therapeutic strategies targeting their unique oncogenic and microenvironmental drivers, which remain critical to improving patient outcomes.

1.2.1 Glioblastoma

Glioblastoma (GBM) is the most common primary malignant brain tumor. GBM presents with a worldwide incidence rate of 3.20 cases per 100,000 individuals[4, 5]. The median age of GBM diagnosis is 64 years old with a slight male predominance[4, 5]. GBM is classified as a Grade IV glioma developing as a de novo primary tumor (85-90%) or as a secondary GBM that has progressed from a lower-grade glioma[5]. Patients exhibit symptoms such as seizures or intracranial pressure followed by diagnosis via MRI and brain tissue biopsy[1, 6, 7]. GBM has a dismal life expectancy of 15 months with a 5-year survival of less than 6%[4, 5].

GBM patients undergo maximal surgical resection followed by treatment with temozolomide (TMZ) and radiation[1, 5, 7]. Methylation of the MGMT promoter, which is a DNA repair gene, results in epigenetic silencing yielding improved survival of patients treated with TMZ[8]. GBM tumors are highly invasive often infiltrating into critical brain structures prohibiting complete resection of the tumor and ultimately resulting in recurrence[5]. Numerous factors prohibit therapeutic success such as inter- and intratumoral heterogeneity, limited diffusion of drugs across the blood-brain barrier as well as the presence of GBM stem cells (GSCs) which exhibit resistance to DNA-damaging agents and are capable of unlimited self-renewal[9-12].

Numerous pathways are altered in GBM where they regulate key malignancy parameters such as proliferation, evasion of apoptosis, invasion, migration, angiogenesis, and GBM drug resistance. The p53-ARF-MDM2 pathway is deregulated in 85% of GBM patients[13-15]. The p53 protein is activated in response to DNA damage or other cellular stress activating cell cycle arrest and induction of apoptosis[15]. The MDM2 protein is an E3 ubiquitin-ligase that acts as an oncogene by degrading p53[15]. MDM2 is amplified in 14% of GBM patients[14, 15]. The CDKN2A locus functions as a tumor suppressor with CDKN2A coding for the $p16^{INK4a}$ and $p14^{Arf}$ proteins[16]. The $p16^{INK4a}$ proteins acts as a cyclin-dependent kinase inhibitor binding and inhibiting CDK4 and CDK6[16]. The $p14^{Arf}$ protein arrests the cell cycle by degrading MDM2 preventing the degradation of p53[16]. The CDKN2A locus is homozygous deleted in 61% of GBM patients[14].

Receptor Tyrosine kinases (RTK) signaling is significantly deregulated in 90% of GBM patients[13, 14]. One key RTK mutation is in the Epidermal Growth Factor Receptor [17] which is mutated or amplified in 45% of GBM patients[14]. EGFR acts as an oncogene that influences key processes such as proliferation, invasion, and inhibition of apoptosis[17, 18]. The PI3K/AKT signaling pathways are altered in GBM with PI3-kinase mutations or mutation/deletion of PTEN deregulated in 25% and 41% of patients respectively[14]. The PI3K/AKT pathway regulates various malignancy parameters including proliferation, inhibition of apoptosis, angiogenesis, and motility[19]. Targeted therapies for EGFR and PI3K have shown some efficacy and received FDA drug approval in certain cancers but have not improved patient outcomes in GBM with numerous clinical trials ongoing[17, 19]. The lack of therapeutic success for targeted therapies is likely due to signal redundancy, tumor heterogeneity, and compensatory mechanisms requiring the identification of new targets and the use of combination therapies.

The initial RNA-sequencing studies as part of the Cancer Genome Atlas [14] identified numerous subtypes within GBM such as Neural, Proneural, Mesenchymal, and

Classical which were all defined by canonical molecular signatures such as EGFR, NF1, etc[14, 20]. GBM patient biopsies would undergo subtype characterization via pathology which would advise clinicians on which potential targeted therapies to treat patients with. Unfortunately, the majority of the targeted therapies didn't prove efficacious. The potential reason why targeted therapies didn't work was later answered with the advances in single-cell sequencing. The first large study of single-cell RNA-sequencing of GBM tumors demonstrated that within any single tumor, all of the previously defined subtypes exist in varying degrees which would explain why the targeted therapies would fail as they would only deplete that specific population and the tumor would recur with the other populations. Single-cell RNA-sequencing defined the cell states of GBM as Neural precursor like (NPC-like), Oligodendrocyte precursor like (OPC-like, Astrocyte like (AC-like), Mesenchymal like (Mes-like) and cycling (G1-S, G2-M)[21]. Additionally, these studies isolated specific cell state populations that when engrafted into mice yielded tumors that recapitulate the cell populations of the original tumor pointing towards the role of the tumor microenvironment in promoting cell states in the tumor. The contributions of the tumor microenvironment were further elucidated with the technological advancement of spatial transcriptomics. These advances demonstrated that the tumor microenvironment contributes to tumor heterogeneity, resistance to therapies and lack of therapeutic success requiring new therapeutic targets within the tumor and the tumor microenvironment.

1.2.2 Medulloblastoma

Medulloblastoma [22] is a CNS tumor that arises from the cerebellum, primarily in pediatric patients[23]. Pediatric brain and CNS tumors account for over 20% of all pediatric cancers, making it the second most common cancer class within pediatric patients[23, 24]. Further, medulloblastoma accounts for over 60% of all embryonal tumors in US children aged 0-19 with nearly 300 cases of this cerebellar tumor diagnosed in the US per year

[24]. Medulloblastoma incidence rates peak at age 9 with younger children experiencing more severe treatment side effects. While the 5-year survival rate for pediatric medulloblastoma patients is just over 70%, children who undergo standard-of-care treatments frequently experience permanent neurological deficits such as reduced motor and cognitive functions as a result of radiation and chemotherapy [23, 24]. Even though medulloblastoma does occur in adult patients, pediatric medulloblastoma occurs ~10x more frequently than adult medulloblastoma and as such, is the primary focus of this research[25].

Prior to its molecular characterization, MB was classified by histology. The 2007 WHO classifications of medulloblastoma included desmoplastic, medulloblastoma with extensive nodularity (MBEN), large cell, and anaplastic medulloblastomas[26]. While histological findings are still considered today, molecular characterization has become the main determinant of medulloblastoma prognosis and treatment. Following the publication of several medulloblastoma subgrouping papers that argued for four to six medulloblastoma subgroups, a consensus was reached by experts in the field in late 2010 which established the first official classification of medulloblastoma subgroups as: WNT driven, SHH-driven, Group 3, and Group 4[27]. The WNT and SHH MB subgroups have well-characterized oncogenic driver pathways and have better prognoses than Group 3 and Group 4 tumors. Believed to originate from dorsal brain stem progenitor cells or mossy fiber neurons, WNT-driven tumors demonstrate highly activated WNT signaling frequently due to CTNNB1 somatic mutations or APC germline mutations. SHH-driven tumors are believed to be derived from granule cell precursors and display overactive SHH signaling that is promoted by germline mutations or genome amplifications to various signaling molecules in the SHH pathway such as PTCH1, SMO, SUFU, GLI1, and/or GLI2[27, 28] . To date, there are no known genetic drivers for Group 3 and Group 4 tumors even though they comprise the largest number of medulloblastoma patients and represent the most

severe cases. Since a percentage of Group 3 tumors demonstrate MYC amplification or overexpression, some groups have proposed therapies targeting various proteins that mitigate the strong oncogenic functions of MYC [29]. However, none of these proposed therapies have been approved for clinical treatment of Group 3 medulloblastoma. Even less is known about Group 4 medulloblastoma and as such, there is an extremely strong need for better characterization of these two MB subgroups to understand their molecular basis and for therapeutic target identification.

1.2.3 Diffuse Midline Gliomas

Diffuse midline gliomas (DMG) are malignant gliomas that occur in the brainstem, thalamus, or spinal cord. Diffuse midline glioma has a hallmark genetic point mutation in the histone 3 gene, which results in a lysine (K) to methionine (M) at the 27th amino acid position (K27M) resulting in open chromatin and changes in gene expression[30, 31]. DMG has an incidence rate of 0.06 per 100,000 individuals with the median age of diagnosis being 25 years in young adults and an incidence rate of 0.12 per 100,000 individuals in adolescents with a median age of 8 years old[24, 32]. The prognosis for patients with DMG is dismal with an estimated survival of 9-15 months with treatment. Within DMG, tumors occurring specifically within the pons have historically been referred to as Diffuse intrinsic pontine gliomas (DIPG). The typical standard of care for patients with DMG is radiation for 6 weeks followed by chemotherapy. Surgery is typically not recommended due to the neural structures within the brainstem which controls breathing, body movement as well as other functions. Numerous experimental therapies are showing promise for the treatment of DMG, specifically CAR T-cell therapies. The group running the clinical trials identified disialoganglioside GD2 as overexpressed in DMG tumors and developed chimeric antigen receptor T-cells targeting GD2 which showed efficacy in preclinical models[33]. The preclinical data led to Phase 1 and Phase

2 clinical trials with GD2-CAR T cell therapy being used to treat pediatric patients with DMG where the patients showed improvement in neurological benefits as well as subsets of patients showing tumor regression[34, 35].

1.3.0 Cancer Neuroscience

Cancer neuroscience is an interdisciplinary field that recently emerged to examine the interaction of the nervous system and cancer specifically how they affect and interact with each other. This field is particularly important for brain tumors as the central nervous system regulates numerous cell types in the healthy and diseased brain. These interactions are profoundly influenced by the brain's unique microenvironment, which includes neuronal activity, glial cell signaling, and the blood-brain barrier (BBB). Understanding these complex relationships has the potential to reveal novel mechanisms of tumor progression and therapeutic resistance, while also shedding light on how tumors disrupt neural function.

One of the significant discoveries in the cancer neuroscience field was the interaction of neurons with glioma cells. Two independent groups demonstrated that neurons form synaptic connections glioma cells (GBM and DIPG)[36, 37]. The groups demonstrated that both GBM and DIPG are enriched for synaptic genes which aid in the formation of neuron-glioma connections. The groups validated that neuron-glioma synaptic connections were occurring by using electron microscopy to show synaptic clefts between presynaptic neurons and glioma cells. The groups demonstrated that these synaptic connections were functional through the use of electrophysiology and calcium imaging, demonstrating that the neurons were glutamatergic and the glioma cells were receiving excitatory postsynaptic currents. Additionally, the groups further demonstrated these postsynaptic signals were being mediated through AMPA receptors

on glioma cells. At the same time another group found tripartite synapses between neurons and breast-to-brain metastases. These were glutamatergic neurons like the glioma studies but the breast metastasis tumors were being mediated through NMDA receptors which receive glutamate from the neurons[38]. After the discovery of neuronal connections to glutamatergic brain tumors the next step was to examine the relationship of brain tumors with other types of neurons. GABAergic neurons were shown to form synaptic connections with diffuse midline gliomas (DMGs)[39]. These GABAergic-DMG synaptic connections were shown to be functional through electrophysiology and optogenetic studies which modulated tumor growth and proliferation. High-grade gliomas were also examined but were not depolarized by the addition of GABA pointing toward this relationship being specific to DMG. Additionally, DMG tumors were shown to express the GABA receptor genes which facilitated these connections. The majority of initial studies focused on the close proximity of neurons near tumor cells. The circuitry further from the tumor was later investigated to determine if it could promote tumor growth. To investigate this question one group utilize DREDDs on the contralateral side of the brain to activate callosal projection neurons and examine their role on tumor malignancy. The findings demonstrated that callosal projection neurons send signals through the corpus callosum to activate GBM tumors to increase their proliferation and invasion through the upregulation of genes associated with axon projection[40].

To gain further insight into the neuronal-tumor communications two research groups utilized rabies-based retrograde tracing to map the neuronal connectome of glioblastoma[41, 42]. These papers demonstrated the early integration of GBM cells into neuronal circuits where they and receive signals locally as well as long-range circuit signals. Both groups identified for the first time cholinergic neurons forming synaptic connections with GBM tumors. The cholinergic neurons promoted GBM invasion as well

as the influx of calcium into tumor cells. Additionally, the connections of GBM tumors to cholinergic neurons reprogrammed the transcriptional state of tumor cells toward a more motile and invasive state through CHRM3 receptors. Interestingly, radiotherapy of GBM tumors enhanced the neuron-tumor connectivity but inhibition of the neuronal activity with perampanel in combination with radiotherapy disrupted the networks[41]. A similar observation was seen in DMG tumors where cholinergic midbrain neurons promoted growth in thalamic and pontine gliomas in a circuit-dependent manner[43]. Additionally, the DMG tumors acted on the cholinergic neurons promoting their activity reciprocally. Analysis of DMG tumors revealed upregulation of muscarinic receptors CHRM1 and CHRM3 which are receiving acetylcholine from the cholinergic neurons.

Previous studies have described the effects of neurons on brain tumors via direct synaptic connection but there have also been additional studies that have examined paracrine signaling from neurons in the tumor microenvironment. To determine the paracrine signaling from neurons to brain tumors a group utilized in vivo optogenetic mouse models to activate neurons in the premotor cortex and demonstrate that they promote the growth of high-grade gliomas[44]. The group next activated brain slices using optogenetics and collected conditioned media which when added to glioma cells promoted proliferation. To identify the specific mitogenic factors being secreted, they performed mass spectrometry which identified numerous synaptic proteins with the main candidate being neuroligin-3(Nlgn3). Nlgn3 activates PI3K-mTOR signaling as well as MAPK/ERK signaling pathway to regulate synaptic gene expression as well as Nlgn3 shedding[44, 45]. Another neurotropic factor that was identified by mass spectrometry was brain-derived neurotrophic factor [46]. The normal function of BDNF is promoting adaptive plasticity of synaptic connectivity which DIPG tumor cells utilize to promote malignancy parameters[47]. BDNF signaling is activated through binding the receptor

tropomyosin-related kinase B (TrkB) which is overexpressed in DIPG tumors. The activation of the TrkB receptor promoted AMPA receptor tracking to the glioma membrane surface via CAMKII. The enhanced AMPA receptor tracking increased the amplitude of currents that were evoked by glutamate. Additionally, BDNF-TrkB signaling regulated neuron-glioma synapse formation while increasing the synaptic strength and promoting proliferation of glioma cells. Pharmacological inhibition of TrkB significantly prolonged survival in xenograft models of DIPG as well as GBM.

The tumor can also act on the tumor microenvironment which is detrimental to the normal cells in proximity within the brain. One of the main ways by which GBM is diagnosed is the presence of seizures which is due to the elevated levels of glutamate which causes excitotoxicity resulting in neuronal death. One group found that glioma cells overexpress the system XC cysteine-glutamate transporter (SLC7A11) which allows the glioma cells to intake cysteine and exports glutamate into the tumor microenvironment[48, 49]. This excessive glutamate from the tumors results in hyperexcitability, resulting in epileptic seizures. GBM tumors that have elevated expression of SLCA11 exhibit more peritumoral hyperexcitability and exhibit a worse survival. Additional studies have studied somatic mutations of PIK3CA, which is overexpressed in GBM tumors and demonstrated that particular variants of the gene result in hyperexcitability and synaptic remodeling around the tumors. The group found that this particular variant's downstream signaling resulted in secretion of glypcan 3 (GPC3) which was driving gliomagenesis and hyperexcitability[50-52]. To gain additional insights into the relationship between the tumor and microenvironment one group elucidated the effect on neuronal circuits by attaching electrodes to GBM tumors during surgery with patients undergoing cognitive assessments to examine how the tumor impacts known neuronal circuits. The GBM tumors remodel the functional neuronal

circuits associated with cognitive functions compared to healthy normal brain controls. Site-directed biopsies of the tumors for high functional connectivity followed by single-cell RNA-sequencing showed that these tumors were exhibiting high levels of thrombospondin-1 (TSP1) which showed higher remodeling with neurons with the tumors.

1.4.0 T-type calcium channels

Influx of calcium from the extracellular space to the cytosol is regulated by voltage-gated calcium channels. Voltage-gated calcium channels are divided into two groups based on the voltage required for their activation (L, N,P/Q and R-type) and low-voltage activated (T-type)[53]. These channels regulate the influx of calcium for processes such as atrial pacemaking, neuron firing, proliferation and other physiological processes[53, 54]. T-type calcium channels (TTCC) are activated at low-voltages near resting membrane potential. TTCC are made up of three different channels that differ in their α1 subunit: Cav3.1(*CACNA1G*), Cav3.2 (*CACNA1H*), and Cav3.3 (*CACNA1I*)[53, 56].

T-type calcium channels are expressed within various regions of the nervous system specifically the thalamus, cortex, cerebellum and basal ganglia[56-58]. T-type calcium channels regulate neuronal excitability through low-threshold spikes, particularly in thalamocortical circuits[59]. T-type calcium channel neuronal regulation has been shown to contribute to sleep-wake transitions, epileptogenesis and visual response[58, 60, 61]. Additionally, dysregulation of T-type calcium channels has been implicated in the absence epilepsy where excessive activation leads to pathological burst firing[60, 62].

T-type calcium channels also influence neuronal plasticity through their modulation of intracellular calcium dynamics, which impact synaptic strength and gene transcription. These channels contribute to dendritic excitability and long-term potentiation (LTP) by providing localized calcium influx that activates calcium-dependent signaling cascades,

including those involving calmodulin-dependent kinases and CREB-mediated transcription[58]. Expression of T-type calcium channels in the hippocampus and cortex have been shown to regulate experience-dependent plasticity and memory consolidation[63, 64]. T-type calcium channels have been shown to control presynaptic glutamate release regulating NMDA and AMPA synaptic transmission in the absence epilepsy[65]. Additionally, T-type calcium channels have been shown to regulate GABA release in thalamic relay neurons as well as cortical and hippocampal interneurons impacting neurodevelopmental disorders, epilepsy and anxiety[59, 66-68]. T-type calcium channels have been implicated in cancers such as prostate, retinoblastoma, breast and glioblastoma[69-71]. Increases of intracellular calcium that are regulated by TTCC have been shown to influence GBM proliferation and cell death[71-74]. Human glioma samples and patients have been reported to express multiple splice isoforms of Cav3.1[75].

Mibefradil is an FDA-approved TTCC blocker previously used for the treatment of hypertension. Mibefradil blocks TTCC at 1-10μM and L-type channels at 100-300μM[76]. Mibefradil was later recalled from market due to adverse side effects when taken in combination with β-blockers[77]. Mibefradil has been examined in preclinical studies using glioblastoma xenografts with mibefradil alone or in combination with either radiation or TMZ slowing growth and enhancing survival[78-80]. Mibefradil received FDA orphan drug status for GBM and has been recently evaluated in Phase I clinical trials in recurrent GBM with TMZ and radiation that demonstrated the drug is safe and noted promising responses[81-83].

Our lab has previously characterized the role of Cav3.2 in GBM. We demonstrated that Cav3.2 is overexpressed in GBM cell lines as well as Glioma Stem Cells (GSCs). Additionally, Cav3.2 is overexpressed in GBM tumors compared to normal brain. Inhibition of Cav3.2 with mibefradil significantly decreased GSC growth, induced cell death and differentiated the GSCs. To demonstrate the effect was not resulting from off-target effects

of the drug we silenced Cav3.2 with siRNA which recapitulated the effects of mibefradil. Next, we examined the mechanism of Cav3.2 in GBM utilizing reverse phase protein arrays [84] and RNA-sequencing which identified altered pathways in mTor signaling, cell death and proliferation. Lastly, we examined the effect of mibefradil on GSC growth in vivo in conjunction with temozolomide (TMZ). Mibefradil alone reduced tumor size and prolonged mouse survival compared to vehicle controls. Additionally, mibefradil synergized with TMZ significantly reducing tumor volume, prolonging mouse survival and decreasing tumor growth.

Calcium levels are highly regulated within multiple cellular compartments of the cell. The levels of calcium in the cytosol are ~0.1mM, whereas the levels of extracellular calcium are ~1mM (10 times higher)[85]. The endoplasmic reticulum also contains increased levels of calcium compared to the cytosol[85, 86]. Activation of calcium signaling occurs via influx of calcium from outside the cell or release of calcium from intracellular stores, mediated by channels, pumps and exchangers[86]. Calcium acts as a second messenger regulating numerous cellular processes essential for cancer such as proliferation, apoptosis, invasion and gene transcription[87-93]. The transition from G1 to S phase in the cell cycle is regulated by calcium via regulation of transcription factors controlling expression of G1 cyclins (FOS, JUN, MYC, CREB-ATF1, and NFAT)[94-96]. Additionally, calcium directly regulates cyclins, CDKs and CKIs preventing the assembly and activation of CDK complexes for progression from G1 to S phase[94]. Calcium has been shown to regulate oncogenic signaling such as RAS activation by Ca^{+2} through regulation of GEFS (RASGRF1, RASGRF2, RASGRP1) as well as GAPs (CAPRI and RASAL1) which activate/inactivate RAS signaling in a Ca^{+2} dependent manner. Cancer cells exploit calcium signaling to achieve growth advantages such as regulating cell proliferation by upregulating calcium channels on the plasma membrane[94]. Cancer cells escape cell death by downregulating ER release channels which prevents the release of

calcium from ER stores preventing cell death cascades[94]. The regulation of numerous cellular processes through calcium signaling dictates calcium channels like T-type calcium channels as ideal therapeutic targets in brain tumors.

1.5.0 Rationale and Hypothesis

Glioblastoma (GBM) and medulloblastoma (MB) are highly aggressive primary brain tumors with poor prognoses and limited therapeutic options. GBM, the most common malignant brain tumor in adults, exhibits extensive intratumoral heterogeneity and resistance to conventional therapies. MB, the most prevalent malignant pediatric brain tumor, is molecularly diverse and categorized into distinct subgroups with variable clinical outcomes. Despite advances in molecular profiling, the neurobiological underpinnings that drive tumor progression, invasion, and recurrence remain incompletely understood.

The emergence of cancer neuroscience sheds light on the numerous factors contributing to brain tumor growth requiring the examination of the tumor as well as the contribution of the other cell types in the microenvironment. The majority of cancer neuroscience studies examined the effects of the neurons on the tumor cells but haven’t examined the mechanism in the neurons driving the pro-tumor signaling events. Glioblastoma is a heterogenous tumor with numerous cell states existing within the same tumor with cells from the tumor microenvironment driving certain tumor populations. The mechanism of targeting particular cell states and the microenvironmental contributions driving cell states requires further elucidation.

T-type calcium channels are low-voltage-activated calcium channels with established roles in neuronal excitability, neuronal plasticity, proliferation, and

differentiation. T-type calcium channels are expressed within the various regions of the nervous system specifically thalamus, cortex, cerebellum and basal ganglia. Calcium signaling regulates a plethora of cancer-associated cellular processes including cell proliferation, apoptosis, motility, angiogenesis, differentiation, gene transcription as well as neurotransmission and synaptic plasticity. T-type calcium channels are aberrantly expressed in multiple cancers, including gliomas, where they may contribute to tumor cell proliferation, migration, and therapy resistance. The majority of the studies of T-type calcium channels in cancer have focused primarily on the role of the channels in driving malignancy parameters such as proliferation, migration, and invasion. The role of T-type calcium channels in the other cell types within the tumor microenvironment has yet to be examined.

We hypothesize that T-type calcium channels play a critical role in glioblastoma and medulloblastoma pathogenesis by modulating tumor cell proliferation, invasion, and interactions with the neural microenvironment. We hypothesize that TTCC upregulation drives GBM growth via multiple molecular and cellular mechanisms that involve tumor cell-intrinsic and microenvironment-dependent mechanisms. Specifically, we hypothesize that microenvironmental Cav3.2 plays an essential role in regulating the tumor microenvironment and influencing glioblastoma malignancy. We hypothesize that loss of microenvironmental Cav3.2 impact tumor growth through decreased synaptic connections by decreasing the OPC-like cell state of GBM tumors. We hypothesize that neuronal Cav3.2 is promoting neuron-GBM connections promoting GBM proliferation. For the medulloblastoma project we hypothesize that T-type calcium channel upregulation drives medulloblastoma growth. We hypothesize that inhibition of T-type calcium channels through mibefradil or siRNA silencing will reduce medulloblastoma malignancy parameters. We hypothesize that in vivo administration of mibefradil will

significantly decrease tumor volume and prolong mouse survival compared to vehicle control mice. Overall, our study aims to establish T-type calcium channels as key regulators of glioblastoma and medulloblastoma progression and to evaluate their inhibition as a promising therapeutic strategy for these aggressive brain tumors.

Chapter 2-Microenvironmental T-type calcium channels regulate neuronal and glial processes to promote glioblastoma growth

Collin J. Dube[1], Ying Zhang[1], Shekhar Saha[1], Michelle Lai[1], Myron K. Gibert[1], Miguel Escalante[2], Kadie Hudson[1], Doris Wong[3], Pawel Marcinkiewicz[1], Ulas Yener[4], Yunan Sun[1], Esther Xu[1], Aditya Sorot[1], Elizabeth Mulcahy[1], Benjamin Kefas[5], Farina Hanif[6], Fadilla Guessous[7], Ashley Vernon[1], Manoj K. Patel[8], David Schiff[9,10], Hui Zong[1,10], Benjamin Purow[7,10], Eric Holland[11], Swapnil Sonkusare[12], Harald Sontheimer[2,10], Roger Abounader[1,9,10*]

[1]Department of Microbiology, Immunology & Cancer Biology, University of Virginia, Charlottesville, VA 22908, USA.

[2]Department of Neuroscience, University of Virginia, Charlottesville, VA 22908, USA.

[3]Department of Biochemistry and Molecular Genetics, University of Virginia School of Medicine, Charlottesville, VA 22908, USA.

[4]Department of Neurosurgery, Stanford University School of Medicine, Stanford, California, USA.

[5]Pharmacy, University of Virginia, Charlottesville, VA 22908, USA.

[6]Department of Biochemistry, Dow International Medical College, Dow University of Health Sciences, Karachi, 75270, Pakistan.

[7]Laboratory of Onco-Pathology, Biology and Cancer Environment, Faculty of Medicine, Mohammed VI University of Sciences and Health, Casablanca, Morocco

[8]Department of Anesthesiology, University of Virginia, Charlottesville, VA, United States

[9]University of Virginia Department of Neurology, Charlottesville, VA 22908, USA

[10]University of Virginia Comprehensive Cancer Center, Charlottesville, VA 22908, USA.

[11]Fred Hutchison Cancer Center, Seattle, WA

[12]Department of Molecular Physiology and Biological Physics, University of Virginia, Charlottesville, VA 22908

2.1.0 Abstract

Background

Glioblastoma [19] is the most common primary malignant brain tumor. The aim of this study was to elucidate the role of microenvironment and intrinsic T-type calcium channels (Cav3) in regulating tumor growth and progression.

Methods

We grafted syngeneic GBM cells into Cav3.2 knockout mice to assess the role of microenvironment T-Type calcium channels on GBM tumor growth. We performed single-cell RNA-seq (scRNA-seq) of tumors from WT and Cav3.2 KO mice to elucidate the regulation of tumors by the microenvironment. We used neurons from WT and Cav3.2 KO mice in co-culture with GBM stem cells (GSC) to assess the effects of Cav3.2 on neuron/GSC synaptic connections and tumor cell growth.

Results

Cav3.2 KO in the microenvironment led to significant reduction of GBM growth and prolongation of animal survival. scRNA-seq showed that microenvironment Cav3.2 regulates neuronal and glial biological processes. Microenvironment Cav3.2 downregulated numerous genes associated with regulating the OPC cell state in GBM tumors such as SOX10 and Olig2. Neuronal Cav3.2 promoted neuron/GSC synaptic connections and GSC growth. Treatment of GSCs with the Cav3 blocker mibefradil downregulated genes associated with neuronal processes. The Cav3 blocker drug mibefradil synergized with temozolomide (TMZ) and radiation to reduce in vivo tumor growth and prolong animal survival.

Conclusions

Together these data reveal a role for microenvironment Cav3 in promoting GBM tumor progression through regulating neuronal and glial processes particularly associated with the OPC-cell state. Targeting both intrinsic and microenvironment Cav3 with the inhibitor mibefradil significantly enhanced the anti-GBM effects of TMZ and radiation.

2.2.0 Key Points

- Microenvironment Cav3.2 promotes GBM progression
- Microenvironment Cav3.2 promotes neuronal and glial processes
- Pharmacological targeting of intrinsic and microenvironment Cav3 synergizes with TMZ/radiation

2.3.0 Importance of the Study

In this study, we demonstrate for the first time that microenvironment Cav3.2 contributes to GBM progression and growth by regulating neuronal and glial processes. Our findings highlight the importance of T-type calcium channels in the microenvironment as well as the tumor and provides preclinically relevant data for the use of mibefradil to inhibit GBM growth in combination with standard of care therapies.

2.4.0 Introduction

Glioblastoma [19], grade IV wildtype-IDH glioma, is the most common primary malignant brain tumor. GBM has a dismal prognosis of around 15 months despite aggressive standard of care therapy that includes surgery, chemotherapy and radiation [97, 98]. Gliomas have been shown to interact with the tumor microenvironment to promote growth and resistance to therapy. Gliomas form synaptic connections with neurons and neuronal activity drives growth and invasion through paracrine and electrical signaling [36, 37, 40] [44, 45, 47, 99]. Gliomas also influence the neuronal circuits around them, increasing excitability and neuronal activity [48, 50, 52, 100-102]. Neuronal signals from the tumor microenvironment influence neuronal gene expression and cell state of the tumor. For example, increased neuronal signaling in the tumor microenvironment promotes neuronal connections between oligodendrocyte precursor-like cells (OPCs) and neural precursor-like cells (NPCs) in the tumor with surrounding neurons [21, 103]. Importantly, GBM patients with high neural signatures exhibit decreased overall survival and progression free survival compared to patients with low neural signatures [104]. Gliomas utilize numerous mechanisms of neuronal interactions to collectively create a pro-tumor environment for growth, invasion and resistance to therapies. However, the exact nature and underlying mechanisms of neuron/GBM interactions and therapeutic strategies to disrupt these interactions have not been fully explored.

T-type calcium channels (Cav3) are a class low voltage gated calcium channels which are encoded by three genes (Cav3.1, Cav3.2, Cav3.3). Cav3 are expressed throughout the body, specifically within the central nervous system [57, 58, 105-107]. Cav3 are found both presynaptically and postynaptically throughout the central nervous system where they regulate presynaptic glutamate release as well as postsynaptic plasticity [65, 107, 108]

[65, 109]. Cav3.2 specifically has been shown to regulate neuronal firing in central nervous pathologies such as anxiety, memory disorders, epilepsy and chronic pain [110-113]. Our lab and others previously showed that Cav3 are overexpressed in GBM and regulate malignancy parameters such as growth, invasion, death and stemness [114-117]. However, the role of microenvironment Cav3 in GBM progression has not been investigated to date.

This study aimed to elucidate the role of microenvironment Cav3.2 on GBM tumor parameters including neuron/GBM interactions and malignancy, and to assess the therapeutic effects of targeting microenvironment and cell intrinsic Cav3. We hypothesized that loss of Cav3.2 within the brain tumor microenvironment would decrease tumor growth as well as neuron-GBM signaling processes. We grafted syngeneic GBM cells into whole body Cav3.2 KO mice to elucidate the effect on tumor growth, survival and proliferation. Loss of Cav3.2 in the microenvironment decreased neuronal and glial processes in the tumor, specifically those associated with the OPC cell state. Co-cultures of Cav3.2 KO neurons with GSCs showed decreased neuron/GBM projections and decreased tumor cell proliferation. Inhibition of Cav3 in GSCs significantly decreased genes associated with neuronal processes. Blockage of microenvironment and intrinsic Cav3 with the FDA-approved repurposed Cav3 blocker mibefradil sensitized tumors to temozolomide and radiation therapy. This is the first study elucidating the role of microenvironment Cav3.2 in promoting GBM tumor growth through regulating neuronal and glial processes.

2.5.0 Methods

Cell lines: The mouse GBM cell lines GL261 and CT2A were cultured in 500 mL Dulbecco's modified eagle media (DMEM) (Gibco) containing 5 mL pen/strep, and 50 mL

FBS. Glioblastoma Stem cell lines (GSCs) G34 were cultured in neurobasal (L-glutamine negative) media (Gibco, #.21103-049) containing 5 mL pen/strep, 5 mL B-27 without Vit-A (Gibco), 2.5 mL N-2 (Gibco), one mL EGF, one mL FGF, and 1.25 mL L-Glutamine. All cell media contained 5 µL Plasmocure reagent to prevent mycoplasma contamination.

Orthotopic xenografting: For all xenografts male and female mice were used equally. For constitutive Cacna1h (Cav3.2) knockout studies, C57Bl6 wildtype (WT) and Cav3.2 knockout mice (The Jackson Laboratory) were used. Mice were anesthetized with ketamine and placed in a stereotactic apparatus. The cranium was exposed via a midline incision and 20,000 tumor cells (GL261 and CT2A) in 1 µl of sterile PBS was intracranially injected into the cortex; stereotactic coordinates used were as follows: 0.5mm lateral to midline, 1.0 mm anterior to bregma, -1.8 mm deep to the cranial surface. For drug studies in Nude athymic mice (Foxn1nu, Envigo), 100,000 tumor cells (G34) were injected in 1 µl of sterile PBS into the striatum; stereotactic coordinates used were as follow: 0.5 mm lateral to midline, 1.0 mm posterior to bregma, 2.5 mm deep from cranial surface. Brains were scanned with magnetic resonance imaging [118] on a 7 Tesla Bruker/Siemens ClinScan small animal MRI on the 18th day after cell transplantation. Tumor volumes were quantified using OsiriX Lite software (Version 12.5.2). For survival studies mice were monitored carefully and sacrificed when they displayed symptoms of tumor development including lethargy and head tilt.

RCAS/TVA mouse model: For all RCAS/TVA mouse experiments, male and female mice were used equally. DF-1 cells were transfected with plasmids of RCAS-Scrambled, RCAS-shCav3.1, RCAS-Cav3.2, RCAS-PDGFB, and RCAS-Cre. Mice used in this experiment are the XFM model which is *Ntv-a Ink4a-Arf-/- LPTEN [119]. Mice used for this experiment were 4 to 6.5 weeks old. Two microliters (1:1 mixtures of RCAS-PDGFB, RCAS-CRE and*

either RCAS-Scrambled, RCAS-shCav3.1, RCAS-shCav3.2) of 4 x 10^4 transfected DF-1 cell suspensions were injected into the SVZ zone with the stereotactic coordinates 1.0 mm lateral to midline, 1.0 mm anterior to bregma, -2.5 mm deep from the cranial surface. Brains were scanned with a 7 Tesla Bruker/Siemens ClinScan small animal MRI on the 88th day after cell transplantation. Tumor volumes were quantified using OsiriX Lite software (Version 12.5.2). For survival studies mice were monitored carefully and sacrificed when they displayed symptoms of tumor development.

Neuron-GBM co-cultures: Neurons were isolated from the brains of P1-P3 C57/BL6 WT, Cav3.2 or C57/BL6 Cav3.2 KO mice (The Jackson Laboratory) using the Neural Tissue Dissociation Kit- Postnatal Neurons (Miltenyi Biotec), followed by the Neuron Isolation Kit, Mouse (Miltenyi Biotec) as per the manufacturer's instructions. After isolation, 300,000 neurons were plated on glass coverslips that were pretreated with poly-L-lysine for 1 hr at room temperature followed by 5 µg/ml mouse laminin for 3 hrs at 37C. Neurons were maintained in neurobasal medium (Invitrogen) supplemented with B27 supplement (2% v/v) and L-glutamine (0.5mM). After 5 days GSCs (50,000) were added and co-cultured in neurobasal medium. For EdU proliferation assays, co-cultures were plated for 48 hrs before treatment with EdU (10 µM) and incubated for a further 24 hrs. Following incubation, the cultures were fixed with 4% paraformaldehyde (PFA) for 20 mins at room temperature and stained using the Click-iT EdU cell Proliferation Kit (Thermo Fisher Scientific). The cells were then stained with mouse anti-nestin (1:500 Abcam), chicken anti-neurofilament (1:500, Aves Lab) overnight at 4°C. Following washing steps, the coverslips were incubated in secondary antibodies Alex 555 donkey anti-mouse IgG and Alex 647 donkey anti-chicken IgG and mounted using Prolong Gold Mounting medium (Life Technologies). Images were collected on a Leica Stellaris and the proliferation index was quantified at percentage of EdU-labeled GSCs [120] over total GSCs.

Immunohistochemistry: Tumor-bearing mice were anesthetized with isoflurane inhalation followed by cervical dislocation followed by transcardial perfusion with 20 ml of PBS. Brains were dissected out and fixed in 4% PFA overnight at 4C. Afterwards brains were transferred to 30% sucrose. Brains were embedded in Tissue plus OCT (Thermo Fisher) then sectioned in the coronal plane at 10 μM using a cryostat (Thermo Cryostar NX50). For immunohistochemistry, coronal sections were incubated in a blocking solution (5% normal donkey serum, 0.3% Triton X-100 in PBS) at room temperature for 20 minutes. Chicken anti-GFP (1:500, abcam), rabbit anti-Ki67 (1:500, SantaCruz), rabbit anti-Neun (1:500, Abcam), mouse anti-Nestin (1:500, Abcam), mouse anti-Vglut1 (1:500, Abcam) were diluted in primary diluting solution (5% normal donkey serum, 0.3% Triton X-100 in PBS) and incubated overnight at 4^{o}C. Sections were washed four times in PBT and incubated with Alexa 488 donkey anti-mouse, Alexa 555 donkey anti-rabbit, Alexa 647 donkey anti-chicken all at 1:250 (Thermo Fisher) in secondary diluting solution at room temperature for two hours. Sections were washed with PBT and mounted with ProLong Gold Antifade Mountant with DAPI (Thermo Fisher). Images were collected on a Leica Stellaris 8. Proliferation index was quantified at percentage of Ki67+ GFP+ cells over total GFP cells. Percentage of VGLUT1-GFP was calculated as VGLUT1+GFP+ over total GFP cells.

Single-cell RNA-Sequencing: Tumor-bearing mice were anesthetized under isoflurane inhalation followed by cervical dislocation. Brains were dissected under fluorescent microscope with GFP positive tumors isolated and placed on ice. One male and one female mouse was isolated from each group to control for sex-dependent variability. Tumors were mechanically and enzymatically dissociated using a papain-based brain tumor dissociation kit (Miltenyi Biotec). Samples were washed with PBS and red blood cell

removal was performed as described (Miltenyi Biotec). Samples were next subjected to Debris removal as described (Miltenyi Biotec). Following this, the cells were stained with Live dead dye (7-AAD). Samples were subjected to FACS sorting (Influx Cell Sorter) for live cells. Samples were processed and sequenced using 10X Genomics *according to validated standard operating procedures established by the University of Virginia Genome Analysis and Technology Core, RRID:SCR_018883.*

Single-cell RNA-seq analysis: Sequencing files were downloaded for each flow cell lane and fastq files were merged. Reads were mapped to the mouse genome mm10 using 10X CellRanger (7.1.0). For single-cell sequencing analysis standard procedures for filtering, mitochondrial gene removal, doublet removal, variable gene selection, dimension reductionality and clustering were performed using Seurat (version 5.0.2). A cell quality filter of greater than 200 features but fewer than 7500 features per cell and less than 25% of read counts attributed to mitochondrial genes was used. Dimensionality reduction was performed using principal component analysis and visualized with the Elbowplot function to find neighbors and clusters (resolution 0.3). Uniform manifold approximation and projection was performed for visualizing cells. Cell populations were identified using singleR with the celldex mouse RNA-seq data set as reference along with FindAllMarkers and the inferCNV [121] algorithm to annotate clusters. Differentially expressed genes in tumors between WT and Cav3.2 KO were identified by FindMarkers using default settings. Gene Ontology Biological Pathways, Cellular Compartments and Molecular Functions of DEGS were performed using ClusterProfiler. Single-cell RNA-Seq data can be found at the NIH GEO database (GSE273629).

Identification of co-expressed genes within the tumor cells was carried out using hdWGCNA (v0.2.23). Meta cells were constructed using harmony dimensionality

reduction with 25 neighboring cells [122] using the function construct metacells. Modules were identified using the ConstructNetwork function (setDatExpr=FALSE) below the optimal soft threshold. To identify module feature genes, the ModuleEigenees function was used followed by computing the module connectivity to identify hub genes with the ModuleConnectivity function. To identify differentially expressed module eigengenes between WT and Cav3.2 KO, the FindDME function was used. Module scores representing the average expression of all the modules on the corresponding WGCNA modules were computed using the AddModuleScore function in Seurat. Pathway enrichment analysis of gene modules was performed using enrichR (v3.2).

Cell communication analysis was carried out using CellChat (v2.1.2). CellChat objects were created using createCellChat followed by inference of cell-cell communication using computeCommunProb. CellChat objects were created for both WT and KO samples then merged using MergeCellChat for comparison between the samples using the compare Interactions function. Differential number of interactions and interaction strength were visualized between WT and KO using NetVisual_heatmap. Dysfunctional signaling of Ligand-Receptor pairs was performed using IdentifyOverExpressedGenes then visualized based on sender and receiver cell types using NetVisual_bubble.

Publicly available datasets: To examine the expression of Cav3 in publicly available single-cell datasets the Single-cell Portal was used [123]. Expression of Cav3 was queried in the Neftel dataset [21] and visualized by cell state using the single-cell portal. Expression of Cav3 was queried in the Richards dataset [124] using the single-cell portal. Expression of Cav3 was examined in publicly available spatial transcriptomic using the Ravi et al datasets [122] which is accessible using the SPATA2 tool box (v2.0.4).

Statistical analysis: Comparisons between means of samples were performed using Students t-tests and one-way ANOVA. All quantitative results are shown with means ± SEM. Molecular experiment tests and computational experiment tests were performed using RStudio.

2.6.0 Results

Cav3.2 expression in the microenvironment promotes GBM progression and reduces survival

To elucidate the role of microenvironment Cav3.2 in glioma growth, we generated syngeneic GBM tumors using GL261 expressing Green fluorescent protein (GFP) into Cav3.2 KO (Cacna1h$^{-/-}$) or WT C57/BL6 mice. After 21 days of engraftment of GBM cells, MRI scans to visualize and measure the tumors were performed. The MRI showed significant reduction in tumor volume in Cav3.2 KO mice compared to WT mice (Fig. 2-1A,B, Fig. S2-1A,B). We next sought to determine if microenvironment Cav3.2 KO was sufficient to extend survival of syngeneic GBM tumor-bearing mice. Cav3.2 KO mice survived significantly longer than WT mice implanted in two syngeneic GBM models using GL261 and CT2A cells (Fig. 2-1C,D). Next, we assessed whether microenvironment Cav3.2 KO impacted tumor proliferation through histological analysis of Ki67 stained tumor sections. We found a significant reduction in the proliferation index in tumors in the Cav3.2 KO compared to WT mice (Fig. 2-1E). Taken together, these findings indicate that microenvironment Cav3.2 promotes tumor growth and cell proliferation and decreases survival.

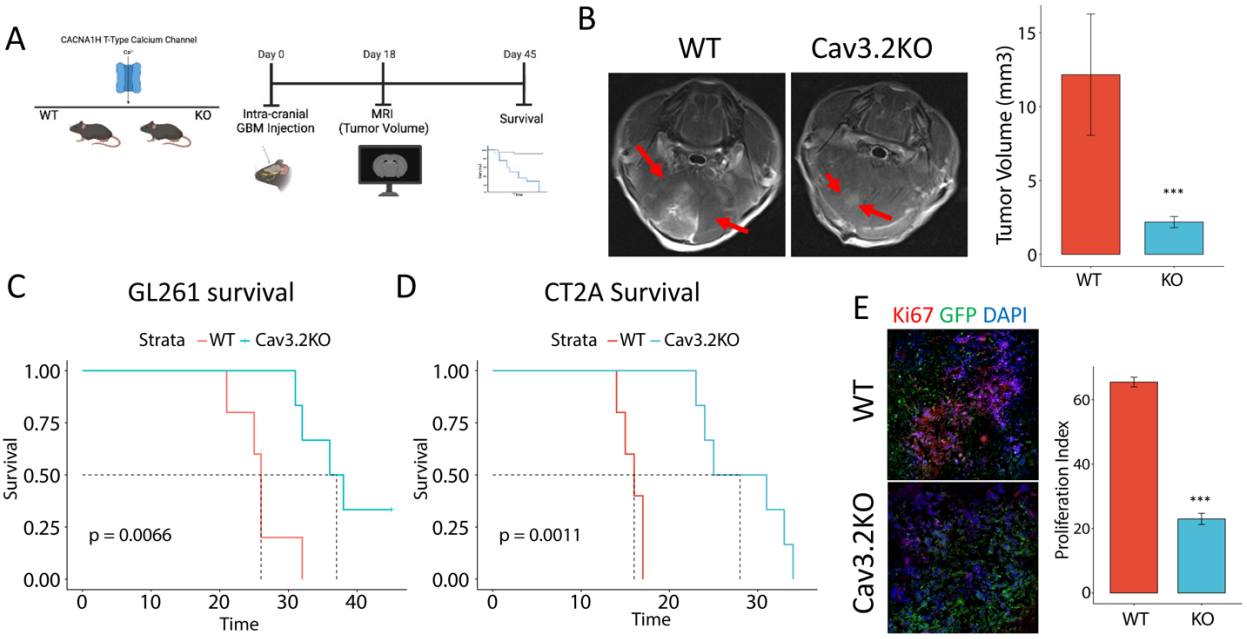

Figure 2-1: Microenvironment Cav3.2 promotes tumor progression and reduces survival. A) Schematic of experimental workflow for WT and Cav3.2 KO experiments. B) Representative MRIs and quantification showing that microenvironment Cav3.2 KO leads to significant reduction in GBM (GL261) tumor volume. Red arrows indicate the tumor location. C & D) Kaplan Meir survival curves for WT and Cav3.2 KO mice in GL261 and CT2A xenograft tumors respectively. E) Representative immunofluorescence staining of Ki67 in WT and Cav3.2 KO with quantification showing a significant reduction in proliferation index. ***<0.001

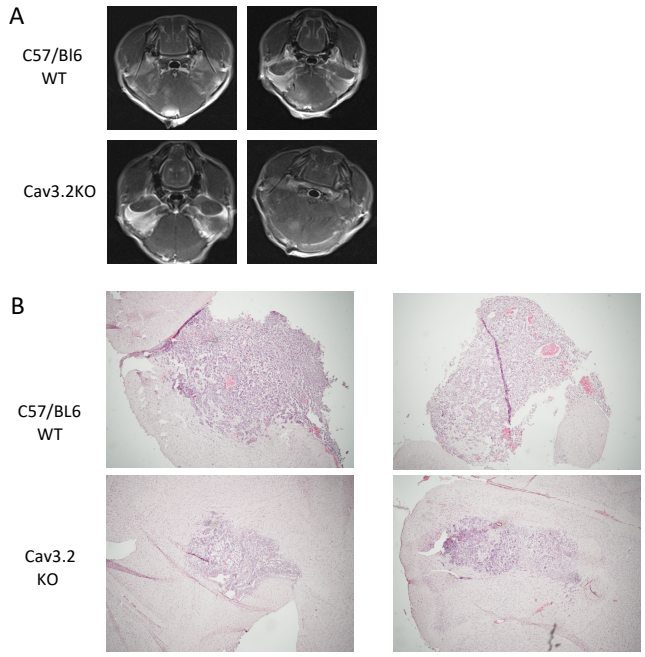

Figure S2-1: MRI and H&E Staining. A) Representative MRI images of GL261 xenografts in WT and Cav3.2KO mice. B) Representative H&E staining of tumor sections from GL261 xenografts from WT and Cav3.2 KO mice.

Microenvironment Cav3.2 regulates genes important for neuron-GBM interactions

To molecularly define the effects of microenvironment Cav3.2 on GBM tumors we performed single-cell RNA-seq (scRNA-seq) on syngeneic tumors implanted in WT and Cav3.2 KO mice (Fig. 2-2A). We utilized established markers as well as the infercnv package to differentiate microenvironment populations from tumor cells (Fig. 2-2B, Fig. S2-2A-H). We performed differential gene expression analysis of the WT and Cav3.2 KO tumors to identify the downregulated genes in the tumor and assess how loss of Cav3.2 in the microenvironment impacts tumor signaling. To gain insight into what the downregulated genes were doing we performed Gene Ontology (GO) Biological pathway analysis which showed downregulation of nervous system processes including

gliogenesis, glial cell differentiation, regulation of synapse organization, structure or activity and axon guidance in GBM cells in the Cav3.2 KO compared to WT tumors (Fig. 2-2C,D, Fig. S2-3A,B). Gene ontology cellular compartment analysis of the downregulated genes showed enrichment of genes associated with neuronal processes such as postsynaptic specialization, neuron to neuron synapse, asynaptic synapse, postsynaptic density and distal axon (Fig. 2-2E,F). Analysis of the upregulated genes showed enrichment for biological pathways associated with positive immune response, phagocytosis and T-cell activation (Fig. S2-3C,D). These data indicate a role of microenvironment Cav3.2 in regulating neuronal (synapse organization, axon guidance) and glial processes (gliogenesis, glial cell differentiation) in the tumor, which are important for regulating connections of the tumor to the other cell types such as neurons and astrocytes.

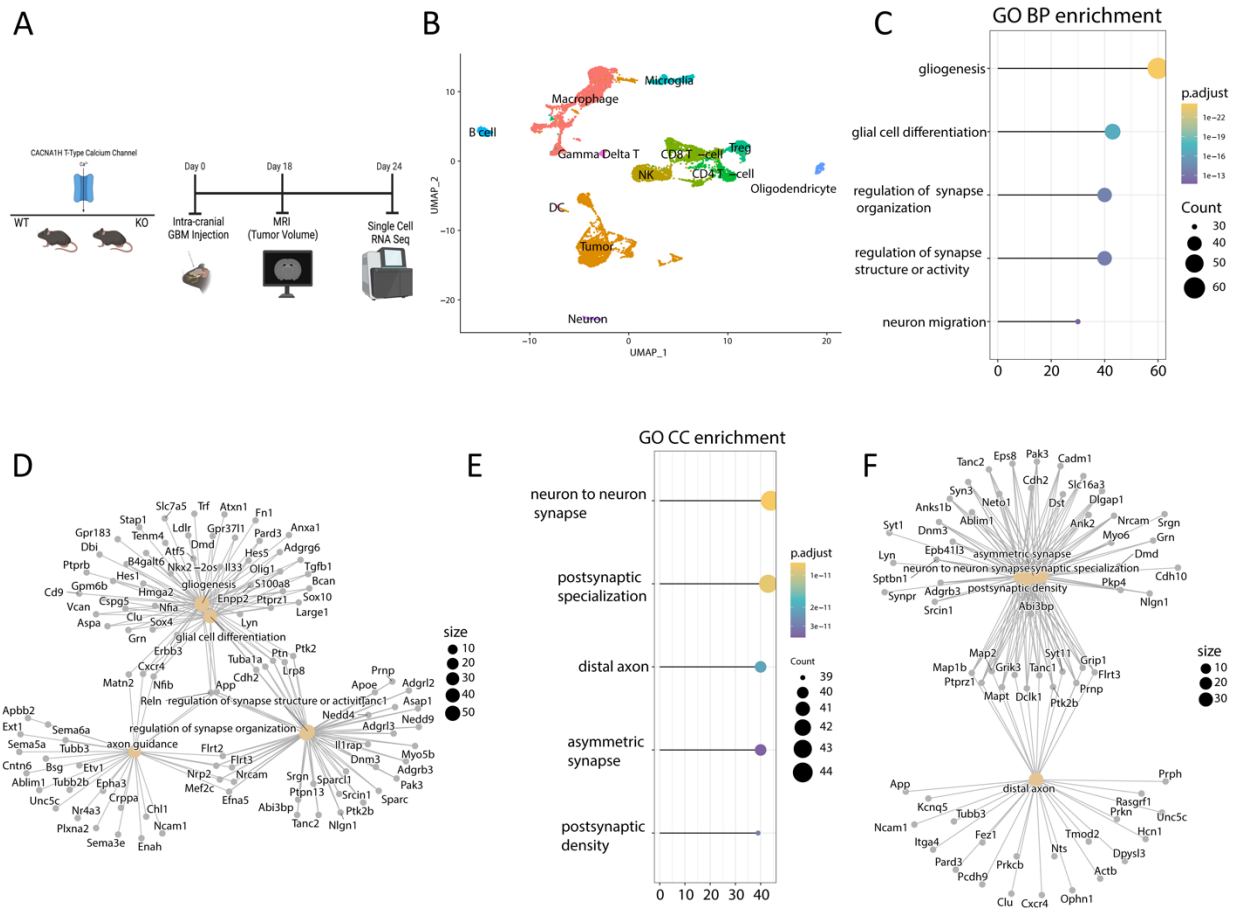

Figure 2-2: Microenvironmental Cav3.2 regulates neuronal and glial processes. A) Schematic showing the experimental workflow for single-cell RNA-seq tumor isolation. B) UMAP of the distinct cell types isolated from WT and KO mice. C) Gene ontology Biological Pathways of downregulated genes in Cav3.2 KO tumors. D) Cnetplot of GO BP pathways and associated genes. E) Gene ontology Cellular Compartment of downregulated genes in KO tumors. F) Cnetplot of GO CC pathways and corresponding genes.

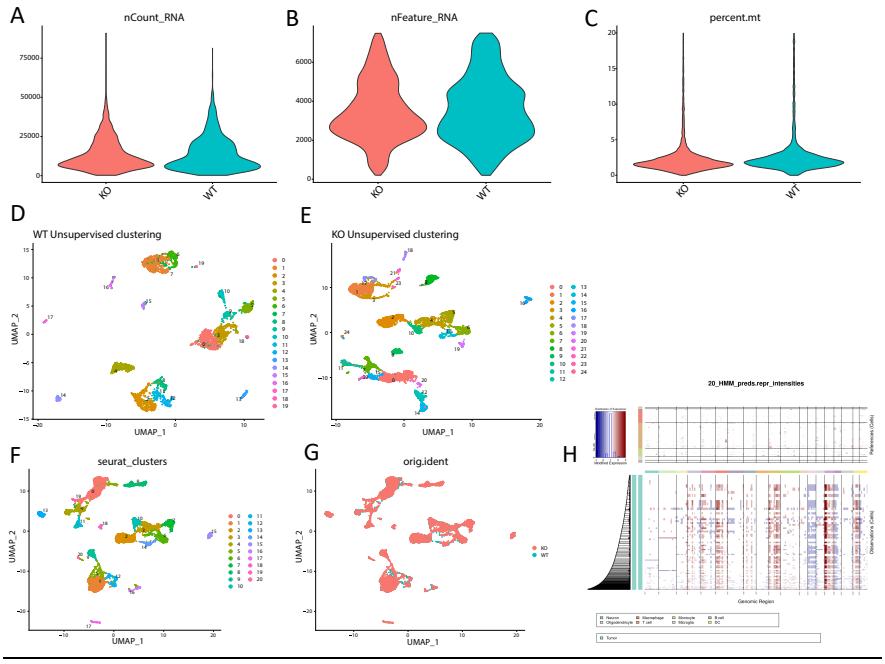

Figure S2-2: Single-cell RNA sequencing QC. Single-cell RNA sequencing of Wild type (WT) and Cacna1H-/- (KO) tumors. A-C. Quality control of sequenced tumors from WT and KO tumors. D,E) Unsupervised clustering of WT and KO tumors. F Seurat clusters for the merged object of WT and Cav3.2 KO tumors. G) UMAP showing the overlap of WT and Cav3.2 KO tumors in the merged object. H) Heatmap of inference of chromosomal CNAs with the top rows being non-malignant cells followed by tumor cells.

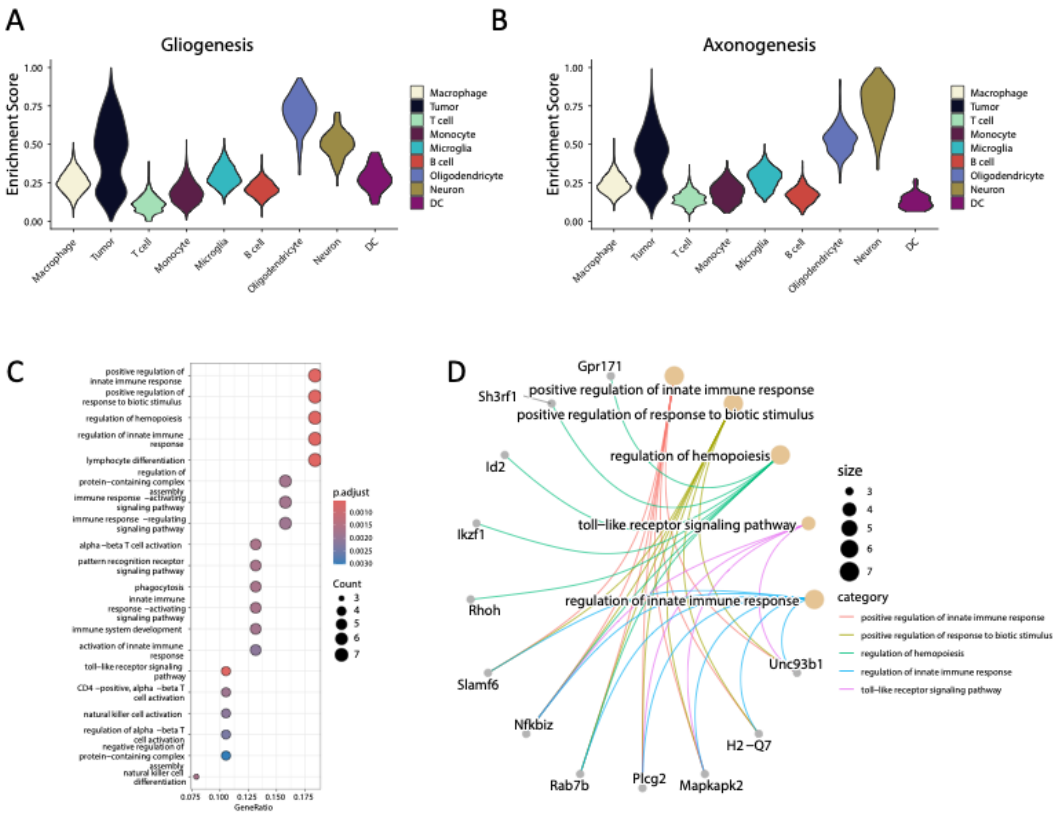

Figure S2-3: Cav3.2 KO Deregulation A) Enrichment score of Gliogenesis genes across cell types. B) Enrichment score of Axongenesis genes across cell types. C) Gene Ontology Biological pathway analysis of upregulated genes in Cav3.2 KO tumors. D) Cnetplot of upregulated biological pathways and corresponding genes with each process.

Microenvironmental Cav3.2 regulates OPC-related genes and cell states in GBM cells

To gain further insight into the role of microenvironment Cav3.2 in the context of GBM, we utilized single-cell weighted gene co-expression network association analysis [125] on tumor cells from WT and Cav3.2 KO mice (Fig. S2-4A,B). This analysis identifies modules of co-expressed gene regulatory networks across multiple cell clusters. Gene ontology of

the tumor modules identified numerous biological pathways associated with the specific modules such as antigen receptor mediated signaling pathways and synaptic pruning (Fig. S2-4C). After identifying the co-expression modules, we performed differential module eigengene (DME) analysis to examine which modules are upregulated and downregulated in Cav3.2 KO tumors (Fig. S2-4D). The analysis identified tumor module 4 as downregulated in tumors from Cav3.2 KO mice. The most co-expressed genes in this module form an interconnected graph and consist of genes associated with oligodendrocyte differentiation (PTPRZ1, SOX6, SOX10) and nervous system development (RBFOX2, NAV3, S100B, GPM6B, ADGRL3) based on GO (gene ontology) pathway analysis (Fig. 2-3A,B). Additionally analysis of the tumor 4 module and differentially expressed genes revealed an overlap of genes associated with the OPC cell state (Fig. S2-4E,F). We examined the OPC cell state and found a decreased enrichment of the OPC cell state in Cav3.2 KO compared to WT microenvironment tumors (Fig. 2-3C). We then characterized the tumors by cell state according to Neftel, which demonstrated that tumors from Cav3.2 KO microenvironment exhibit a decrease in OPC cell states and a shift towards an increase in AC cell state (Fig. S2-5A). We next assessed the differential regulon activity of tumors, which revealed a decreased activity of Olig2 and Sox10 in OPC and NPC cell states (Fig. S2-5B). The decreased enrichment of the OPC cell state as well as the activity of OPC-related transcription factors led to the examination of SOX10 and Olig2 specifically, which showed downregulation in tumors in the Cav3.2 KO microenvironment (Fig. 2-3D,E, Fig. S2-5C). The OPC cell state has been shown to interact with neurons in the tumor microenvironment [103]. Therefore, we examined publicly available spatial transcriptomic data by Ravi et al [122] and found that enrichment of SOX10 and Olig2 in the transition and infiltration region of the tumors, specifically OPC-like cells, indicative of connections with neurons in the microenvironment (Fig. 2-3F, Fig. S2-5D). The cell state of GBM regulates the ability of tumor cells to interact with the various

cell types of the tumor microenvironment. Our data suggest that microenvironment Cav3.2 regulates the OPC cell state of the tumor through SOX10 and Olig2 which are important transcription factors for regulating genes responsible for the OPC-like cell state.

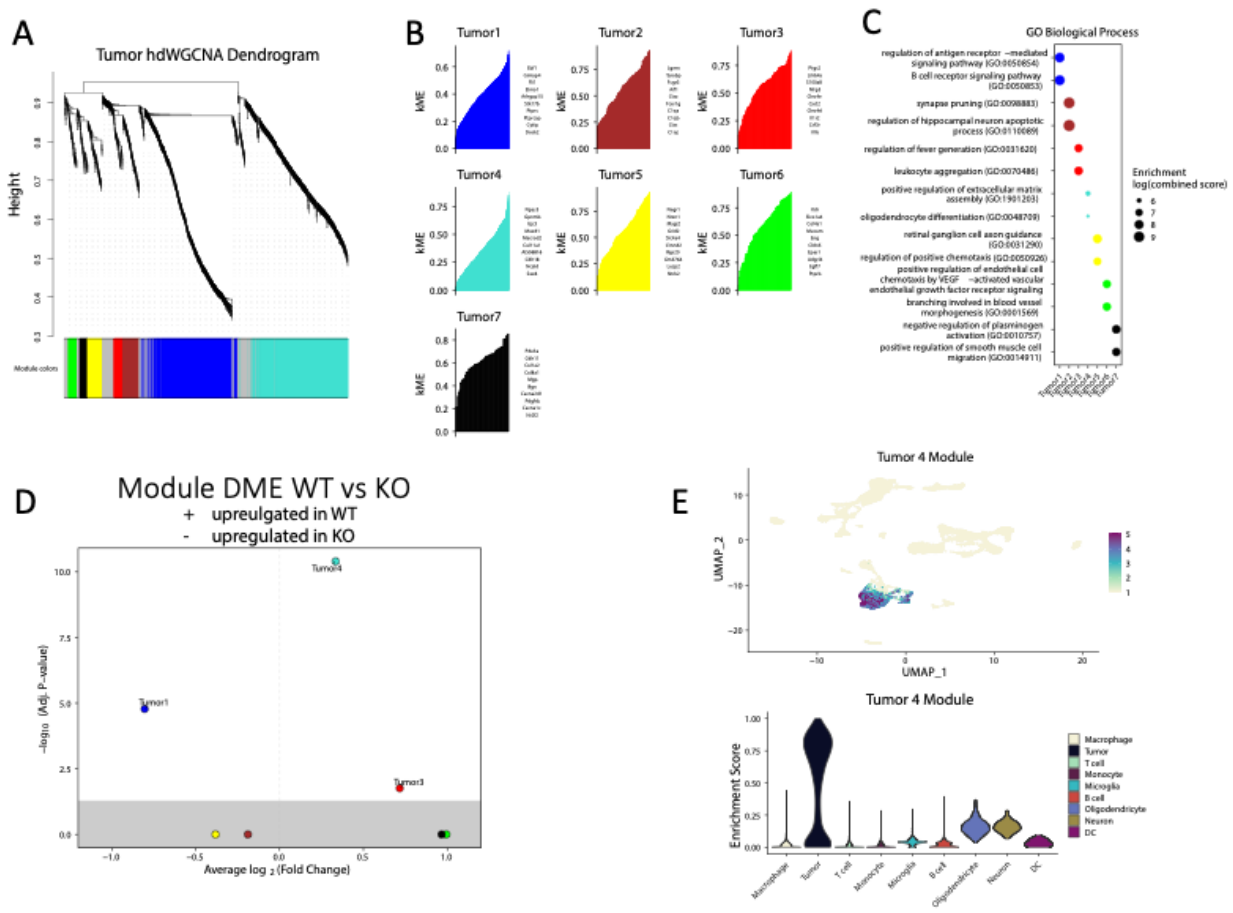

Figure S2-4: hdWGCNA analysis. A) Dendogram of co-expression modules single-cell RNA seq tumors. B) kME for the tumor modules identified in hdWGCNA. C) Gene ontology biological processes for each of the tumor modules. D) Volcano plot of the differential module eigene between WT and Cav3.2 KO tumors. E) Feature plot showing overlay of tumor 4 module with corresponding Violin plot showing enrichment of the tumor 4 module in the cell types.

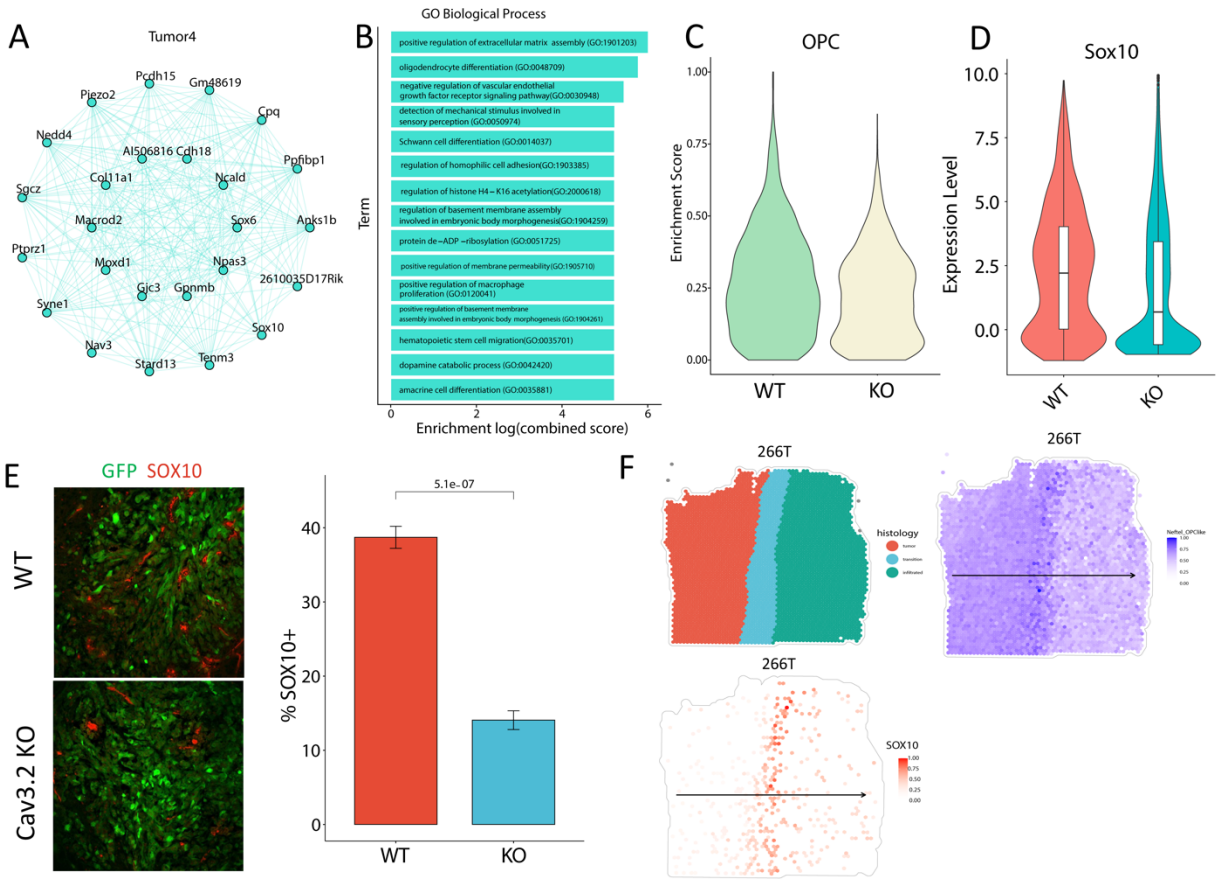

Figure 2-3: Cav3.2 KO downregulates OPC cell state genes. A) Network graph of the top 25 co-expressed genes in the Tumor 4 module of the hdWGCNA analysis. B) Gene Ontology Biological Pathways for the Tumor module 4. C) Enrichment score of the OPC cell state in WT and Cav3.2 KO tumors. D) Expression of Sox10 in WT and Cav3.2 KO tumors showing decreased expression. E) Representative immunofluorescent staining of SOX10 (Red) in WT and Cav3.2 KO tumors (GFP) with quantification of %SOX10 positive cells on the right. F) Spatial transcriptomic data of 266T showing the different zones of tumor infiltration (Left), OPC-like cells (Right) and Sox10 expression (Bottom) demonstrating enrichment of Sox10 in the OPC-like cells in the transition zone.

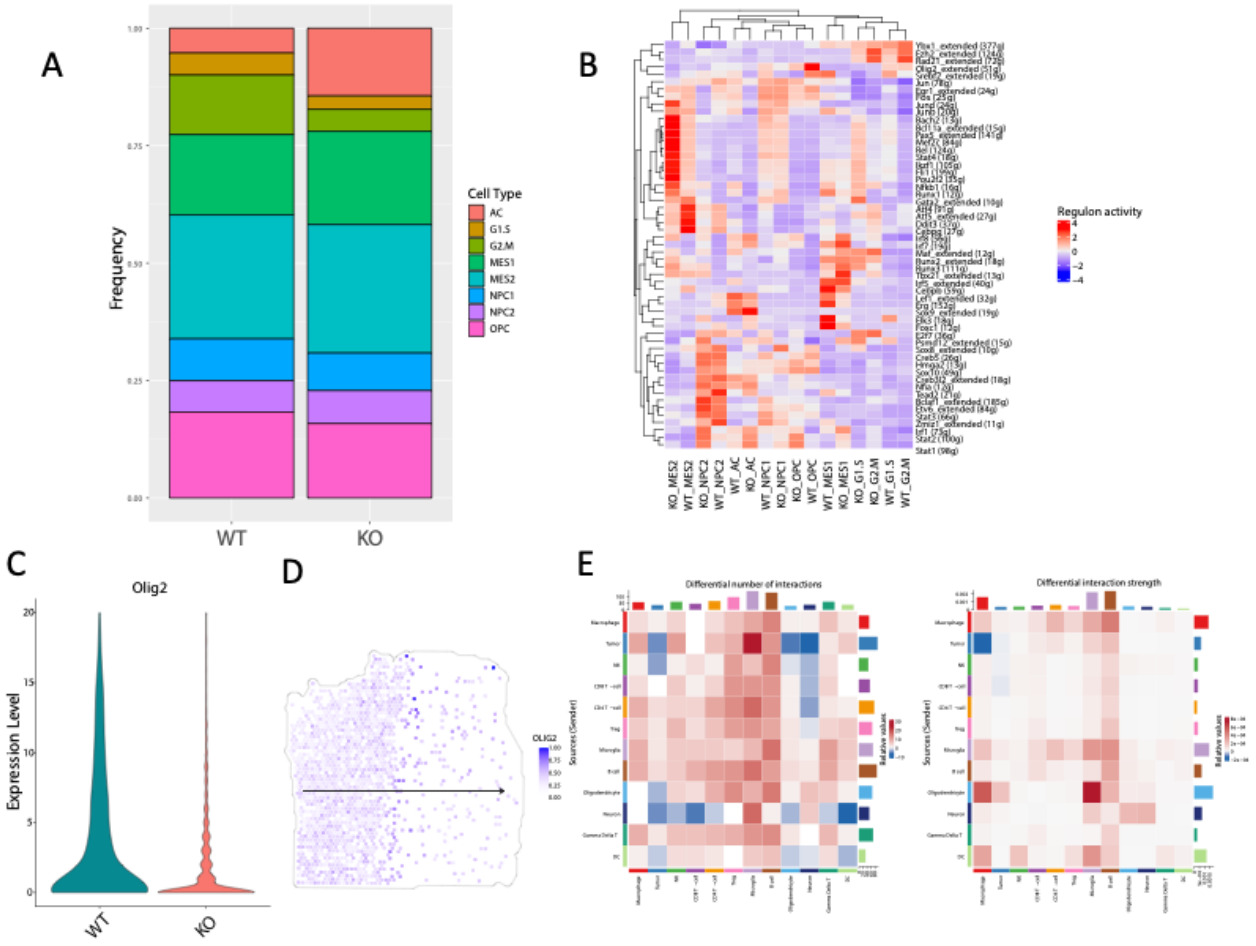

Figure S2-5:Cell state and CellChat analysis A) Frequency of cell states in WT and Cav3.2 KO Tumors. B) Heatmap of regulon activity of transcription factors from Scenic analysis for each cell state within WT and Cav3.2 KO tumors. C) Expression of Olig2 in WT and Cav3.2 KO tumors showing decreased expression. D) Spatial transcriptomic data of 266T showing the Olig2 expression. E) Heatmap of differential number of interactions and interaction strength of cell senders and receivers between WT and Cav3.2 KO cellchats.

Neuronal Cav3.2 enhances GBM growth and guides neuron/GBM connections

The downregulation of neuronal genes and neuronal processes in tumors from Cav3.2 KO led us to examine the role of Cav3.2 in neurons in the GBM microenvironment as Cav3.2 is expressed in glutamatergic neurons. To elucidate the role of Cav3.2 in neurons, we isolated neurons from WT and Cav3.2 KO mice for co-culture experiments with GBM stem cells (GSCs). The co-culture of WT neurons with GSCs enhanced the proliferation index of the GSCs (Fig. 2-4A). The enhanced proliferation was abolished when the GSCs were co-cultured with neurons isolated from Cav3.2 KO mice (Fig. 2-4A). To demonstrate that the proliferation effect was coming specifically from the neurons we utilized tetrodotoxin (TTX) to inhibit the neuronal activity which abrogated the additive effect of WT neurons on GSC growth (Fig. 2-4A). Next, we assessed whether direct contact was necessary to attenuate the growth effect. To this end, we applied conditioned medium from WT and Cav3.2 KO neurons to GSCs and found that this mirrored the results of the co-culture experiments (Fig. 2-4B). We also assessed the connections between WT and Cav3.2 KO neurons with GSCs in co-culture and found that Cav3.2 KO neurons exhibited less projections toward GSC cells compared to WT neurons (Fig. 2-4C). We assessed neuron innervation in WT and Cav3.2 KO tumors which showed significant decrease in glutamatergic neurons (Vglut1) present in the Cav3.2 KO tumors compared to WT tumors (Fig. 2-4D). This observation is consistent with the single-cell Gene Ontology analysis which showed decreases in genes associated with axon guidance. To gain insight into how neurons affect GBM cells, we utilized CellChat to examine the ligand-receptor relationships between neurons and tumor cells. Examination of neurons-tumor showed decreased signaling associated with the glutamate pathway while upregulating GABA signaling in the Cav3.2 KO microenvironment (Fig. S2-5E, Fig. S2-6A-C). These data demonstrate the importance of neuronal Cav3.2 in regulating GSC growth as well as neuron/GBM connections.

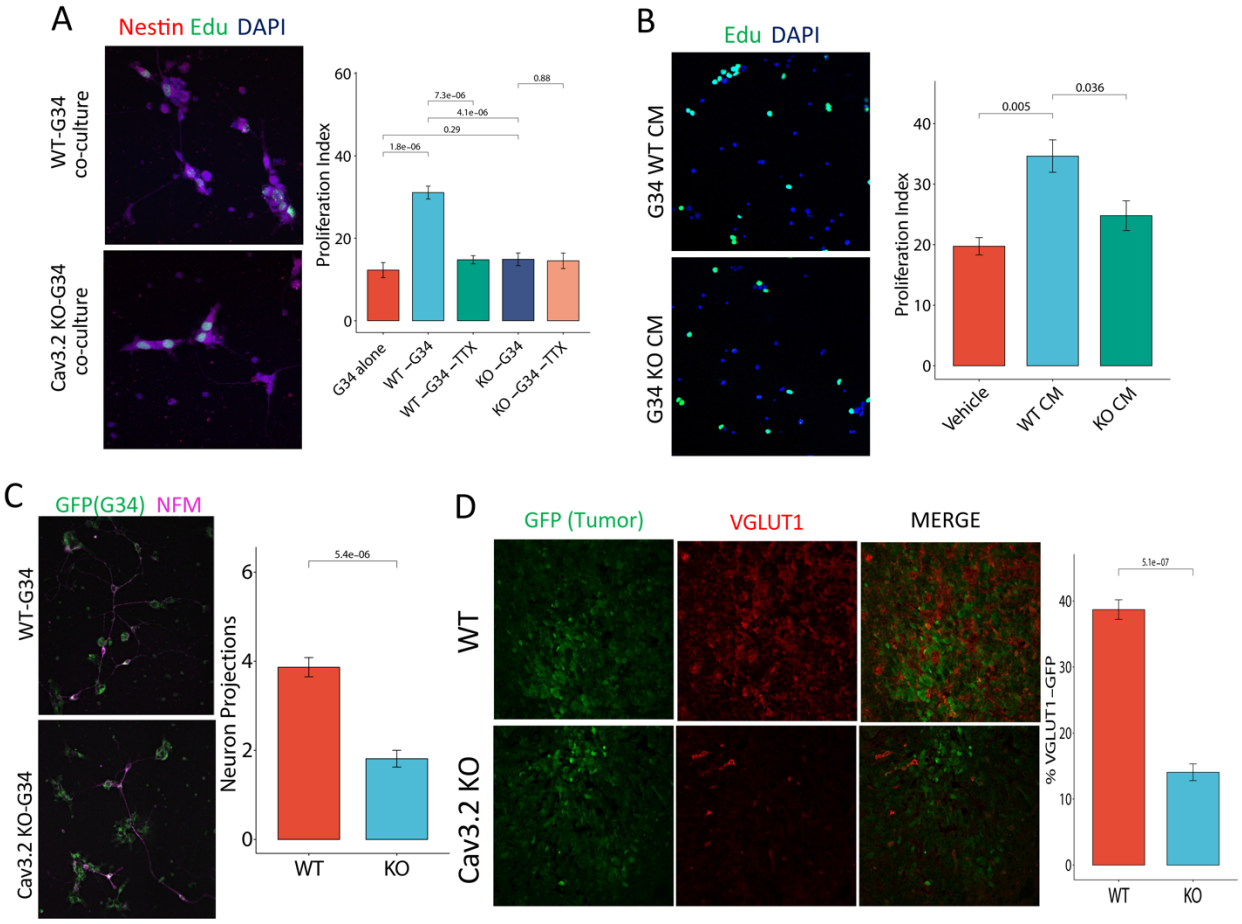

Figure 2-4: Neuronal Cav3.2 promotes GSCs growth and neuronal connections. A) Representative immunofluorescent images of Glioma Stem cells G34 (Red) co-cultured with WT and Cav3.2 KO neurons. Proliferative cells are labeled with EDU (Green) with quantification of proliferation index to the right. B) Representative immunofluorescent images of G34 cells subjected to WT and Cav3.2 KO Conditioned medium with quantification of proliferation index to the right. C) Representative immunofluorescent images of Glioma Stem cells G34-GFP (Green) co-cultured with WT and Cav3.2 KO neurons labeled with Neurofilament (Pink) with quantification of neuron projections to the right. D) Representative immunofluorescent staining of VGLUT1 (Red) in WT and Cav3.2 KO tumors (GFP) with quantification of percent VGLUT1-GFP positive cells on the right.

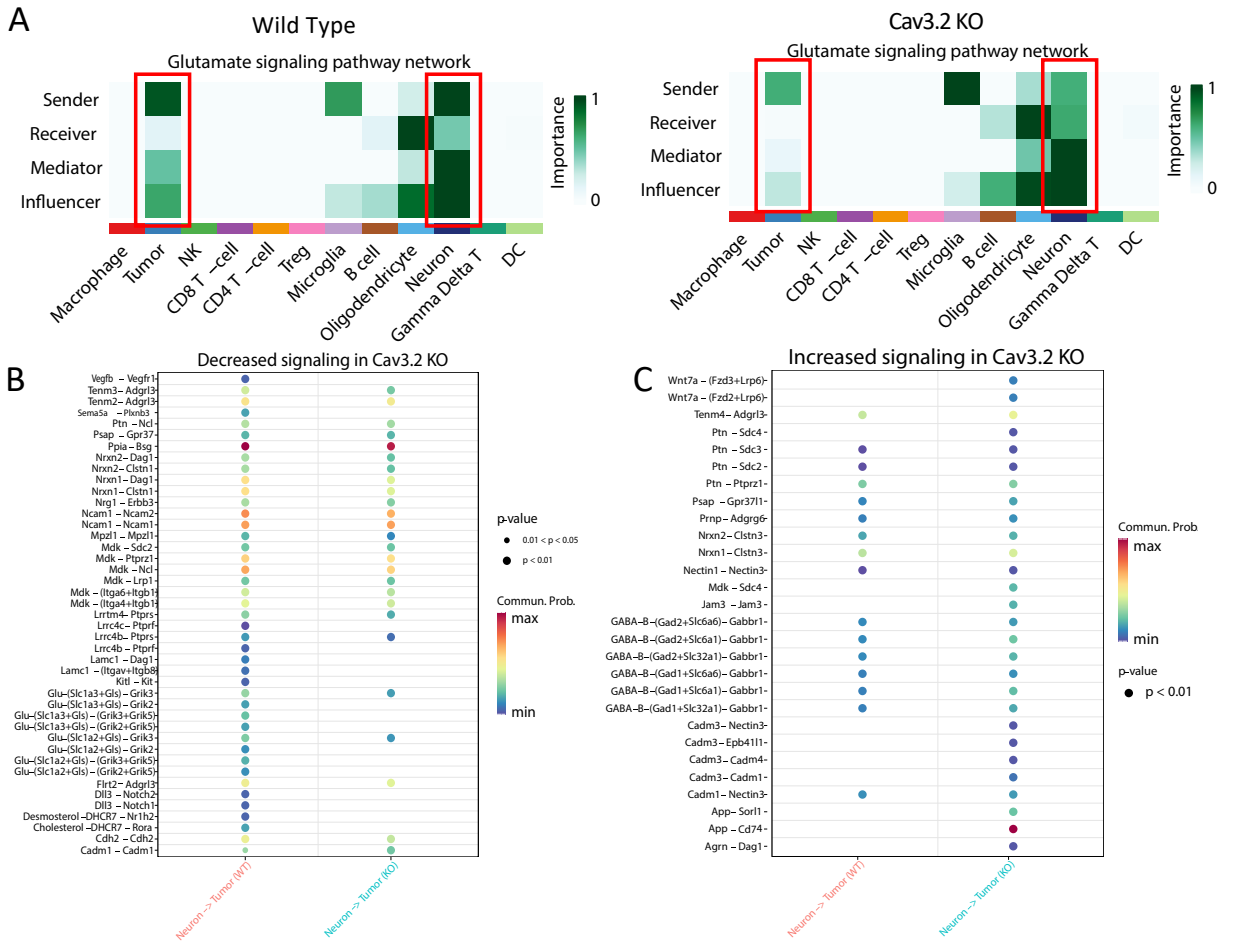

Figure S2-6: Glutamate signaling is altered in Cav3.2 KO. Microenvironmental Cav3.2 regulates glutamate release. A) Heatmap of Glutamate signaling pathway network in WT and Cav3.2 KO tumors showing a decrease in glutamate signaling in the Cav3.2 KO tumors and neurons. B) Analysis of decreased signaling pathways from neurons to tumors in WT and Cav3.2 KO. The red boxes highlight glutamate and neuron-related signaling pairs. C) Dotplot of increased signaling in Cav3.2 KO tumors from neurons to tumor cells.

Therapeutic targeting of both tumor intrinsic and microenvironment Cav3 inhibits GBM growth

We next assessed the therapeutic value of targeting tumor cell intrinsic and microenvironment Cav3 in GBM. We previously showed a role for tumor intrinsic Cav3.2 in promoting GBM growth using a xenograft model [114]. To validate and expand these findings, we used the RCAS/TVA mouse model to deliver shRNA for Cav3.1 and Cav3.2 to GBM tumors generated by implanting vector-infected chicken fibroblast cells (DF-1) into the SVZ of the XFM mouse model(*Ntv-a Ink4a-Arf-/- LPTEN*)[119]. Mice received DF-1 cells with RCAS-PDGFB, RCAS-Cre and either RCAS-Scrambled or RCAS-shCav3.1, RCAS-shCav3.2. We found a significant reduction in tumor volume as well as significantly prolonged survival of mice in which tumor Cav3 was knocked down as compared to control mice (Fig. S2-7A-D). We then assessed the effects of targeting both tumor intrinsic and microenvironment Cav3 on tumor growth using the repurposed FDA-approved Cav3 blocker mibefradil that blocks all three Cav3 isoforms in humans and mice [126]. We tested the effects of mibefradil in combination with GBM standard of care therapy consisting of temozolomide (TMZ) and radiation. GSCs were stereotactically implanted into the striata of immunodeficient mice [98]. Six days after implantation mibefradil (24 mg/kg body weight) was administered by oral gavage every 6 hours for 5 days. TMZ (100 mg/kg body weight) was concurrently administrated via IP injection once a day for 4 days. Radiation (70 cGy) was administered in a small animal irradiator (Rad Source RS-2000) once a day for 4 days. MRI scans were performed 18 days after surgery and tumor volume was assessed. The effect of mibefradil alone significantly reduced tumor volume compared to control (Fig. 2-5 A,B). The triple combination of mibefradil with temozolomide and radiation significantly reduced tumor volume compared to the TMZ/radiation only group suggesting

mibefradil gives an additive effect (Fig. 2-5 A,B). These data suggest that the inhibition of Cav3 in the microenvironment and in tumors enhances standard of care GBM therapy.

The therapeutic effects of targeting Cav3 are associated with inhibition of neuronal processes

To confirm that the therapeutic effects of Cav3 inhibition are associated with the alteration of neuronal processes, we treated GSCs with mibefradil and performed RNA-sequencing. Mibefradil treatment downregulated key neuronal genes such as Synpo, Syn1, Vgf, Sema7a, Nxph4 (Fig. 2-5C). Analysis of differentially expressed genes revealed enrichment of biological processes associated with neuronal processes such as glutamatergic synapse, postsynaptic density and neuron-to-neuron synapse (Fig. 2-5D). The mibefradil data gave a similar effect as the Cav3.2 KO single-cell RNA-seq data in downregulating genes associated with neuronal processes. We also analyzed TCGA data and found that Cav3 are co-expressed with genes associated neuronal processes such as axon Sema6a, Sema6c, Plxna2, Kcnc1, Grin2b, Shank2, Shank3, which are associated with neuronal processes such as axon guidance, synapse organization, neuron project and ionotropic glutamate receptor binding (Fig. S2-8A,B). We also analyzed publicly available single-cell RNA-seq [21] and found that Cav3.2 is enriched in NPC-like GBM cells (Fig. S2-8C). We also found that Cav3.2 are enriched in the developmental transcriptional signatures compared to injury response signatures within the Rchards dataset (Fig. S2-8D), which is important as the developmental signatures are more likely to interact with the neurons [124]. Additionally, analysis of publicly available spatial transcriptomic data of GBM shows enrichments of Cav3 in the NPC cell state and neuronal development spatial transcriptional program (Fig. S2-8e) [122]. The above data

demonstrate that Cav3 are co-expressed with neuronal genes and that the inhibition of Cav3 with mibefradil downregulates genes important for neuron-GBM processes.

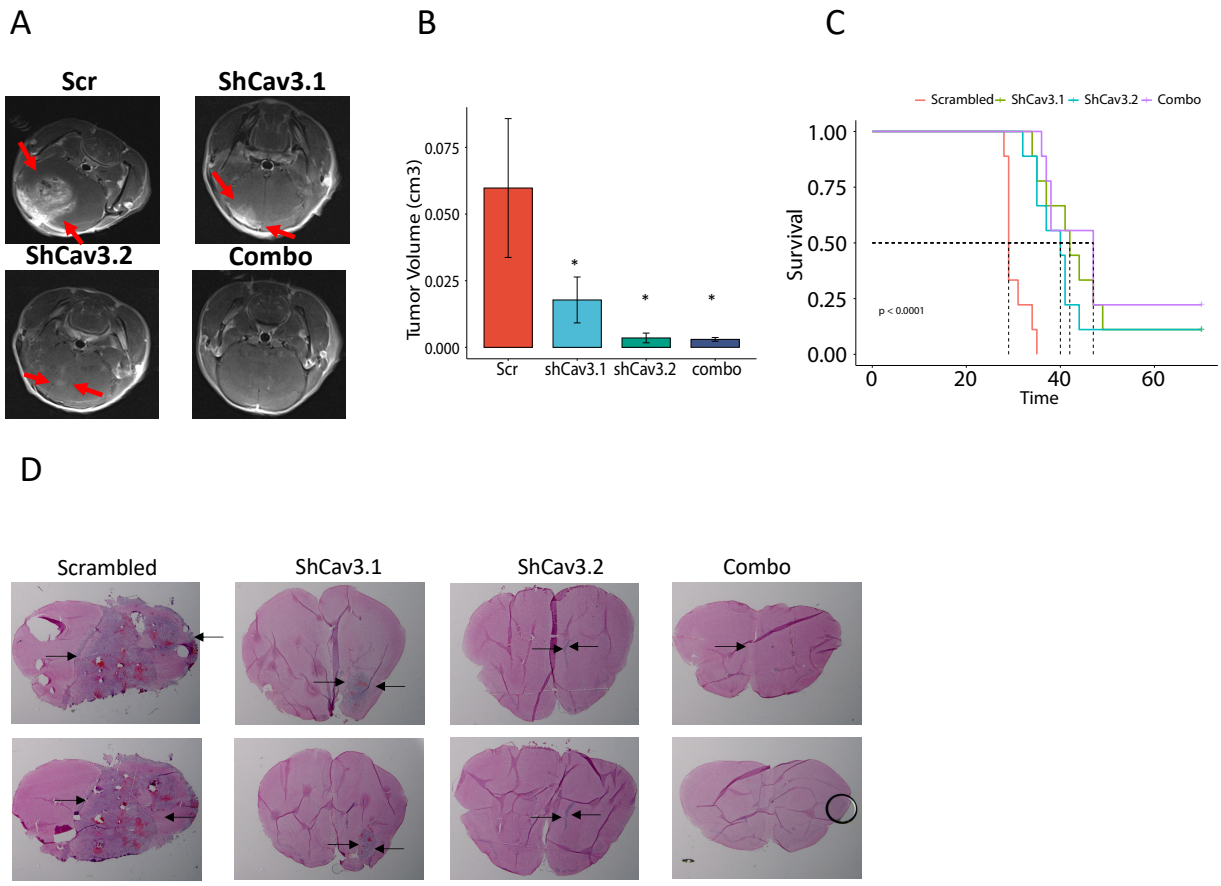

Figure S2-7:Silencing of TTCC in RCAS/TVA mouse inhibits GBM growth and prolongs mouse survival. A) Representative MRI of RCAS/TVA mouse models with Scr, ShCav3.1, Sh-Cav3.2, Combo [127]. B) Quantification of tumor volume in the RCAS/TVA mouse model. C) Kaplan Meier survival curves of the RCAS/TVA mouse model. D) H&E staining of RCAS/TVA mouse model for Control group, shCav3.1, shCav3.2 and combo (shCav3.1+ shCav3.2).

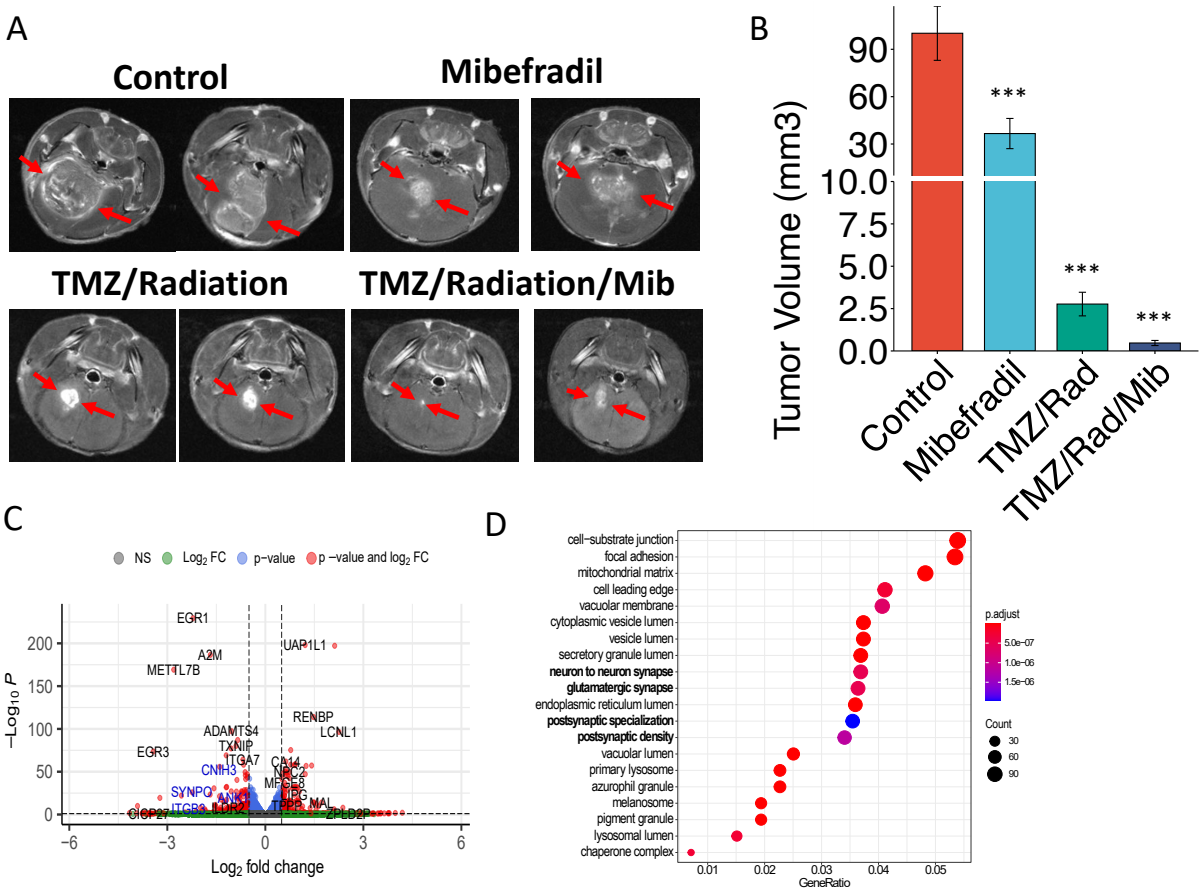

Figure 2-5: Mibefradil synergizes with standard of care to reduce tumor volume and downregulate neuronal processes. A) Representative MRIs of Vehicle, Mibefradil, TMZ + Radiation, Mibefradil + TMZ+ Radiation. B) Quantification of tumor volume. C) Volcano plot of the differentially expressed genes from GSCs treated with mibefradil. D) Dotplot of the Gene ontology Biological Pathway for the deregulated genes upon GSC treatment. ***<0.001

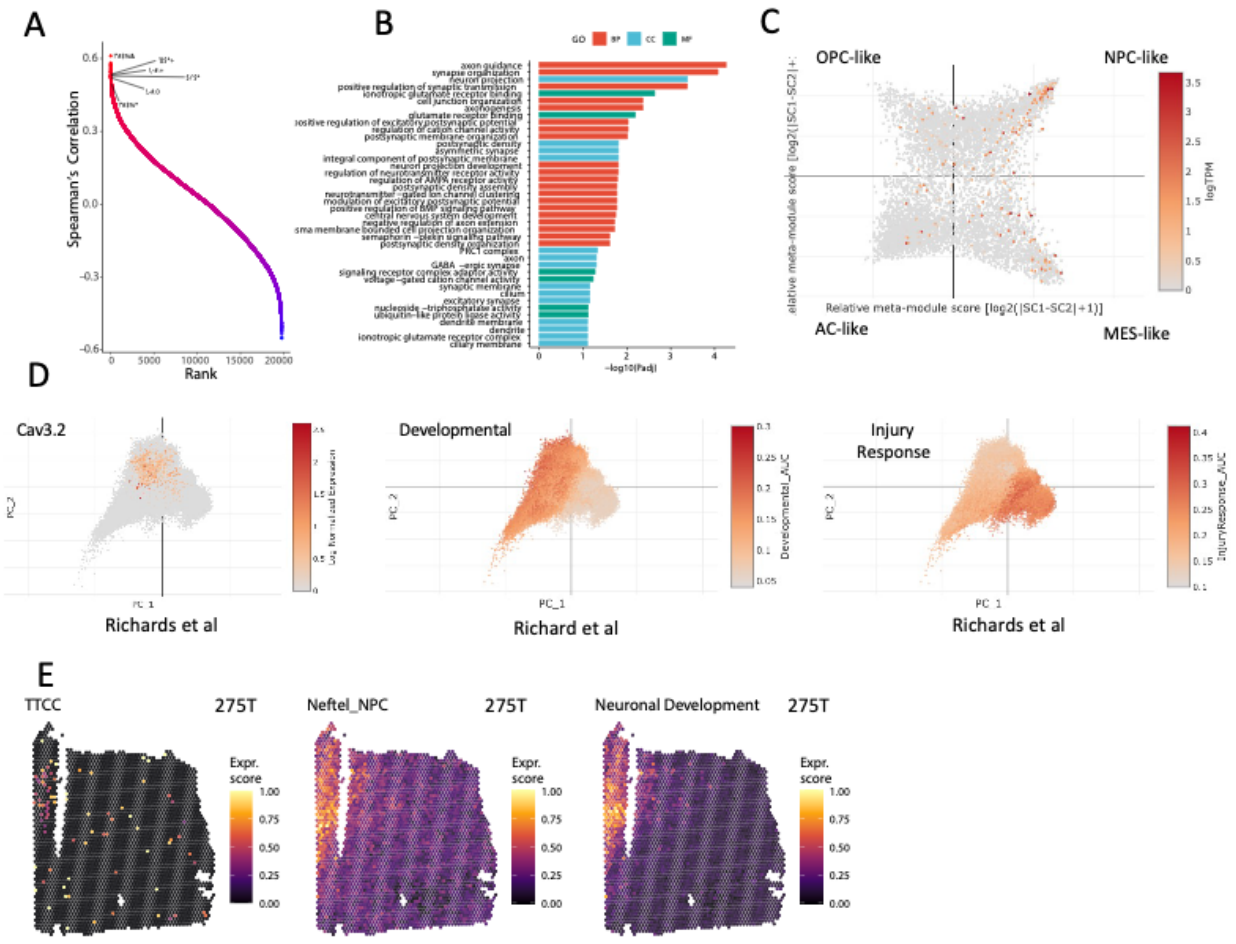

Figure S2-8:T-type calcium channels are co-expressed with neuronal genes and processes. T-type calcium channels are expressed with neuronal genes. A) Spearmen correlation top genes correlated with Cav3.2 within GBM TCGA dataset. B) Gene ontology of Biological pathways (BP), Cellular Compartment [80], Molecular Function (MF) of the top positive correlated genes with Cav3.2 in GBM TCGA dataset. C) Expression of Cav3.2 in Neftel dataset showing enrichment within NPC-like cells. D) Expression of Cav3.2 (Left) in the Richards dataset which overlaps with Developmental cells (middle) compared to injury response (right). E) Expression scores of spatial transcriptomics 275T tumor of T-type calcium channels (Left), Neftel NPC (Middle), Neuronal Developmental Signature (Right).

2.7.0 Discussion

Cell state is important for receiving signals from the microenvironment with the NPC/OPC cell states previously shown to form synaptic connections with tumors promoting growth and infiltration [103]. GBM tumor microtubules, which have been shown to connect to neurons, are more resistant to chemotherapy and radiation [128, 129]. Patients with high neural signatures exhibit decreased overall survival and progression-free survival in GBM and high-grade gliomas [104]. The mechanism of neuron-tumor interaction is still understudied and requires further elucidation of both the neurons and tumors. Cav3 are expressed in glutamatergic neurons and regulate glutamate release as well as glutamate receptor plasticity [65]. Our study aimed to elucidate the role of Cav3 in the microenvironment and its effects on tumor growth.

We investigated the role of Cav3.2 in the GBM microenvironment by first utilizing whole body knockout mice which revealed that loss of Cav3.2 the microenvironment inhibited tumor growth, proliferation and increased survival. To gain insight into the mechanism of inhibition of tumor growth we performed single-cell RNA-sequencing, which revealed that loss of Cav3.2 in the microenvironment decreased expression of genes associated with neuronal and glial processes such as gliogenesis, axon guidance and regulation of synapse organization. Among the downregulated genes were genes associated with regulating the OPC cell state such as Sox10 and Olig2 which had decreased regulon activity in Cav3.2 KO tumors. Sox10 is a transcription factor that is involved in development by shifting neural crest cells toward oligodendrocyte precursor cells [130, 131]. In glioma Sox10, has been shown to induce gliomagenesis, regulate oligodendrocyte lineage and suppress astrocyte lineage [132, 133]. Sox10 has also been identified as a master regulator of the RTK1 epigenetic subtype which is associated with proneural

signatures and loss of Sox10 shifts GBM cells towards a mesenchymal-like state [134]. Microenvironmental Cav3.2 regulating OPC cell state as well as neuronal and glial processes points toward its role in regulating tumor connections to neurons. To validate these findings, we examined the role of neuronal Cav3.2 using neuron/GBM co-cultures and found that loss of Cav3.2 in the neurons led to a significant decrease of GSC proliferation in co-cultures as well as in conditioned media from neurons. Additionally, Cav3.2 KO neurons exhibited fewer neuronal projections towards GSCs. Additionally, Cav3.2 KO tumors showed less glutamatergic neuron innervation compared to WT tumors. Analysis of the single-cell RNA-seq data with CellChat, which is used to infer cell-cell communication, showed that in the Cav3.2 KO microenvironment neuron-tumor communication is associated with a decrease in glutamatergic signaling and an increase in GABAergic signaling, which can inhibit glioma growth [135].

By analyzing publicly available single-cell and spatial transcriptomic datasets we also found that Cav3 are enriched in NPC-like and OPC-like cell states as well as neurodevelopmental transcriptional signatures. Additionally, Cav3 was positively correlated with genes associated with neuronal processes. The inhibition of Cav3 downregulated neuronal-associated genes specifically for processes associated with synapse formation and communication. The combination of mibefradil, temozolomide and radiation significantly decreased tumor volume compared to TMZ/radiation alone, presumably via the inhibition of both tumor intrinsic and microenvironment Cav3. These data support the use of mibefradil to complement standard GBM therapies and warrant testing this combination in clinical trials. The Cav3 inhibitor mibefradil has been examined in clinical trials in recurrent gliomas demonstrating safety and potential activity in combination with temozolomide [136]. Mibefradil was also assessed in a clinical trial in combination with radiation therapy in recurrent GBM patients which demonstrated safety

and potential activity with radiation therapy [137]. Recent studies have modified mibefradil to improve the drug to create better radiosensitizers for treatment of GBM [117]. Our data along with the clinical trial data suggest that a phase 2 trials in newly diagnosed GBM patients is warranted.

In conclusion, our results represent the first characterization of Cav3.2 in the GBM microenvironment. Microenvironment Cav3.2 promotes GBM growth, proliferation and decreased survival. Microenvironmental Cav3.2. regulates GBM neuronal and glial cell processes and regulates OPC cell state within the tumor through Sox10. Neuronal Cav3.2 promotes glioma stem cell proliferation and neuronal connections. Within GBM tumors Cav3 channels are enriched in neurodevelopmental transcriptional states and correlated with neuronal genes. Blockage of Cav3 enhances the effects of standard GBM therapies most likely by altering tumor intrinsic as well as microenvironmental factors, supporting evaluation of mibefradil in future clinical trials.

2.8.0 Authorship, Data Availability, Conflict of Interest, Funding

Authorship: Designing research studies: CD and RA. Conducting experiments and acquiring data: CD, YZ, SS, ML, MG, ME, KH, DW, PM, UY, YS, EX, AS, BK, FH, FG, AV. Analyzing Data: CD, RA. Conceptual input: CD, RA, MKP, DS, HZ, BP, SS HS. Writing manuscript: CD and RA. Reviewing and editing of manuscript: All authors

Data Availability: Single-cell RNA-sequencing data has been deposited in the NCBI Gene Expression Omnibus (Geo) under accession number GSE273629. Bulk RNA-seq is accessible under GSE95106.

Conflict of Interest: The authors have declared that no conflicts of interest exist

Funding: Supported by NIH/NINDS RO1 NS122222, NIH/NCI UO1 CA220841, NIH/NINDS 1R21NS122136, NCI Cancer Center Support Grant P30CA044579, a University of Virginia Comprehensive Cancer Center Pilot Grant, a Schiff Foundation grant (all to R.A.). NCI 5T32CA009109-47 Grant and Parson Weber Parsons Fellowship (C.J.D). Support was also provided by the University of Virginia Advanced Microscopy Core Facility and Molecular Imaging Core

Chapter 3- T-type calcium channels regulate medulloblastoma and can be targeted for therapy[+]

Collin J. Dube[1], Michelle Lai[1], Ying Zhang[1], Shekhar Saha[1], Ulas Yener[2], Farina Hanif[1,3], Kadie Hudson[1], Myron K Gibert Jr[1], Pawel Marcinkiewicz[1], Yunan Sun[1], Tanvika Vegiraju[1], Esther Xu[1], Aditya Sorot[1], Rosa I. Gallagher[6], Julia D Wulfkuhle[6], Ashley Vernon[1], Lily Dell'Olio[1], Rajitha Anbu[1], Elizabeth Mulcahy[1], Benjamin Kefas[4], Fadila Guessous[5], Emanuel F. Petricoin[6], Roger Abounader[1,7,8*]

[1]Department of Microbiology, Immunology & Cancer Biology, University of Virginia, Charlottesville, VA 22908, USA.

[2]Department of Neurosurgery, Stanford University School of Medicine, Stanford, California, USA.

[3]Department of Biochemistry, Dow International Medical College, Dow University of Health Sciences, Karachi, 75270, Pakistan.

[4]Department of Pharmacy, University of Virginia, Charlottesville, VA 22908, USA.

[5]Laboratory of Onco-Pathology, Biology and Cancer Environment, Faculty of Medicine, Mohammed VI University of Sciences and Health, Casablanca, Morocco

[6]George Mason University Center for Applied Proteomics and Molecular Medicine, Manassas, VA 20155, USA

[7]University of Virginia Department of Neurology, Charlottesville, VA 22908, USA

[8]University of Virginia Comprehensive Cancer Center, Charlottesville, VA 22908, USA.

* Corresponding author: Roger Abounader, University of Virginia, PO Box 800168, Charlottesville VA 22908, USA, Phone: (434) 982-6634, ra6u@virginia.edu

[+]Adapted from Dube, C. J., Lai, M., Zhang, Y., Saha, S., Yener, U., Hanif, F., ... & Abounader, R. (2025). T-type calcium channels regulate medulloblastoma and can be targeted for therapy. *Journal of Neuro-Oncology*, 1-10.

3.1.0 Abstract

Purpose: The goal of this study was to investigate the role and therapeutic targeting of T-type calcium channels in medulloblastoma, a common and deadly pediatric brain tumor that arises in the cerebellum.

Methods: T-type calcium channel expression was assessed in publicly available bulk and single-cell RNA-seq datasets. The effects of T-type calcium channel blocker mibefradil on cell growth, death and invasion were assessed with cell counting, alamar blue, trypan blue and transwell assays. Proteomic-based drug target and signaling pathway mapping was performed with Reverse Phase Protein Arrays [84]. Co-expression modules of single-cell RNA-seq data were generated using high dimensional weighted gene co-expression network analysis (hdWGCNA). Orthotopic xenografts were used for therapeutic studies with the T-Type calcium channel blocker mibefradil.

Results: T-type calcium channels were upregulated in more than 30% of medulloblastoma tumors and patients with high expression associated with a worse prognosis. T-type calcium channels had variable expression across all the subgroups of medulloblastoma at the bulk RNA-seq and single-cell RNA-seq level. Mibefradil treatment or siRNA mediated silencing of T-type calcium channels inhibited tumor cell growth, viability and invasion. RPPA-based protein/phosphoprotein signal pathway activation mapping of T-type calcium channel inhibition and single-cell hdWGCNA identified altered cancer signaling pathways. Oral administration of mibefradil inhibited medulloblastoma xenograft growth and prolonged animal survival.

Conclusion: Our results represent a first comprehensive multi-omic characterization of T-type calcium channels in medulloblastoma and provide preclinical data for repurposing mibefradil as a treatment strategy for these relatively common pediatric brain tumors.

3.2.0 Introduction

Medulloblastoma is a CNS tumor that arises in the cerebellum, primarily in pediatric patients[138, 139]. The 5-year survival rate for pediatric medulloblastoma patients is ~ 70%[138]. Patients often experience permanent neurological deficits such as reduced motor and cognitive functions as a result of radiation and chemotherapy [23, 24]. Medulloblastoma is classified into four molecular subgroups: SHH, WNT, Group 3 and Group 4[2, 27, 28]. SHH and WNT have a better prognosis than Group 3 and Group 4. Current treatment options for medulloblastoma include surgical resection and radio and chemotherapy but patients frequently experience permanent neurological deficits such as reduced motor and cognitive functions, reducing their overall quality of life [140-142].

T-type calcium channels are voltage gated channels that are active around resting membrane potential. They channel calcium from the extracellular space into the cell. Calcium signaling regulates numerous important cellular processes such as proliferation, migration, invasion and apoptosis[143, 144]. T-type calcium channels are deregulated in some cancers including colon carcinoma, breast cancer and gliomas[114, 145-147]. Inhibition of T-type calcium channels with the selective inhibitor mibefradil has shown significant anti-tumor effects in gliomas in preclinical models [114-116]. These studies formed the foundation for a Phase 1 clinical trial of mibefradil with temozolomide in recurrent glioma patients. The trial showed that mibefradil was safe with minimal side effects and elicited responses in select patients[136]. However, a comprehensive study of the expression, functions and therapeutic targeting of T-type calcium channels in medulloblastoma has, to our best knowledge, not been published to date.

This study aimed to elucidate the role of T-type calcium channels in medulloblastoma using a multi-omic approach incorporating transcriptomic, proteomic/phospho-proteomics, coupled to functional analyses, and experimental therapy. We hypothesized that T-type calcium channels act as oncogenes to promote medulloblastoma malignancy parameters. We analyzed publicly available data and found that T-type calcium channels are upregulated in medulloblastoma tumors and that expression correlates with patient survival. Inhibition of T-type calcium channels with mibefradil significantly reduced medulloblastoma cell growth and invasion. Additionally, mibefradil significantly reduced tumor volume in vivo and prolonged animal survival. Mechanistically, we demonstrated that inhibition of T-type calcium channels regulates numerous cellular pathways such as cell proliferation and apoptosis. Also, T-type calcium channels are co-expressed in gene modules regulating numerous cellular pathways in medulloblastoma tumors. This is the first study elucidating the roles and therapeutic targeting of T-type calcium channels in medulloblastoma.

3.3.0 Methods

Cell Lines. Three medulloblastoma cell lines were used in this study. PFSK, DAOY and ONS-76 were grown in RPMI-1640 media supplemented with 10% FBS. All cells were cultured in media in a 37 °C incubator with 5% CO_2 and 20% O_2. All cell lines underwent testing for species identity and mycoplasma infection using Mycoplasma Detection Kit-QuickTest.

Pediatric Brain Tumor Atlas analysis. Pediatric Brain Tumor Atlas data was downloaded from PedCbioPortal [148, 149]. Medulloblastoma tumors were sub-setted for analysis of the expression of the T-type calcium channels. Oncoplots of mutational

status and survival curves of T-type calcium channels were generated using pedcbioportal.com with RNA-expression z-scores set to 2.0.

Single-cell RNA seq analysis. The count matrix from a published dataset (GSE155446)[150] was analyzed using the Seurat (v5) package in R (v3.4.1). The dataset underwent standard preprocessing using Seurat. Cell type categorization was conducted using the annotations published alongside GSE155446. T-type calcium channels were sub-setted for > 0 for plotting the violin plots.

hdWGCNA. Identification of co-expressed genes within tumor cells was carried out using hdWGCNA (v0.2.23)[125]. Meta cells were constructed using harmony dimensionality reduction. Modules were identified using the ConstructNetwork function below the optimal soft threshold. To identify module feature genes, ModuleEigenees function was used followed by computing of the module connectivity to identify hub genes with ModuleConnectivity functions. FindDME function was used to identify differentially expressed module eigengenes between cells that express Cav3.1 or Cav3.2 vs cells that had no expression. Pathway enrichment analysis of gene modules was performed using enrichR (v3.2).

Transfection. Cells were transfected with either 30 nM of a scrambled negative control (Thermofisher #AM4635) or 30 nM of a siRNA for Cav3.2 (ThermoFisher #AM16708) using RNAiMax reagent. Cells were harvested 48 hours post-transfection for various analyses, including RNA isolation, cDNA synthesis, qPCR, or functional assays.

Cell death and proliferation assays. Medulloblastoma cell lines were either drug treated (mibefradil 1-10 μM) or transfected with siRNA for Cav3.2. Cell death was

assessed by trypan blue assay. The Alamar Blue assay which measures cell viability was utilized according to the manufacturer's instruction. Cell proliferation was assessed by cell counting for five days as previously described [114, 151, 152]. All experiments were performed three times.

Invasion Assay. Medulloblastoma cell lines were either drug treated (mibefradil 10 μM) or transfected with siRNA for Cav3.2. After 72 hours cells were seeded at 100,000 cells per chamber in 0.01% FBS media in collagen IV coated chambers. The chambers were incubated in complete media with 10% FBS in 24 well plate in triplicates. After 8 hours of incubation the chambers were gently rinsed with PBS and stained with 0.1% crystal violet solution in 20% methanol. Chambers were imaged on Evos XL Core microscope. The images were quantified with ImageJ software [153].

Reverse Phase Protein Arrays. Proteomic screening was performed by Reverse Phase Protein Array [84] as previously described [154-156]. One hundred protein and phosphoprotein analytes were chosen for analysis based on their involvement in key aspects of tumor biology. All antibodies were validated as previously described [154-156]. For proteomic screening, ONS-76 and DAOY cells were treated with vehicle control or mibefradil 10 μM.

Immunoblotting. Immunoblotting was performed as previously described [157]. Antibodies used were Ki67 (ab16667), BAK (ab32371), BAD (ab32445), CDK2 (SC-163), HSP90 (SC-13119) and GAPDH (SC-166545).

In vivo experiments. Medulloblastoma DAOY cells ($3x10^5$) were stereotactically implanted into the cerebellum of immunodeficient mice (n= 7 per treatment group). Seven weeks after tumor implantation, the brains were scanned with magnetic resonance imaging on a 7 Tesla Bruker/Siemens ClinScan small animal MRI. After confirmation of tumor presence, the animals were randomized and treated with control (H_2O) or mibefradil (24 mg/kg) by oral gavage every 6 hours once a day for four days. Mice were treated for two cycles (Days 49-52, 55-58). Brains were scanned with magnetic resonance imaging [118] following treatment cycles. Tumor volumes were quantified using OsiriX Lite software. For survival studies mice were monitored carefully and sacrificed when they displayed symptoms of tumor distress including lethargy and head tilt.

Statistical analyses. Comparisons between means of samples were performed using Students t-tests and one-way ANOVA. All quantitative results are shown as means ± SEM. Molecular experiment tests, and computational experiment tests were performed using RStudio.

3.4.0 Results

T-type calcium channels are deregulated in medulloblastoma patient samples and expression correlates with survival

To determine expression of T-type calcium channels in medulloblastoma, we analyzed 121 medulloblastoma samples in the Pediatric Brain Tumor Atlas (PBTA)[148] and identified T-type calcium channels as amplified or upregulated in greater than 30% of patients (Figure 3-1A). This ranks T-type calcium channels as one of the most frequently deregulated genes in medulloblastoma. Patients with alterations in T-type calcium channels demonstrated a correlation toward worse survival compared to patients with no alteration of T-type calcium channels (Figure 3-1B). We examined expression of T-type

calcium channels across medulloblastoma subgroups in the Pediatric Brain Tumor Atlas and found high expression of T-type calcium channels across multiple subgroups (Figure 3-1C). We also examined expression of T-type calcium channels in medulloblastoma cell lines and found high expression of Cav3.2 in medulloblastoma cell lines (Figure 3-1D). We examined expression of T-type calcium channels in publicly available single-cell RNA-seq datasets and found that expression of Cav3.1 across all subtypes and Cav3.2 expression in SHH, Group 3 and Group 4 tumors (Figure 3-1E & F)[150]. Cav3.3 was examined in the dataset but there weren't enough positive cells to visualize them, so we focused primarily on Cav3.1 and Cav3.2. These data demonstrate that T-type calcium channels are upregulated in human medulloblastoma tumors and cell lines.

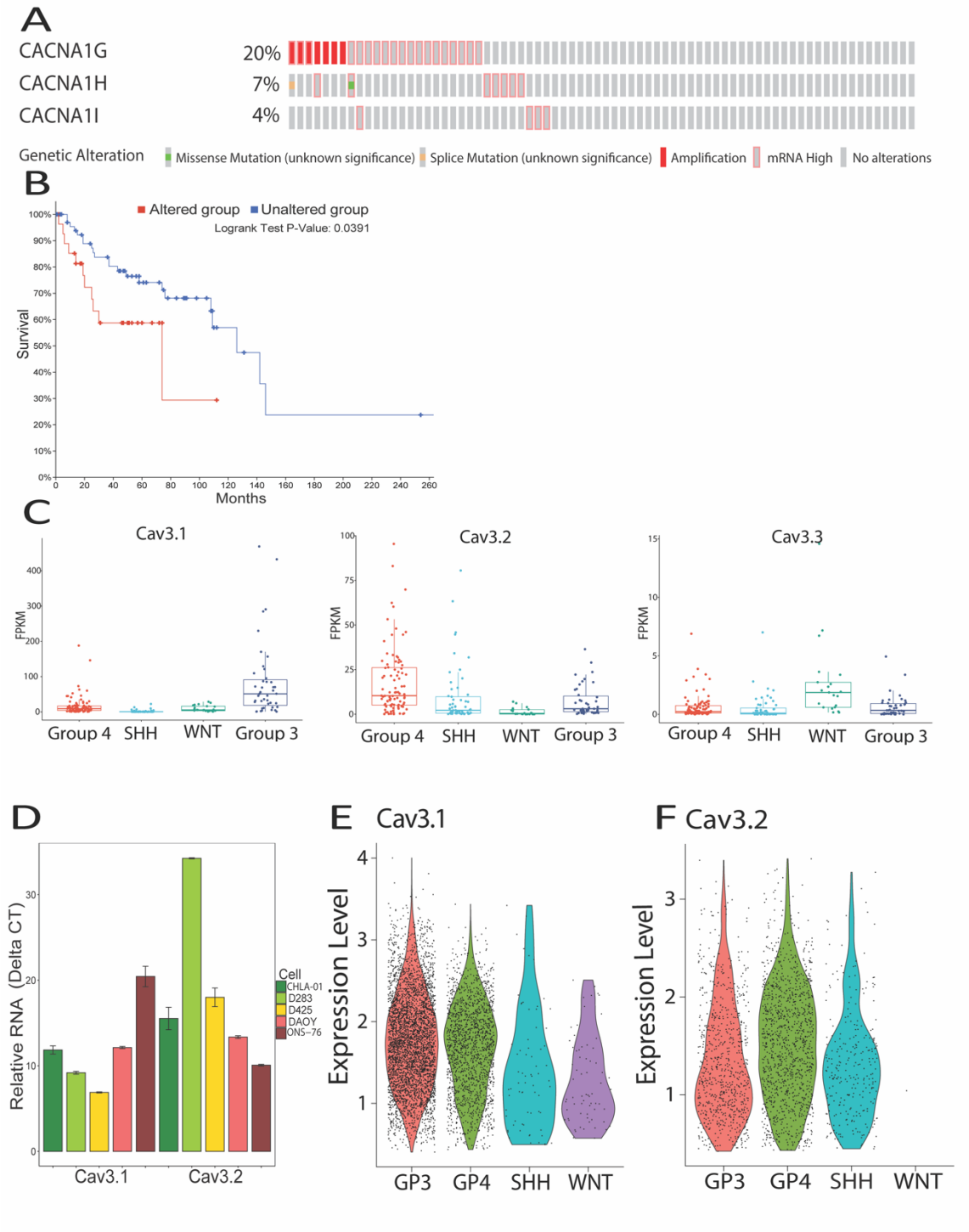

Figure 3-1: T-type calcium channels are dysregulated in medulloblastoma. A) Genetic dysregulation of T-type calcium channels in medulloblastoma samples of the Pediatric Brain Tumor Atlas (PBTA). B) Correlation of T-type calcium channel dysregulation with patient survival based on PBTA analysis. C) Analysis of T-type

calcium channel expression in subgroups from the Pediatric Brain Tumor Atlas (PBTA). D) Relative expression Cav3.1 and Cav3.2 expression in medulloblastoma cell lines via RT-qPCR. E & F) Violin plot showing expression of Cav3.1 and Cav3.2 in the different medulloblastoma subtypes in scRNA-seq data.

Single-cell high dimensional weighted gene co-expression network analysis (hdWGCNA) provides additional insights into the roles of T-type calcium channels in medulloblastoma

To gain further insight into the role of T-type calcium channels in medulloblastoma we performed single-cell high dimensional weighted gene co-expression network analysis (hdWGCNA) on publicly available single-cell RNA seq medulloblastoma tumors[150]. We focused on the malignant cells of each subgroup to identify the co-expression networks for each subgroup of medulloblastoma. We identified 6 unique co-expression modules for SHH, 8 co-expression modules for Group 3, 3 co-expression modules for Group 4 and didn't have enough statistical power to identify modules of the WNT subgroup.

To gain insight into which modules the T-type calcium channels are impacting, we performed Differential Module Eigengene (DME) analysis between cells expressing one of the T-type calcium channels and cells which didn't express them. We prioritized Cav3.1 and Cav3.2 since they are widely expressed in tumor cells, but we didn't have enough Cav3.3 positive cells for follow-up analysis. Within the Group 3 tumors, Module 2 was most upregulated in Cav3.1 positive tumors and Module 4 was most upregulated in Cav3.2 positive tumors (Figure 3-2A & B, Figure S3-1A-E). Interestingly the Cav3.1 and Cav3.2 positive cells exhibit opposite trends in their differential modules pointing toward different potential cell states between the Cav3.1 and Cav3.2 positive Group 3 tumors. We then performed Gene ontology pathway analysis to gain insight into what biological pathways were associated with the different modules. Module 2, which was upregulated in Cav3.1 positive tumors, was associated with biological processes related to histone methylation and microtubule movement (Figure 3-2A). Module 4 which was upregulated in Cav3.2 positive tumors was associated with biological processes related to negative

regulation of hippo signaling, regulation of secretion and regulation of synaptic vesicle pruning (Figure 3-2B).

We next examined the DME of Cav3.1 and Cav3.2 positive tumor cells in the SHH modules. Module 5 was the most upregulated module in Cav3.1 positive tumors whereas Module 2 was the most upregulated module in Cav3.2 positive tumors (Figure 3-2C & D, Figure S3-2A-E). We observed a similar trend in the SHH tumors where the Cav3.1 and Cav3.2 positive cells exhibited opposite regulation of their top modules. Analysis of biological pathways of Module 5 showed processes associated with neuronal functions such as synaptic localization and neurotransmitter transport (Figure 3-2C). The analysis of the biological pathways of Module 2 revealed processes associated with signaling pathways such as TOR and regulation of growth hormone receptors (Figure 3-2D). Analysis of Group 4 tumors identified three modules but no modules were differentially expressed between Cav3.1 and Cav3.2 positive tumor cells (Figure S3-3A-D). These data demonstrate that T-type calcium channels regulate numerous signaling pathways in the different subgroups of medulloblastoma.

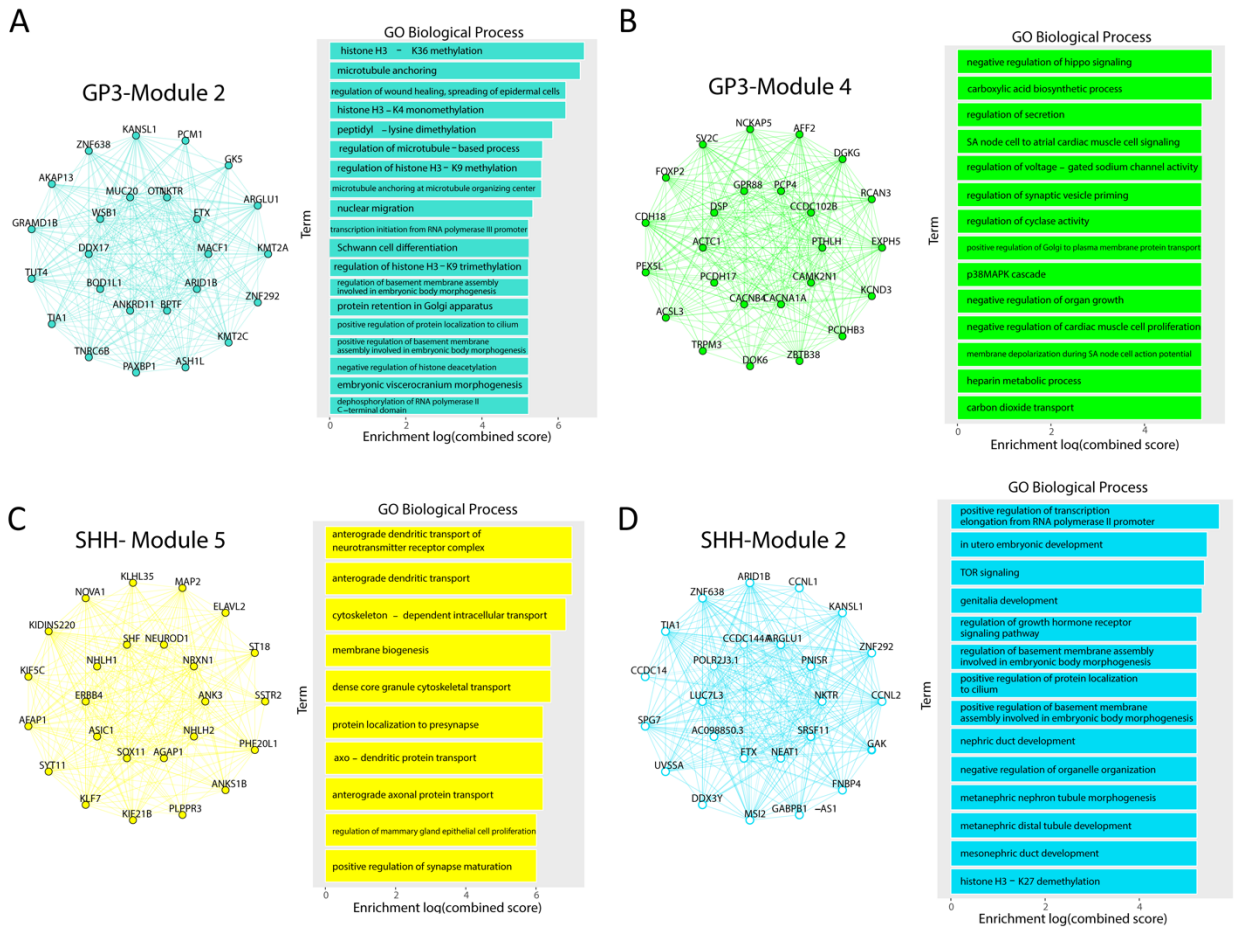

Figure 3-2: Cav3.1 and Cav3.2 are co-expressed with different pathways. A) Network plot of top differentially expressed module for Cav3.1 positive cells in Group 3 tumors and associated biological processes. B) Network plot of the top differentially expressed module for Cav3.2 positive cells in Group 3 tumors and associated biological processes. C) Network plot of the top differentially expressed module for Cav3.1 positive cells in SHH tumors and associated biological processes. D) Network plot of the top differentially expressed module for Cav3.2 positive cells in SHH tumors and associated biological processes.

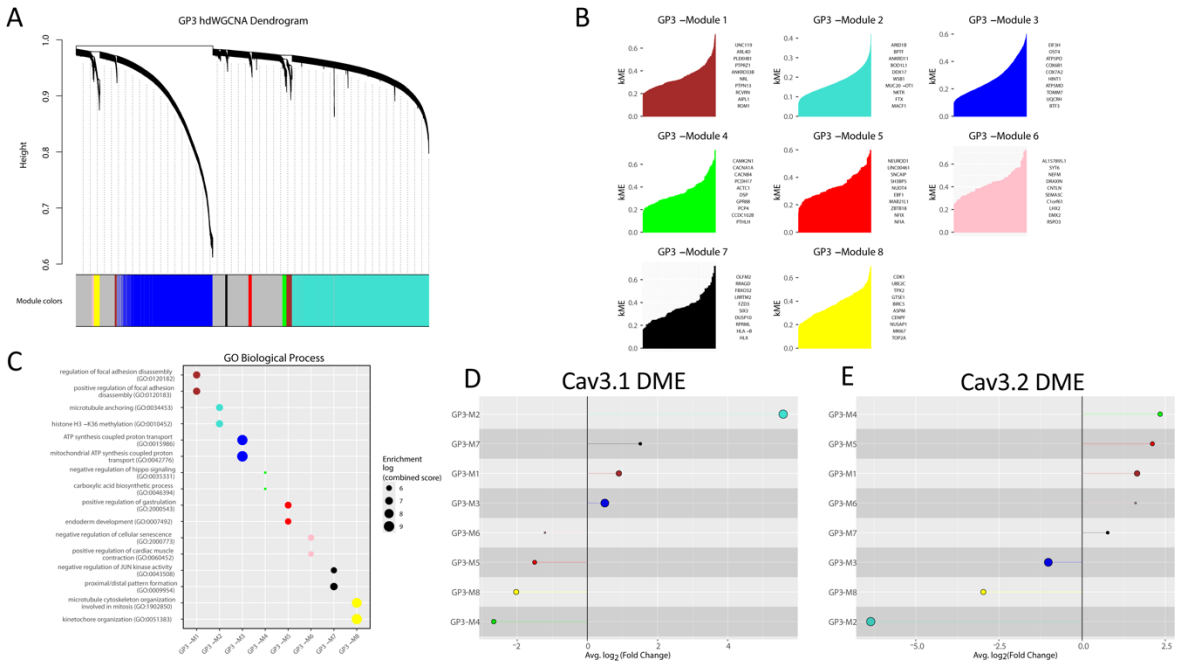

Figure S3-1: Co-expression data for Group 3 tumors. A) Dendogram of co-expression modules single Group 3 tumor cells. B) kME for the Group 3 modules identified in hdWGCNA. C) Gene ontology biological processes for each of the Group 3 modules. D) Lollipop plot of the DME of Cav3.1 positive cells in Group 3 tumors. E) Lollipop plot of the DME of Cav3.2 positive cells in Group 3 tumors

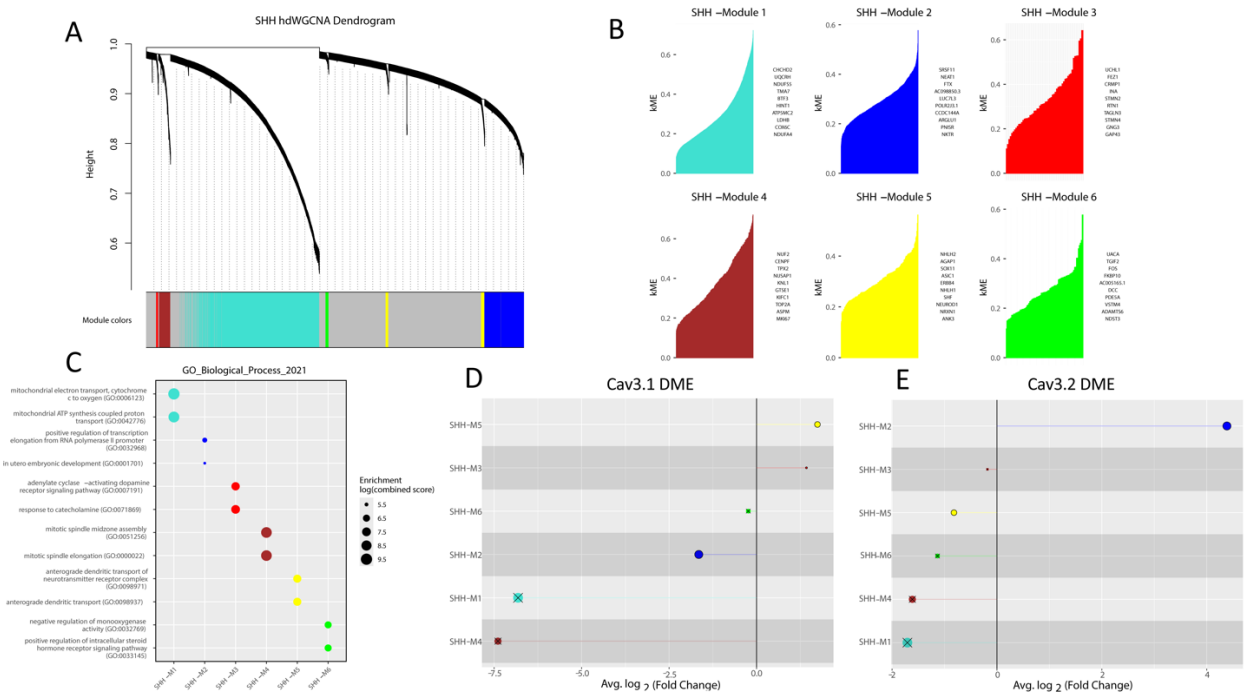

Figure S3-2: Co-expression data for SHH tumors. A) Dendogram of co-expression modules single SHH tumor cells. B) kME for the SHH modules identified in hdWGCNA. C) Gene ontology biological processes for each of the SHH modules. D) Lollipop plot of the DME of Cav3.1 positive cells in SHH tumors. E) Lollipop plot of the DME of Cav3.2 positive cells in SHH tumors

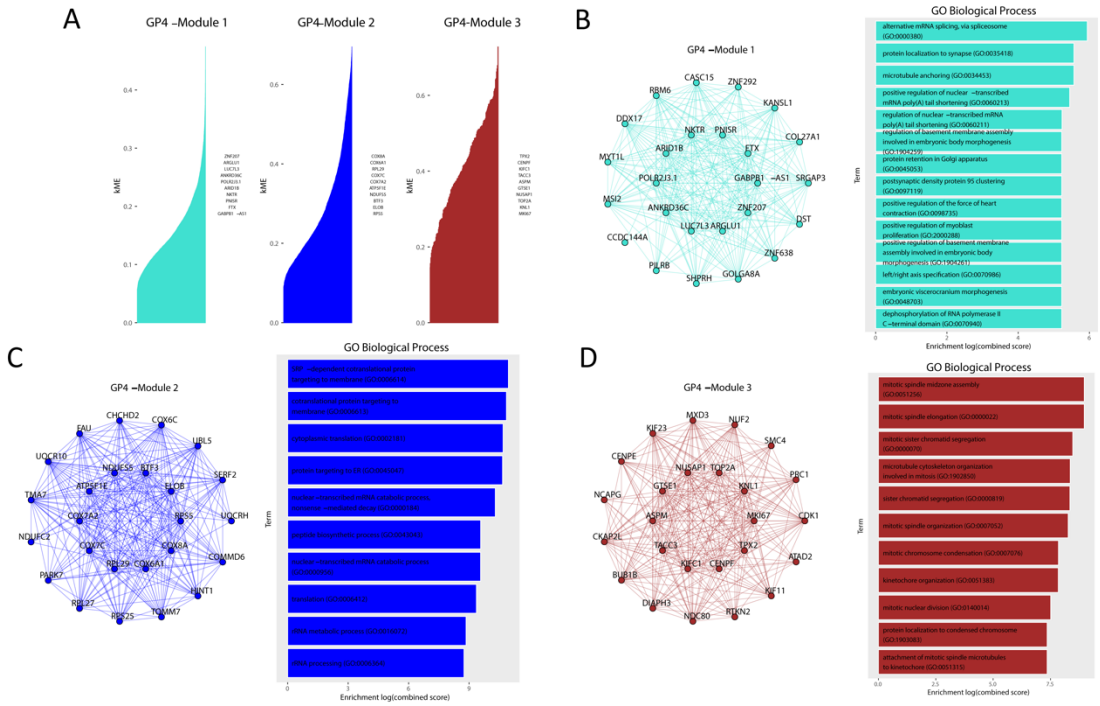

Figure S3-3: Co-expression data for Group 4 tumors. A) kME for the Group 4 modules identified in hdWGCNA. B) Network plot of top 25 genes in Group 4-M1 module and Gene ontology biological processes for the module. C) Network plot of top 25 genes in Group 4-M2 module and Gene ontology biological processes for the module. D) Network plot of top 25 genes in Group 4-M3 module and Gene ontology biological processes for the module.

Blockade of T-type calcium channels with mibefradil inhibits cell growth, invasion and induces cell death.

To examine the functional effects of blockage of T-type calcium channels on medulloblastoma, we utilized T-Type calcium channel blocker mibefradil to assess the effects of channel blockade on cell growth, invasion, proliferation and death. Medulloblastoma cell lines (PFSK, ONS-76, DAOY) were treated with vehicle or mibefradil (1-10 μM) and assessed for cell viability by alamar blue assay. The results demonstrate a dose dependent response to mibefradil inhibiting cell growth in all the medulloblastoma cell lines (Figure 3-3A, Figure S3-4A). To determine the effects of mibefradil on cell death, we treated medulloblastoma cell lines with vehicle or mibefradil and performed trypan blue assay, which showed significant cell death upon mibefradil treatment (Figure 3B, Figure S3-4B). To determine the effects of mibefradil on cell proliferation medulloblastoma cell lines were treated with mibefradil and counted over 5-7 days. Mibefradil significantly inhibited cell proliferation in all medulloblastoma cell lines (Figure 3-3C, Figure S3-4C). To determine if mibefradil impacts cell invasion we treated medulloblastoma cells as described above, then performed invasion assays. The results revealed that mibefradil significantly inhibited medulloblastoma invasion in all cell lines (Figure 3-3D). Altogether these data demonstrate that mibefradil is a strong inhibitor of medulloblastoma cell growth, viability and invasion.

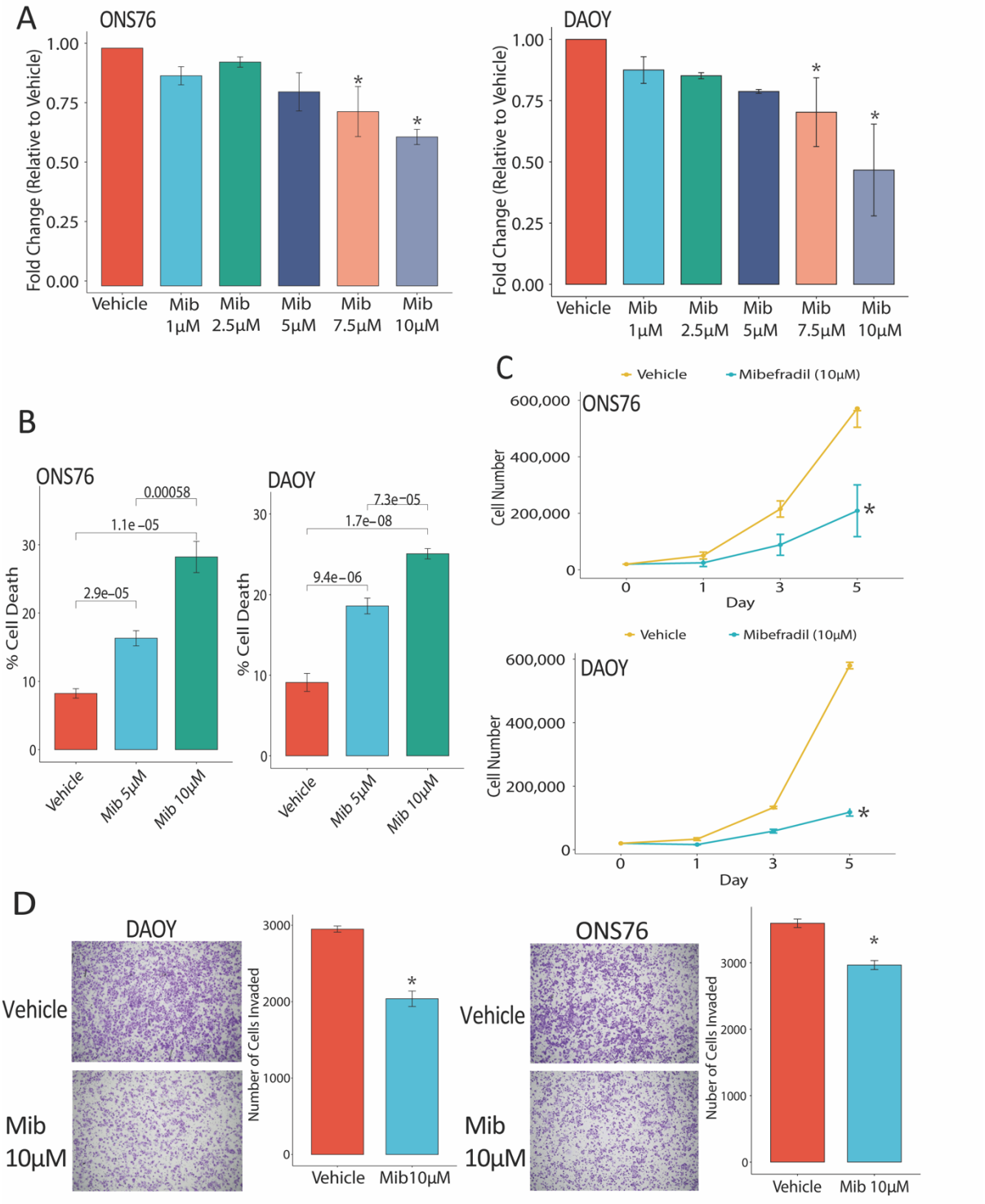

Figure 3-3: T-type calcium channel blocker mibefradil inhibits cell growth and induces cell death in medulloblastoma. A) ONS-76 and DAOY cells were treated with vehicle or mibefradil (1-10 μM) and assessed cell viability changes by alamar blue 72

hours later. B) ONS-76 and DAOY cells were treated with vehicle or mibefradil and cell viability was assessed 48 hrs later by trypan blue cell counting. C) Cell growth assay of vehicle and mibefradil treated cells (ONS-76. DAOY). D) Representative images of invaded cells and quantification of invasive cell number in vehicle and mibefradil treated cells. N=3 independent experiments for all assays. *p<0.05

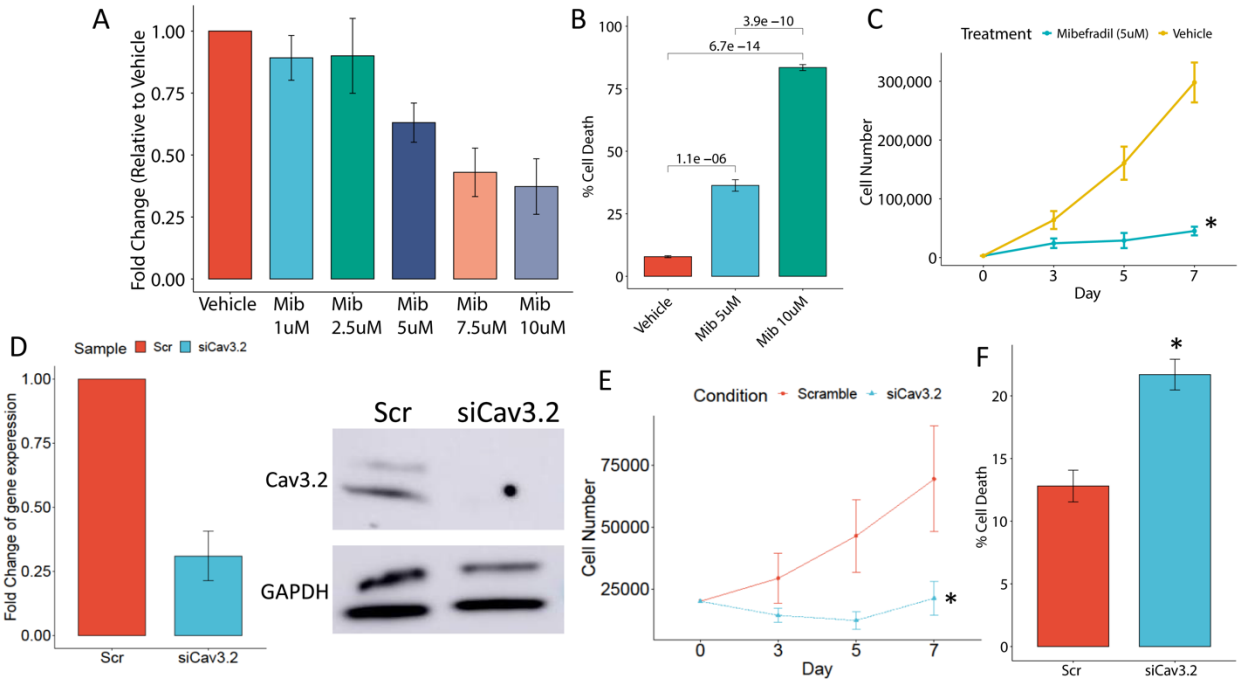

Figure S3-4: Mibefradil and siRNA mediated silencing of T-type calcium channels induces cell death and inhibits cell growth. A) PFSK cells were treated with vehicle or mibefradil (1-10 μM) and assessed for cell viability changes with Alamar Blue 48 hours later. B) PFSK cells were treated with vehicle or mibefradil and cell death was assessed 48hrs later by trypan blue cell counting. C) Cell growth assay of vehicle and mibefradil treated cell lines (PFSK). D) qPCR and western blot confirmation of Cav3.2 knockdown in ONS-76 cells. E) ONS-76 cells were transfected with Scrambled or siRNA for Cav3.2 and assessed for proliferation by cell counting over 7 days. F) Cell death was assessed by trypan blue assay. N=3 independent experiments for all assays *p<0.05

Silencing of Cav3.2 inhibits cell growth and induces cell death

To ascertain that mibefradil-induced cell death and growth suppression are specifically due to T-type calcium channel inhibition, we silenced Cav3.2 in medulloblastoma cells using siRNA and assessed cell death and growth. Cells were transfected with either a scrambled siRNA or siRNA for Cav3.2. Knockdown was confirmed by qPCR which demonstrated 75% knockdown, as well at the protein level via Western Blot (Figure S3-4D). Knockdown of Cav3.2 significantly inhibited cell growth (Figure S3-4E). To assess how silencing of Cav3.2 impacts cell death, we utilized trypan blue cell counting. Silencing of Cav3.2 significantly increased cell death compared to scrambled control (Figure S3-4F). These data demonstrate that gene silencing of Cav3.2 significantly impacts medulloblastoma cell growth and death, comparable to mibefradil.

Inhibition of T-type calcium channels induces apoptosis pathways and inhibits cell proliferation pathways

To investigate the mechanism of action of T-type calcium channels we treated medulloblastoma cells with mibefradil or vehicle control and performed RPPA on the resultant lysates. Mibefradil treatment significantly induced widespread changes in medulloblastoma signaling (Figure S3-5A). There were significant changes in the induction of apoptosis signaling activation of BAK and BAD (Figure 3-4A). Additionally, mibefradil treatment affected molecules associated with cell proliferation such as the decrease of CDK6, CDK2 and Ki67 (Figure 3-4B). These results were verified by immunoblotting (Figure 3-4C and Figure S3-5B). We also examined the overlap the

RPPA and hdWGCNA which revealed important regulators of medulloblastoma tumor signaling with 6 targets overlapping in SHH (Ephrin A3, FOXM1, Histone H2A, Ki67, Survivin and Synaptophysin), 12 overlapping targets in Group 3 (EGFR, FoxM1, Glucocorticoid receptor, Histone H2A, Ncam1, p38 MAP kinase, PTEN, CDK6, Ki67, LC3B, Survivin, and Twist) and 3 overlapping targets in Group 4 tumors (FoxM1, Ki67 and Survivin). The above data show that mibefradil inhibition of T-type calcium channel regulates medulloblastoma cell signaling including apoptosis and cell proliferation associated molecular events

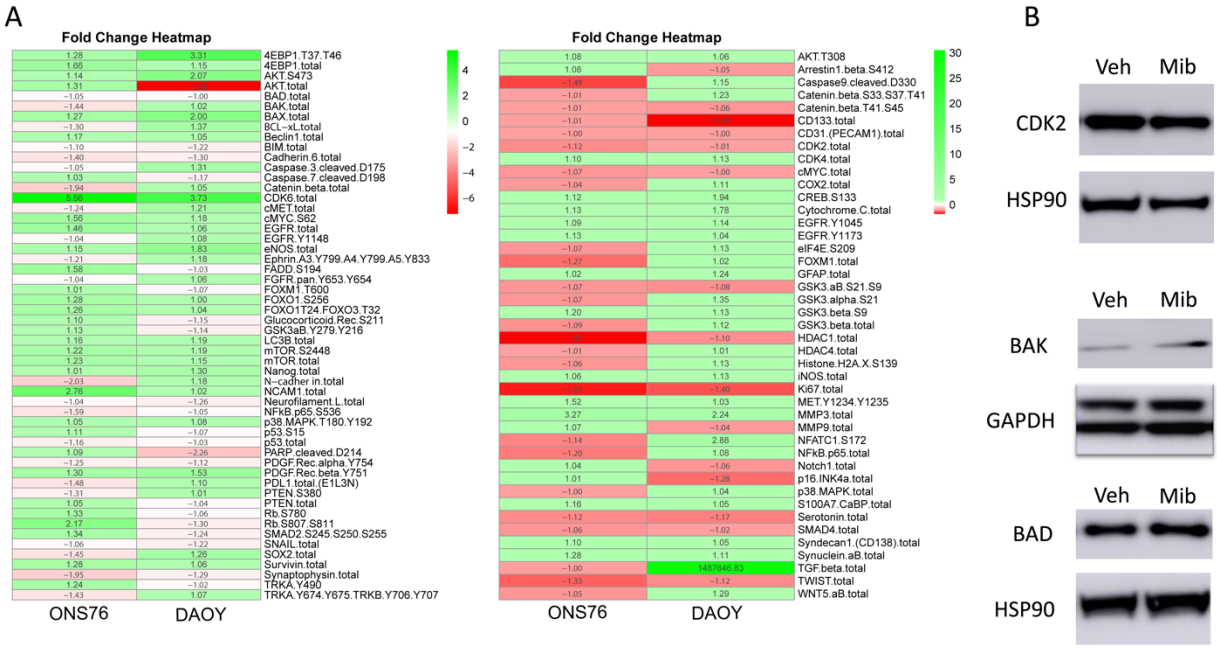

Supplemental Figure 3-5: Mibefradil significantly alters medulloblastoma signaling. A) Heatmap summarizing the fold change of mibefradil treated ONS-76 and DAOY across the RPPA analytes that were screened. B) Western Blot confirmation showing downregulation of CDK2, BAD and upregulation of BAK in mibefradil treated ONS-76 cells.

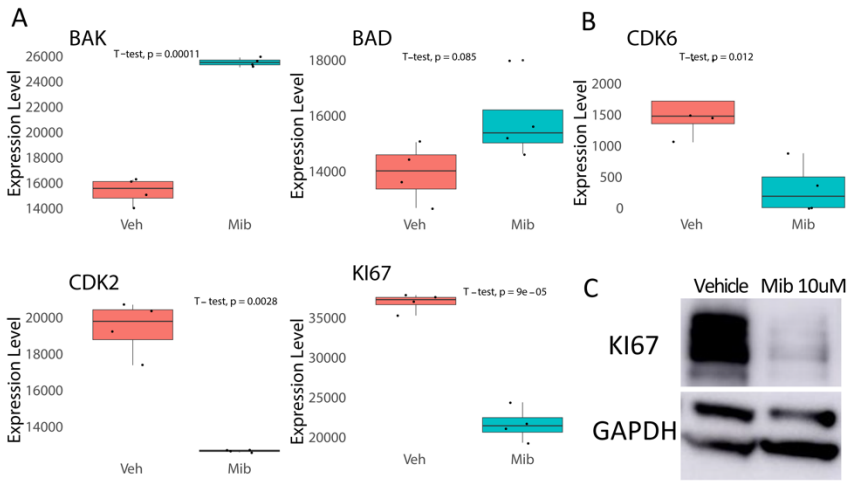

Figure 3-4: Mibefradil downregulates important apoptosis and growth-regulating proteins. A) Reverse phase protein array of mibefradil-treated cells showed upregulation of BAK and BAD in medulloblastoma cells. B) Reverse phase protein array of mibefradil treated cells showed downregulation of cell growth and cell cycle proteins such as CDK6, CDK2 and Ki67. C) Western blot confirmation showing downregulation of Ki67 in mibefradil-treated ONS-76 cells.

T-type calcium channel blockage inhibits in vivo tumor growth and prolongs animal survival.

To determine the effects of blockade of T-Type calcium channels with the FDA approved repurposed channel blocker mibefradil on tumor growth in vivo, we utilized medulloblastoma xenografts in immunodeficient mice. DAOY cells ($3x10^5$) were stereotactically implanted in the cerebellum and tumor formation was monitored by MRI. Seven weeks after tumor implantation the mice were subjected to MRI. Pre-treatment baseline measurements were recorded followed by treatment of either vehicle (H_2O) or mibefradil (24 mg/kg body weight) which was administered per oral gavage every six

hours for 4 days (Figure 3-5A,B). The treatment plan was repeated three days later. MRI scans were performed two weeks after drug treatment and tumor volume was quantified. Animal survival was also assessed. Mibefradil significantly inhibited tumor growth (Figure 3-5B). Additionally, mibefradil significantly prolonged survival compared to vehicle-treated mice (Figure 3-5C). These data show that inhibition of T-type calcium channels with mibefradil significantly reduces tumor volume and prolongs survival of mice, providing support for the use of mibefradil as a therapeutic drug in future clinical trials in medulloblastoma patients.

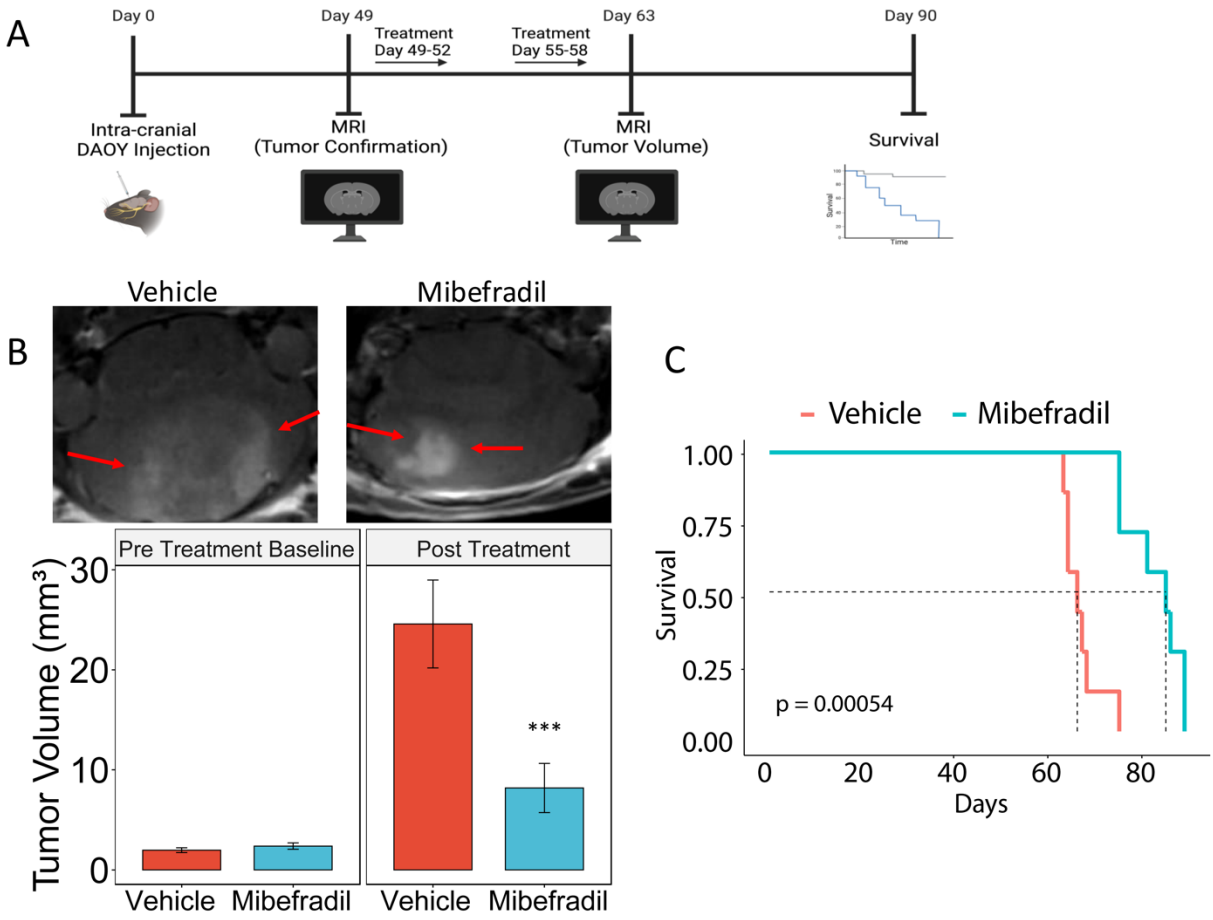

Figure 3-5: Mibefradil inhibits DAOY xenograft growth and prolongs survival. A) Schematic of in vivo experimental design. B) Representative MRIs of the tumor with quantification of tumor volume at the pretreatment time point as well as the post treatment timepoint for both Vehicle and Mibefradil-treated mice. C) Kaplan-Meier survival curves of vehicle and mibefradil-treated mice. N=7 mice per group. ***p<0.001

3.5.0 Discussion

Calcium signaling regulates a plethora of cellular processes such as proliferation, migration, invasion and apoptosis. Calcium channels are deregulated in cancers, where they can serve as a therapeutic target. Mibefradil is an orally bioavailable blocker of T and L type calcium channels, marketed by Roche as Posicor for the treatment of hypertension and previously in clinical trials for cancer.

We demonstrated that T-type calcium channels are upregulated in medulloblastoma tumors and cell lines. Patients that exhibit alterations in T-type calcium channels had worse survival compared to patients with no alterations. Patients with alterations in T-type calcium channels typically exhibit a mutation in one of them with little co-occurrence between the three channels, suggesting that deregulation of any single channel isoform is sufficient to promote tumor growth. A previous study reported pharmacological inhibition of T-type calcium channels with mibefradil decreased medulloblastoma cell growth and invasion and increased cell death. Pharmacological inhibition of Group 3 and Group 4 medulloblastoma cell lines with mibefradil-induced apoptosis and altered metabolic pathways[158]. Silencing of T-type calcium channels decreased cell growth and increased cell death demonstrating that the effect seen with mibefradil was specific to the inhibition of the T-type calcium channels.

To gain insight into the mechanism of T-type calcium channels in medulloblastoma we performed RPPA-based protein activation mapping of key signaling pathways and uncovered that mibefradil decreased expression of proliferative genes such as Ki67, CDK2, CDK6 and increased expression of apoptotic pathways genes BAD and BAX. We utilized publicly available single-cell RNA-seq data to perform co-expression analysis to gain additional insight into mechanisms of T-type calcium channels in medulloblastoma.

Co-expression analysis of T-type calcium channel in medulloblastoma tumors identified tumor modules representing numerous important biological processes associated with neuronal processes, cell signaling pathways, regulation of histone methylation, and cell division. We observed that modules for Cav3.1 and Cav3.2 typically trended in opposite directions. In the SHH tumors Cav3.1 had upregulation of SHH-Module 5 which was downregulated in Cav3.2 positive cells. Cav3.2 positive cells showed upregulation of SHH-Module 2 which was downregulated in Cav3.1 positive cells. This trend was also observed in the Group 3 tumors as well, suggesting that Cav3.1 and Cav3.2 regulate different cell states within the subgroups of medulloblastoma. These data demonstrate the T-type calcium channels are involved in various biological pathways in medulloblastoma tumors.

Mibefradil significantly reduced in vivo growth of medulloblastoma tumors and significantly prolonged animal survival. These data provide promising translational significance for the use of mibefradil in the treatment of medulloblastoma tumors. Mibefradil has been tested in clinical trials in recurrent glioblastoma patients in combination with temozolomide (NCT01480050) as well as in recurrent GBM patients with radiation (NCT02202993), which demonstrated that it was safe with some patients exhibiting partial responses[136, 137].

Altogether, this study represents the first fairly comprehensive analysis of the expression, functions, and mechanisms of action of T-type calcium channels in medulloblastoma. The study also indicates that blocking the channels with the repurposed FDA approved drug mibefradil is a promising potential therapy for one of the most common malignant pediatric brain tumors.

3.6.0 Author contributions, Competing interests, Funding

Author contributions: CJD and RA designed this study. CJD, ML, YZ, SS, UY, FH, KH, MGK, PM, YS, TV, EX, AS, AV, LD, RA, EM, FG performed experiments. RIG, JDW performed proteomic screening. CJD, RA, BK and EFP provided conceptual input. CJD and RA wrote the manuscript. All authors reviewed and edited the manuscript.

Competing interests: *The authors have no relevant financial or non-financial interests to disclose.*

Funding: Supported by NIH/NINDS RO1 NS122222, NIH/NCI UO1 CA220841, NIH/NINDS 1R21NS122136, NCI Cancer Center Support Grant P30CA044579, a University of Virginia Comprehensive Cancer Center Pilot Grant, a Schiff Foundation grant (all to R.A.). NCI 5T32CA009109-47 Grant and Parson Weber Parsons Fellowship (C.J.D). Support was also provided by the University of Virginia Advanced Microscopy Core Facility and Molecular Imaging Core

Chapter 4- Future Directions

4.1 Impact And Significance

The demonstration of the importance of T-type calcium channels in glioblastoma as well medulloblastoma malignancy parameters provides ample rationale to examine the role of T-type calcium channels in other brain tumors. The work in Chapter 2 is the first study examining the role of T-type calcium channels in the tumor microenvironment promoting GBM growth and progression. Additionally, the work in Chapter 2 further demonstrated the therapeutic capacity of in the tumor intrinsic and extrinsic properties of T-type calcium channels. The work in Chapter 3 is the first study characterizing the therapeutic target and mechanism of T-type calcium channels in medulloblastoma. The above studies demonstrate the importance of T-type calcium channels in brain tumor biology and form the foundation for follow-up studies in additional brain tumors as well as expansion into synergistic drug combinations with T-type calcium channel inhibitors.

4.2 Future Directions

4.2.1 CRISPR KO screens to identify and test new synthetic lethal druggable targets that increase the therapeutic efficacy of mibefradil in GBM:

Rationale & Impact

Glioblastoma has a dire need for identification of new therapeutic treatments as single targeting of patient alterations has not improved patient outcomes, likely due to signal redundancy, compensatory mechanisms and tumor-promoting microenvironment factors. The data presented in Chapter 2 establishes T-type calcium channels as viable drug targets as they are overexpressed in GBM as well as present in the tumor microenvironment. Mibefradil which inhibits T-type calcium channels crosses the blood brain barrier and inhibits GBM growth as well as synergizes with standard of care. We will perform in vitro and in vivo synthetic lethal CRISPR/Cas9 screens to identify druggable

mibefradil combination targets. This aim will develop and test new efficacious GBM therapies that can be utilized as preclinical data for drug combinations for future clinical trials.

Experimental Plan

The discovery of novel pathways or genes whose inhibition will synergistically improve the therapeutic efficacy of an existing therapeutic agent is a highly desirable goal in cancer research. We propose to use an unbiased CRISPR screening approach to identify effective combinatorial targets that will create a synthetic lethal combination with **mibefradil in GBM** using an established *in vivo* platform. To discover new synthetic lethal drug combinations with mibefradil, we will perform high throughput pooled genetic knock out screenings against the genes **druggable targets**. We will utilize CRISPR technology to knock out thousands of genes in a clinically relevant model of GBM and screen for the fitness of tumor cells to **mibefradil** drug treatment. This project is being done in collaboration with the Adli laboratory which has generated the druggable library and powerful screening tool[159]. Successful completion of this sub-aim would significantly impact GBM therapy as it would lead to the discovery of new synthetic lethal therapeutic combinations that use available drugs. These combinations could be rapidly tested in clinical trials.

As preliminary data we generated U87-Cas9-expressing cells which were infected with the druggable library at an MOI of 0.25. The library positive cells were selected with puromycin and expanded for 14 passages to allow the sgRNA to successfully knockout their target genes. After 14 passages the cells were treated with Vehicle or dose response of mibefradil. After 48 hours of drug treatment all of the cells were collected and DNA was extracted. PCR was performed for library amplification and the addition of sequencing adaptors. The samples were then sequenced using the Illumina MiSeq system. Sequencing files were downloaded and adaptors were trimmed followed by alignment to

identify gene targets. To identify depletion of sgRNA in drug treatment samples we utilized DESeq2 to compare Drug treatment samples versus Vehicle which identified significant targets that were enriched upon drug treatment as well as depleted upon drug treatment (Figure 4-1A). We focused specifically on the genes which were depleted upon drug treatment as these are the targets for synthetic lethality with mibefradil. To gain additional insight into what types of targets mibefradil is synergizing with we took the top depleted genes and performed pathway analysis using enrichR. Analysis of Biological Pathways, Cellular Compartment, and Molecular Function identified typical growth-related processes and functions but additionally identified numerous neuronal-related processes and functions (Figure 4-1B-D). The depletion of neuron-related target genes matches with our mibefradil treated RNA seq (Figure 2-5). Additionally, this provides a strong rationale for performing the screen in vivo, where mibefradil's efficacy is enhanced due to the higher expression of T-type calcium channels in neurons, further reinforcing its potential for synthetic lethality in a physiologically relevant context. The preliminary data was generated with the help of Dr. Shekar Saha.

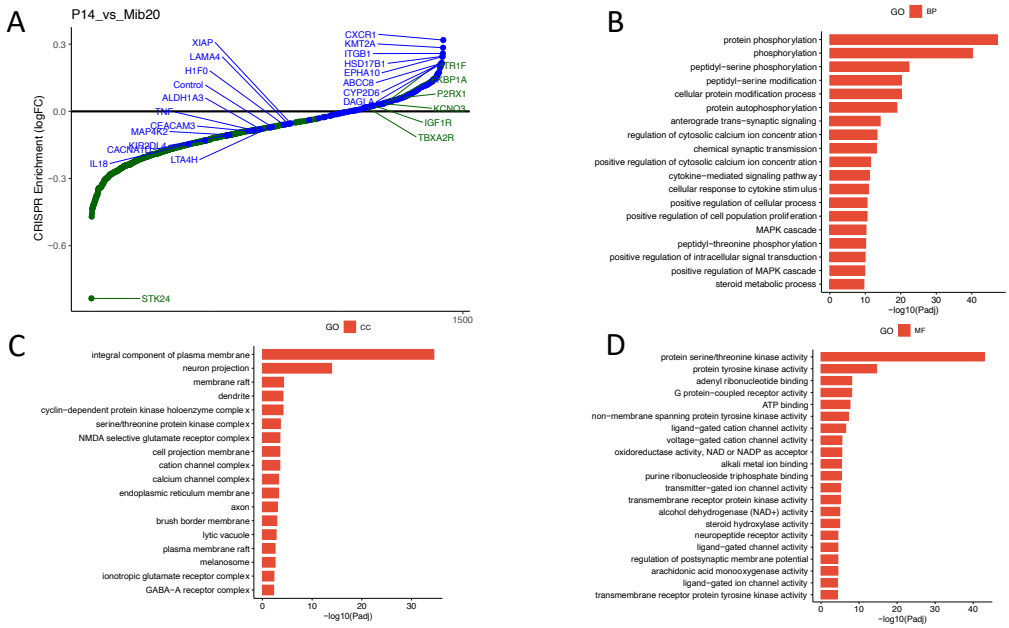

Figure 4-1: Mibefradil synergizes with synthetic lethal drug targets. A)Enrichment plot of the fold change of mibefradil treated synthetic lethal Crispr library showing the target genes that are enriched and depleted upon mibefradil treatment. B) Gene Ontology Biological Pathway analysis of the targets which are depleted upon mibefradil treatment. C) Gene Ontology Cellular Compartment analysis of the targets which are depleted upon mibefradil treatment. D) Gene Ontology Molecular Function analysis of the targets which are depleted upon mibefradil treatment.

Identification of druggable synthetic lethal combinations with mibefradil in GBM: To perform *in vivo* CRISPR KO screening in the xenograft model, we will generate a Cas9-expressing patient-derived three GSC/GBM lines and infect them with the CRISPR library of ~12,000 sgRNAs targeting druggable genes. After drug selection, ~ 2 million infected tumor cells will be in injected into the brain of athymic nude mice. One week later, the mice will be randomized to receive control or mibefradil treatment. After 4 weeks of treatment, tumors will be imaged with volumetric MRI, harvested, and weighed. DNA will be extracted for sequencing to measure relative abundance of each sgRNA. We will analyze the relative abundance of each sgRNA in Day 0 cells, control tumors (n=6) and mibefradil treated tumors (n=6) using the tailored CRISPR screening analysis tools that we developed by improving the previously published analytical tools[160].

Testing of new synthetic lethal drug combinations: After identification of druggable synthetic lethal targets, we will test the in vivo anti-tumor effects of drugging the targets in combination with mibefradil. We will prioritize targets based on the easy availability of clinically applicable drugs that target them and on known involvement of the target in GBM malignancy. We will use the GBM xenograft model described above as well as the RCAS/Tva model when applicable (existence of homology between the human and

corresponding mouse target). Mice xenografted with GSC-derived tumors and RCAS/Tva mice bearing GBM tumors will be generated as described above. The mice will be treated with mibefradil, the synthetic lethal drug, a combination of both or control vehicle. Mibefradil will be administered per oral gavage as described above. The synthetic lethal drug will be administered either orally, intraperitoneally, or intravenously, depending on the drug at various concentrations (depending on IC50). The animals will be monitored for tumor growth by MRI as described above. Tumor sizes will be measured and the effects of single and combination treatments will be compared. We expect that the combination will be synergistically more efficient in inhibiting tumor growth than single treatment. We plan to test ten different combinations. The findings could uncover new combination therapies that can be tested in clinical trials.

4.2.2. Transgenic mouse model to assess the role of Cav3 overexpression in GBM and MB in vivo:

Rationale & Impact

Glioblastoma (GBM) are most common primary malignant brain tumor with poor prognosis and limited treatment options. While in vitro studies using cell lines have provided insights into tumor biology, they fail to fully recapitulate the complexity of patient tumors, including the heterogeneous microenvironment, immune interactions, and developmental context. The work generated in Chapter 2 (Glioblastoma) demonstrated that T-type calcium channels are overexpressed in cell lines and tumors promoting brain tumor growth. The glioblastoma in vivo experiments using shRNA for the T-type calcium channels in the RCAS/Tva mouse model which showed that silencing the channels upon tumor initiation impacted tumor growth. One of the next steps would be to examine the impact of overexpression of T-type calcium channels upon tumor initiation in GBM. This aim will generate new mouse immune competent mouse models that can

be utilized for the study of brain tumors, other cancers as well as the T-type calcium channels in other disease models.

Experimental Plan

To perform Cav3 gain of function experiments in vivo, we will generate transgenic overexpression mice for each Cav3. We constructed transgenes encoding the cDNA and mVenus fluorescent marker driven by a nestin promoter flanked by a nestin enhancer[161]. The transgene for Cav3.2 has been purified and microinjected into fertilized mouse eggs for implantation into foster females. Microinjection and implantation were done by the UVA Genetically Engineered Murine Model Core. Transgene confirmation has been performed in founder mice and pups through genotyping. Incorporation of the Cav3.2 transgene wasn't enough to form tumors alone so the next step is for the mice to be crossed with commercially available $p53^{flox/flox}$ mice (B6.129P2-$Trp53^{tm1Brn}$/J) as well as Nestin-Cre mice (B6.Cg-Tg(Nes-cre)1Kln/J)[162] [163] (Figure 4-2). The mice will be assessed for GBM tumor formation in vivo at different times time points via MRI. After characterizing the time to tumor formation we will validate the tumors are GBM through Immunohistochemistry for canonical GBM markers such as IDH1, ATRX, and TP53. The overexpression of Cav3.2 would impact the calcium influx into tumors so we will perform calcium imaging of tumors. We will examine the tumors' ability to influx calcium using fluorescent calcium measurements utilizing ex vivo calcium imaging. We will euthanize the mice and isolate the brain which will be sliced using a vibratome at 200 μm thick sections. Brain slices will be placed in artificial cerebrospinal fluid (ASCF) where they will be loaded with Rhod-2AM for calcium imaging. The brain slices will be placed under the confocal microscope maintained in warm (30^{o}C) oxygenated (95% O2, 5% CO2). The tumor is identified by locating the mVenus positive cells using the 515nm wavelength and the calcium activity is monitored

using the 555 wavelength to capture the calcium events. The calcium dye Rhod-2AM will allow the monitoring of calcium events in the GME (red sparklets) and the tumor (co-localization with YFP).

The next step would be to assess the mutational landscape of the tumors. To accomplish this we will dissect the tumors under a fluorescent microscope as the tumors are labeled with mVenus. We will focus on the tumor as well as the normal tissue around the tumor for single-cell RNA sequencing to identify the signaling changes occurring within the tumor as well as to the tumor microenvironment. Additionally, we will gain insight into the tumor intrinsic properties of manipulation of Cav3.2 utilizing the Cav3.2 overexpression mouse as well as the RCAS-shCav3.2 mouse for proteomic screening with reverse phase protein arrays. The tumor cells will be isolated using GFP-based or mVenus-based flow cytometry sorting. Reverse-phase protein arrays [84] are a powerful approach for the quantitative screening of protein expression and activation[164-167]. We will use RPPA to determine the expression and activation status of proteins and pathways in response to TTCC manipulations. Cells from TTCC-manipulated or control tumors will be subjected to RPPA as previously described[84, 167]. Tissue lysates will be printed in triplicates on glass-backed nitrocellulose array slides. Arrays will be probed with > 600 phosphorylated, cleaved or total protein validated antibodies. Protein analytes will be chosen based on their known involvement in key aspects of GBM biology and calcium signaling. This work will be done in collaboration with Dr. Emanuel Petricoin who is an RPPA expert and was involved with the work in Chapter 3.

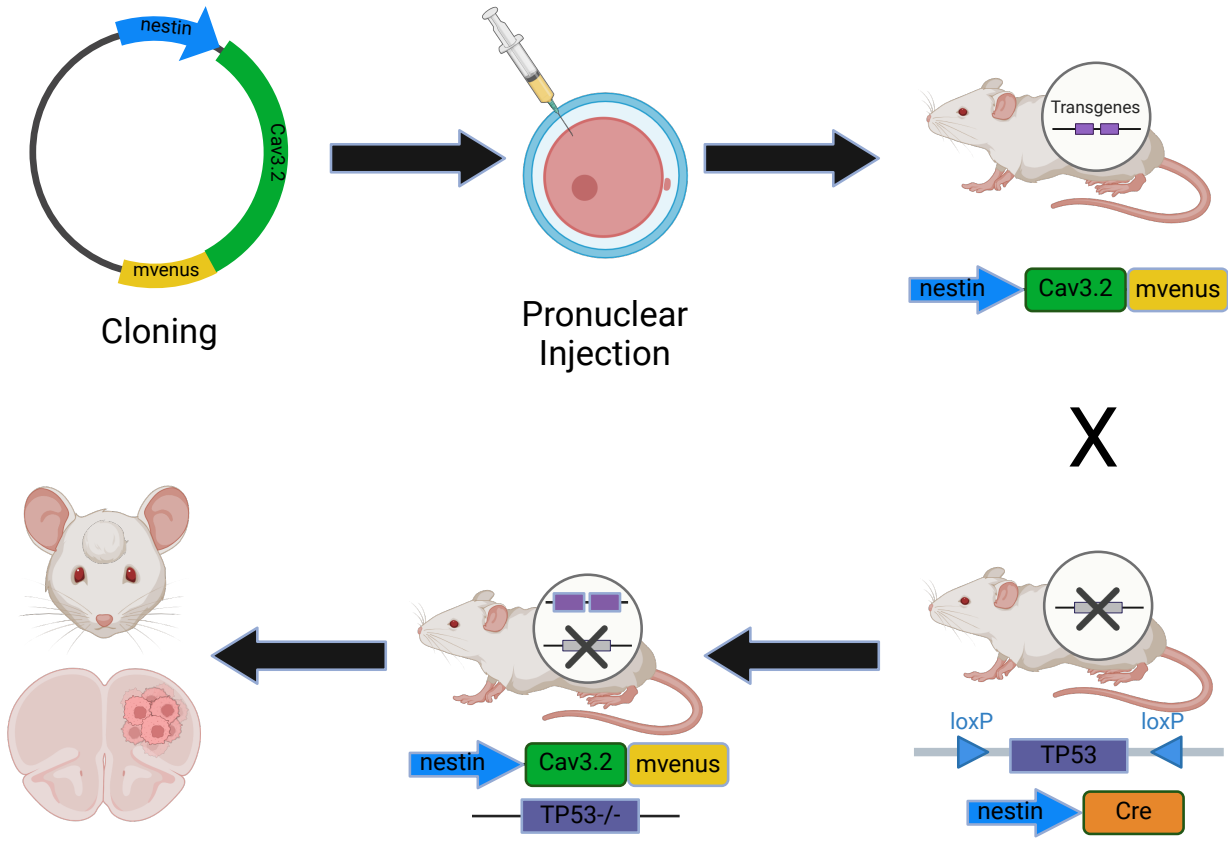

Figure 4-2 Schematic for generation of Cav3.2 overexpression mice in GBM: Schematic for the generation of the spontaneous Cav3.2 overexpression tumors in GBM and MB by crossing the nestin-Cav3.2 with a $p53^{loxp/loxp}$ mouse.

4.2.3. Transgenic mouse model to assess the role of Cav3 overexpression in MB in vivo.

Rationale & Impact

Medulloblastoma (MB) are most common pediatric brain tumor. The 5-year survival rate for pediatric MB patients is ~ 70%. However, patients treated with radiation therapy frequently experience permanent neurological deficits such as reduced motor and cognitive functions requiring identification of new therapeutic targets. The work generated in Chapter 3 (Medulloblastoma) demonstrated that T-type calcium channels

are overexpressed in cell lines and contribute to medulloblastoma malignancy parameters. One of the limitations of medulloblastoma is the cell lines fail to fully recapitulate the complexity of patient tumors, including the heterogeneous microenvironment, immune interactions, and developmental context. Medulloblastoma has several mouse models that are immune-competent and recapitulate the subtypes. The generation of overexpression T-type calcium channel mice would allow the study of the oncogenic capacity of T-type calcium channels in the different subtypes of MB utilizing the corresponding mouse models. This aim will generate new mouse immune-competent mouse models that can be utilized for the study of brain tumors, and other cancers as well as the T-type calcium channels in other disease models. The majority of the data in Chapter 3 on MB utilized SHH cell lines and publicly available data for inferring the role of T-type calcium channels in the other subtypes. The generation of overexpression T-type calcium channel mice in the other subtypes will elucidate the oncogenic capacity and mechanism on T-type calcium channels in Wnt, Group 3 and Group 4 subtypes of medulloblastoma.

Experimental Plan

The overexpression Cav3.2 mouse model can be utilized as a follow-up to the medulloblastoma work as well. The work in chapter 3 demonstrated the importance of T-type calcium channels in medulloblastoma but was limited in scope due to medulloblastoma not having numerous cell lines like GBM. Medulloblastoma does have reliable mouse models which can be utilized with the Cav3.2 overexpression mouse. We can model the different subtypes of medulloblastoma utilizing different mouse models. To model the SHH we will utilize the Math1-Cre mouse, $Ptch1^{loxp/loxp}$ mouse, $p53^{loxp/loxp}$ mouse which will form spontaneous medulloblastoma tumors from granule neuron progenitors (GNPs)[120, 168]. We cross the nestin-Cav3.2-mVenus to form spontaneous

overexpression Cav3.2 SHH medulloblastoma tumors. We will first assess the time to tumor formation compared to control heterozygous mice via MRI at varying time points. We will assess the calcium signaling in the tumor cells and microenvironment using brain slices and Rhod-2AM as described above. Medulloblastoma tumors are similar to glioblastoma tumors in that the other cell types in the tumor microenvironment can promote tumor growth such as astrocytes and microglia requiring the elucidation of how the overexpression of Cav3.2 impacts other cell types in the microenvironment. To address this we will first utilize immunofluorescence to look at the morphonology and markers for astrocytes and microglia to see if they are reactive astrocytes and tumor-associated microglia. Additionally, we can utilize single-cell RNA-seq to examine all the signaling changes occurring within the tumor as well as the tumor microenvironment. We can utilize programs like CellChat to elucidate the cell-cell communication that is altered upon overexpression of Cav3.2 in medulloblastoma tumors. We can use the same approach to model overexpression of Cav3.2 in the Wnt mouse model (*Ctnnb1*$^{lox\ (ex3)}$ × *Trp53*$^{flx\ /flx}$), and the Group 3 mouse model (Glt1-tTA; TRE-MYCN;Trp53$^{-/-}$) which would allow the examine of how Cav3.2 overexpression impacts those subtypes of tumors as well as their tumor microenvironment[169-171]. Additionally, it is important to understand the limitations of these mouse models so we will try to acquire additional medulloblastoma cell lines as well as patient-derived xenografts to validate our findings using numerous approaches. We can also utilize publicly available genomics data to compare the altered pathways from overexpression of Cav3.2 in the mouse models to medulloblastoma tumors that overexpress Cav3.2 utilize programs like WGCNA (bulk RNA-seq) and hdWGCNA [172]. These experiments will expand on the previous medulloblastoma work.

4.2.4 Regulation of malignancy parameters in GBM cells and OPCs by Cav3 in tumors, neurons, and OPCs

Rationale & Impact

Glioblastoma (GBM) is a highly aggressive brain tumor that exploits neural and glial signaling pathways to drive its malignancy. Emerging evidence from cancer neuroscience suggests that GBM growth and invasion are influenced by interactions with both neurons and oligodendrocyte precursor cells (OPCs), key components of the brain microenvironment. T-type calcium channels are widely expressed in neurons and OPCs, where they regulate excitability, differentiation, and migration. The work in Chapter 2 examined the role of Cav3.2 in the tumor microenvironment utilizing a whole-body knockout mouse model for Cav3.2 which demonstrated the importance of microenvironmental Cav3.2 in promoting GBM tumor progression. To demonstrate the effect was coming from neurons we utilized co-culture experiments with WT and Cav3.2KO neurons which decreased GBM proliferation providing evidence that neuronal Cav3.2 promotes GBM growth. The next step would be to generate neuron-specific KO to begin to elucidate the exact nature of neuronal Cav3.2 as other cell types within the microenvironment express Cav3.2. The data in Chapter 2 also found that Cav3.2 KO diminished the OPC-like GBM state and OPC are a cell of origin in GBM. OPCs have been shown to promote GBM malignancy an express T-type calcium channels providing rationale to examine how OPC T-type calcium channels promote GBM malignancy parameters and cell state. The mechanism through which Cav3 affect malignancy is not well understood. The proposed research could shed light on this mechanism and uncover new modes of action of Cav3 in GBM and cancer, especially what pertains to the regulation of glutamate and OPCs as well as the identification of the roles of GME cell-specific Cav3 in regulating tumor growth. The proposed research will generate new transgenic models including microenvironment cell-specific Cav3.2 knockout mice. This

will be the first study examining the role of OPC T-type calcium channels in promoting GBM.

Experimental Plan

To generate neuron specific knockout of Cav3.2 we will utilize Nex-Cre mice [173] (from Dr. Klaus Armin Nave, Max Planck Institute, Germany) crossed with $Cav3.2^{loxP/loxP}$ (a kind gift from Dr. Emanuel Bourinet, CNRS, France) to delete Cav3.2 within neurons in layers II,III and IV of the cortex[174]. We will first xenograft in GL261 and CT2A mouse tumor cell lines to examine how neuron specific knockout of Cav3.2 impacts tumor growth as well as survival. We will next look at how loss of neuronal Cav3.2 impact neuron-GBM connections through examining the presence of connections (Immunofluorescence and TEM) as well as function [175]. We expect neuronal Cav3.2 KO to decrease the neuron-GBM synaptic connections. Another aspect to examine is the glutamate signaling between neurons and tumor as the single-cell RNA-seq data demonstrated decreased glutamate signaling from neurons to tumor cells in the whole body Cav3.2 KO model as depicted in Figure S2-6. We will utilize in vivo glutamate reporters to examine how neuronal Cav3.2 KO impacts glutamate signaling in the tumor as well as the microenvironment. To achieve this we will utilize AAV to deliver the glutamate reporter (iGluSnFR3) which uncages mVenus upon glutamate binding allowing the visualization of glutamate signaling[176]. We will implant cranial windows into our mouse models for glutamate imaging using multiphoton laser scanning microscopy (MPLSM) in real time as well as utilize ex vivo brain slices. We will also examine how neuronal Cav3.2 KO impacts calcium influx into tumors utilizing syngeneic GBM cell lines expressing Tdtomato-GCAMP6 which allows identification of the tumor cells as well as visualizing of influx of calcium. We will examine the effect of influx of calcium in real time using cranial windows as well as ex vivo brain slices where we can

apply different compounds to modulate neuronal activation and inhibition. We will also utilize neuronal Cav3.2 KO neurons in co-cultures GBM/GSC cells to examine the effect on proliferation, calcium influx, glutamate signaling and synaptic connections.

Another cell population in the tumor microenvironment that expresses T-type calcium channels is Oligodendrocyte progenitor cells (OPCs)[177, 178]. OPCs have been shown to promote glioma growth through numerous mechanisms such as neovascularization, invasion, promoting neuronal-GBM connections as well as interacting with macrophages and microglia[47, 118, 179]. Additionally, OPCs are believed to be one of the cells of origin of glioma and exist as a cell state within glioblastoma[21, 180]. The data in Chapter 2 demonstrates that the whole body Cav3.2 KO mouse decreased the OPC cell state within the GBM tumors. We hypothesize that Glioma microenvironmental Cav3.2 drives tumor growth by enhancing the proliferation of OPCs and shifting GBM cells to an OPC-like state.

We will generate Cav3.2 KO-OPC mouse models by crossing the Cav3.2$^{loxP/loxP}$ mouse described above with PDGFRa-Cre mice (commercially available Jackson Labs). We will perform similar experiments described above by first assessing how Cav3.2KO OPCs in the microenvironment impact tumor growth by implanting two syngeneic cell lines (Gl261 & CT2A) and assessing tumor formation via MRI as well as assess animal survival. We expect loss of Cav3.2 in OPCs to decrease tumor volume and prolong animal survival. We will isolate tumor for immunofluorescence staining to assess tumor proliferation and states of other cell types such as astrocytes, neurons, microglia and macrophages. To gain insight into tumor and other cell types in microenvironment are altered we will isolate tumors from WT and Cav3.2 KO-OPC mice for single-cell RNA-sequencing. We will follow the same bioinformatic workflow described in Chapter 2 that was used for analyzing the Cav3.2 whole body KO mouse. We will first examine the

changes in the tumor from WT and Cav3.2 KO-OPC where we expect changes in genes associated with neuronal and glia process as well as decreases in OPC/NPC cell states. We will also examine the other cell types in the tumor microenvironment to assess what cell communication is altered from Cav3.2 KO-OPC. Additionally, we can compare the Cav3.2KO-OPC data to the whole body Cav3.2KO data to see specifically which particular process the Cav3.2KO-OPC contributes.

We will utilize co-cultures of neurons and OPCs to validate the findings from the in vivo models and single-cell data. We will use the following co-culture conditions: 1) WT neurons and WT OPC; 2) Cav3.2-KO neurons and WT OPC; 3) WT neurons and Cav3.2 KO-OPC; and 4) Cav3.2-KO neurons and Cav3.2 KO-OPC. These co-culture combinations will allow us to dissect the roles of neuronal Cav3.2 and OPC Cav3.2 on the growth of OPCs in co-cultures with neurons. The GFP labeled OPCs will be counted under a microscope. The effects of Cav3 on OPC proliferation when co-cultured with neurons will be determined. We will also perform EdU incorporation assays to measure OPC proliferation in co-cultures with neurons. For EdU incorporation assays, slides will be treated with 10 μM EdU. The cells will be fixed and stained using the Click-iT EdU kit and protocol (Invitrogen). The proliferation index will then be determined by quantifying percentage of EdU labelled OPCs (identified by EdU+/GFP+) over total number of OPCs using confocal microscopy. The findings will determine the role neuronal and OPC Cav3 in mediating neuron/OPC functional interactions.

We will also assess the role of Cav3 in mediating OPC growth and competition in vivo in the MADM model. The MADM model will be provided by the Zong lab. The Zong lab has established a new MADM-anti-competition model (MADM-p53,NF1/NF1), which differs from the original MADM-glioma model only by incorporating a global NF1-null OPC

genotype. After induction of early tumor growth, mibefradil (24 mg/kg body weight) will be administered to the animals per oral gavage for 4 days. Three days later, OPC growth and competition will be assessed in the Zong lab**.** These experiments will determine if Cav3 inhibition in the glioma microenvironment affects OPC growth, competition and malignancy and will complement the in vitro experiments described above.

4.2.5 Role of T-type calcium channels in Diffuse Intrinsic Pontine Glioma

Rationale & Impact

Diffuse intrinsic pontine glioma (DIPG) is a highly aggressive and incurable pediatric brainstem tumor with limited treatment options and a devastating prognosis. T-type channels regulate key cellular processes such as proliferation, invasion, and resistance to apoptosis, all of which are hallmarks of DIPG's aggressive nature. Given that the brainstem is a region rich in calcium-dependent signaling, investigating T-type calcium channels in DIPG could uncover novel mechanisms of tumorigenesis and identify potential therapeutic vulnerabilities. Emerging evidence from the field of cancer neuroscience demonstrated that DIPG, co-opt neuronal signaling pathways to drive tumor progression, with a particular emphasis on activity-dependent mechanisms. T-type calcium channels (Cav3.1, Cav3.2, Cav3.3) are predominantly expressed in neurons, where they regulate excitability, synaptic plasticity, and neurotransmitter release. The data in Chapter 2 demonstrate the role of microenvironmental Cav3.2 in promoting GBM growth specifically through neuronal expression. The role of microenvironmental T-type calcium channels can contribute to DIPG growth and progression. This aim would represent the first study of T-type calcium channels in DIPG. Additionally, it would elucidate the intrinsic and extrinsic role of T-type calcium channels in DIPG as well as provide preclinical data for potential T-type inhibitors in clinical trials for DIPG.

Experimental Plan

We expanded into the examination of T-type calcium channels in other forms of glioma specifically Diffuse Intrinsic Pontine Glioma (DIPG). To elucidate the expression, I downloaded the raw reads of RNA-sequencing of diffuse intrinsic pontine glioma cell lines and tumors[181]. I aligned the raw reads using salmon to generate count files which were converted into transcripts per million (TPM) for assessing expression. T-type calcium channels showed variable expression in the tumors with several tumors exhibiting higher expression of Cav3.2 compared to the normal pons samples demonstrating that Cav3.2 is upregulated in DIPG (Figure 4-3). Diffuse intrinsic pontine glioma is a pediatric tumor that exhibits oncohistone mutations specifically H3K27M mutations at histone H3.1 and H3.3. Analysis showed that Cav3.2 showed higher expression in H3.3K27M mutants compared to the tumors that were H3.1K27M (Figure 4-3). Additionally, we examined the expression of T-type calcium channels pediatric high grade gliomas that exhibit oncohistone mutations (H3.1K27M, H3.3K27M and G34R). We observed a similar trend of Cav3.2 exhibiting the highest expression among the T-type calcium channels and it was highest in H3.3K27M mutant tumors.

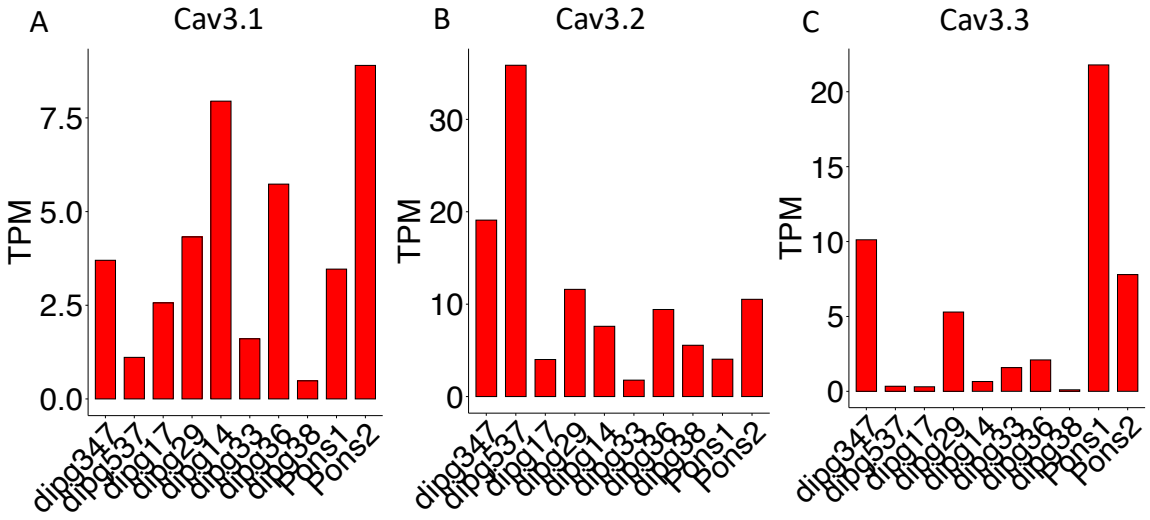

Figure 4-3 Expression of T-type calcium channels in DIPG tumors. A) Expression of Cav3.1 in DIPG tumors and normal pons. B) Expression of Cav3.2 in DIPG tumors and normal pons. C) Expression of Cav3.3 in DIPG tumors and normal pons.

The elevated expression of T-type calcium channels in diffuse intrinsic pontine glioma tumors provide evidence to begin a project examining the role of T-type calcium channels in promoting tumor growth. The elevated expression of T-type calcium channels points towards them acting as oncogenes. To test this hypothesis, we will utilize a combination of T-type calcium channel inhibitors (mibefradil and NNC 55-0396) to inhibit the functions in DIPG cell lines. To determine the functional role of T-type calcium channels in DIPG we will study the effects of TTCC inhibition on DIPG cell proliferation, survival, migration and invasion. Cell proliferation and cell cycle progression will be assessed by cell counting and propidium iodide flow cytometry, respectively. Cell death and apoptosis will be assessed by trypan blue staining and Annexin V-7AAD flow cytometry, respectively. Cell migration and invasion will be assessed by a wound assay and a transwell invasion assay, respectively.

To investigate the role of TTCC in vivo, we will generate and use immune-competent mouse models of DIPG. The models will be generated using the RCAS/Tva system and transgenic approaches. The **RCAS/Tva** system utilizes an avian leukosis virus [119] to somatically transfer genes to cells expressing the Tva receptor, which is not expressed in mammals[182]. Mice can be genetically engineered to express the Tva receptor under control of a tissue-specific promoter resulting in somatic gene transfer to those specific cells[182]. Somatic gene transfer of oncogenes or knockdown/knockout of tumor suppressors can yield spontaneous tumor formation[183]. In our model, Tva receptor expression is driven by the nestin promoter, which is specific for neural stem/progenitor cells [184]. To generate RCAS-Tva mice, we have prepared shRNA targeting the channels individually[55]. We inserted the shRNAs into the RCAS-Y vector. We validated the RCAS-shRNA of TTCCs previously in our RCAS model of GBM which showed significant decrease in tumor growth, survival and knockdown of TTCCs (Figure 2-7). To model DIPG in the RCAS/Tva model we will utilize RCAS-oncohistones [30] along with RCAS-PDGFB and RCAS-shp53 plasmids[185]. We will transfect the RCAS-shRNA plasmid along with above mentioned plasmids into DF-1 cells for the production of the RCAS virus. We will then inject the RCAS-DF1 expressing cells into the brainstem of day 0-2 old pups in the nestin-tva background. We will deliver RCAS-shRNAs individually to assess the role of each Cav3 as well as in combination to examine the impact of all TTCCs.

We will monitor tumor formation using MRI. We will also isolate the tumors for immunohistochemistry to examine proliferation (Ki67), apoptosis (Caspase 3) and stemness (Sox2). We will examine the tumors' ability to influx calcium using fluorescent calcium measurements utilizing ex vivo calcium imaging by loading the GFP labeled

tumors with Rhod-2am to identify tumor specific calcium activity by colocalization. Knockdown of TTCCs is expected to yield smaller tumors, prolonged survival, increased apoptosis, decreased proliferation and stemness and decreased calcium influx.

After demonstrating the importance of T-type calcium channels in DIPG utilizing cell lines in in vitro and in vivo we want to test the therapeutic efficacy of mibefradil in vivo. To do that we will utilize two models of orthotopic DIPG xenografts into nude mice and spontaneous DIPG tumors utilizing the RCAS/Tva mouse model. For the DIPG xenografts we will stereotactically implant 300K DIPG cells into the brainstem of nude mice. We will allow tumors to form for 4 weeks then perform MRIs to confirm the presence of tumors. After tumor confirmation, we will begin treatment with mibefradil (24 mg/kg) via oral gavage every 6 hours in two regiments of 4 days on 3 days off. After the prescribed treatment period we will MRI the vehicle and mibefradil treated mice. We will euthanize a subset of each group for histological analysis while leaving the remainder of the mice for survival studies. Additionally we will utilize the RCAS/Tva mouse model described above with the same timeline for MRI and mibefradil treatment. We expect mibefradil to significantly decrease tumor volume compared to the vehicle cohort in both mouse models. We expect the mibefradil treated mice to exhibit a significant increase in survival compared to the vehicle treated mice. For the histological analysis we will perform Ki67 straining to address how mibefradil impacted proliferation and H&E staining.

We will also examine how mibefradil impacts neuronal-DIPG connections. DIPG has previously been shown to form neuronal synapses with tumor cells specifically through the expression of synaptic genes in within OPC-like cells[36, 44, 45]. The data generated in this thesis has demonstrated that mibefradil treatment in GBM

downregulates genes associated with neuronal processes. Additionally loss of Cav3.2 in the microenvironment downregulates genes associated with neuronal processes and glial processes. The data generated in GBM provides evidence to examine how mibefradil impacts neuronal processes in DIPG. To assess neuronal processes we will perform immunofluorescence of tissue sections from vehicle and mibefradil treated mice. Tumors will be identified as GFP positive cells, Neurons will be identified utilizing neurofilament, presynaptic neuronal connections will be identified using synapsin and post-synaptic connections in the tumor will be identified using PSD95. We will quantify the percentage of colocalization of Synapsin-PSD95 between neurons and tumor in vehicle and mibefradil treated sections. We anticipate seeing a decrease in neuronal-DIPG connections in mibefradil treated sections compared to vehicle.

After demonstrating the importance of T-type calcium channels in malignancy parameters and the therapeutic targeting in DIPG the next step is to elucidate the mechanism. To gain insight into the mechanism of T-type calcium channels in DIPG we will perform single-cell RNA-sequencing of DIPG tumors. We will isolate tumors from the RCAS/Tva mouse models described above with the conditions being RCAS-Scrambled mice and RCAS-shTTCC mice. We will isolate the tumors utilizing a fluorescence dissecting microscope to locate the GFP positive tumor and remove the tumor as well as normal tissue around it to capture the cells in the tumor microenvironment. Tumors will be mechanically and enzymatically dissociated using a papain-based brain tumor dissociation kit followed by red blood cell removal and debris removal. Samples will be strained with live dead dye (7-AAD) and subjected for FACS sorting for live cells followed by processing and sequencing using 10X Genomics kits. Additionally, we will isolate tumors from vehicle and mibefradil-treated DIPG xenografts for single-cell RNA-sequencing.

Reads will mapped to the mouse genome mm10 using 10X CellRanger. For single-cell sequencing analysis standard procedures for filtering, mitochondrial gene removal, doublet removal, variable gene selection, dimension reductionality and clustering will be performed using Seurat. A cell quality filter of greater than 200 features but fewer than 7500 features per cell and less than 25% of read counts attributed to mitochondrial genes will be used. Dimensionality reduction will be performed using principal component analysis and visualized with the Elbowplot function to find neighbors and clusters (resolution 0.3). Uniform manifold approximation and projection was performed for visualizing cells. Cell populations will be identified using singleR with the celldex mouse RNA-seq data set as reference along with FindAllMarkers and the inferCNV algorithm to annotate clusters.

After annotating all the appropriate cell types we will focus specifically on the tumor population to examine the effects mibefradil and silencing of T-type calcium channels has on tumor cell state. We will examine the specific clusters within the tumor populations to identify if mibefradil or silencing of T-type calcium channels creates any unique populations within the tumor cells. We will perform differential expression analysis of the tumor cells between vehicle and mibefradil treated samples as well as Scrambled vs shTTCC tumor cells using FindMarkers with default settings. Gene Ontology Biological Pathways, Cellular Compartments and Molecular Functions of DEGS were performed using ClusterProfiler. Additionally we will assess how drug treatment and silencing of T-type calcium channels alters the cell states of the tumor. DIPG has very well defined cell states based on single-cell RNA-sequencing which are AC-like (astrocytic differentiation), OC-like (oligodendrocytic differentiation) and OPC-like programs which are more stem like[172]. The OPC-like cell state exhibits the stem like

state of DIPG tumors which are enriched for postsynaptic gene signatures which are important for the formation of neuron-glioma synapses[36]. The OPC-like cell state is enriched for genes associated with synaptic processes that allow connections with different types of neurons such as glutamatergic, GABAergic and cholinergic[36, 39, 43]. We hypothesize that mibefradil treatment and silencing of T-type calcium channels would result in a decrease in the OPC-like cell as well as decrease genes associated with synaptic connections as the work of this thesis demonstrated that mibefradil downregulated genes associated with synaptic connections in GSCs.

Synaptic gene signatures within gliomas are important for the regulation and connection of neuron-glioma synapses in GBM as well DIPG. The work in this thesis demonstrated the ability of microenvironment Cav3.2 to regulate neuronal and glial process in GBM which provides rationale for the examination of how microenvironmental Cav3.2 regulates neuronal connections in DIPG. DIPG is a glioma located within the brainstem specifically the pons on the brainstem. Neuronal Cav3.2 has been shown to regulate neuronal firing in the thalamus associated with epilepsy[187, 188]. The thalamus sits above the midline acting as a relay station between the peripheral nervous system and the central nervous system resulting in innervation and interaction with the pons. The interaction of neurons from the thalamus with the pons and the role of neuronal Cav3.2 in neuron regulation in thalamus leads to the hypothesis that microenvironmental Cav3.2 will promote DIPG malignancy parameters. To test this hypothesis, we will first assess how loss of Cav3.2 in the microenvironment impacts tumor growth and survival. We will xenograft in mouse DIPG cells into wild type (WT) and Cav3.2KO mice then assess tumor growth by MRI at 4 weeks. We expect to see significant decrease in tumor volume in the Cav3.2KO mice compared to the WT mice. Next we will asses animal survival where we expect Cav3.2KO mice to significantly live

longer than WT mice. Additionally we will collect tissue sections from both WT and Cav3.2KO mice to asses proliferation via immunofluorescence via Ki67 staining. Next we will assess neuron-glioma interactions between WT and Cav3.2KO tumors. Tumors will be identified as GFP positive cells, Neurons will be identified utilizing neurofilament, presynaptic neuronal connections will be identified using synapsin and post-synaptic connections in the tumor will be identified using PSD95. We will quantify the % colocalization of Synapsin-PSD95 between neurons and tumor in vehicle and mibefradil treated sections. We anticipate seeing a decrease in neuronal-DIPG connections in Cav3.2KO sections compared to Wild type sections.

To gain insight into the mechanism of loss of microenvironmental Cav3.2 has on DIPG tumor growth we will perform single-cell RNA-sequencing. We will isolate tumors from WT and Cav3.2KO mice around 4 weeks removing the tumor as well as the normal cells around the tumor for sequencing. We will dissociate the tumor and performed single-cell RNA-sequencing and quality control for processing the data using the methods described above. We will first focus on the tumor examining the differential expression between WT and Cav3.2KO. tumor cells to identify the downregulated genes in the tumor and assess how loss of Cav3.2 in the microenvironment impacts tumor signaling using FindMarkers with default settings. To gain insight into what the downregulated genes were doing we will perform Gene Ontology (GO) Biological pathway analysis, Cellular compartment analysis and Molecular Function analysis. We hypothesize that microenvironmental Cav3.2KO will downregulate genes associated with neuronal and glial processes which are important for synaptic connections of neurons to tumor. To gain additional insight we will perform CellChat to examine how the tumor cells are interacting with other cells in the microenvironment. We will focus on the interaction with the neurons and tumor cells to identify which signaling pathways are altered

between WT and Cav3.2KO. The combination of the downregulated genes and interactions between neurons and tumor cells will provide insight into how microenvironmental Cav3.2 is promoting neuron-DIPG connections.

To further demonstrate that the effect is coming from neurons we will isolate neurons from WT and Cav3.2 KO mice for co-culture experiments with DIPG cells. We will assess the proliferation index of DIPG cells in the co-culture setting with WT and Cav3.2KO neurons. We expect the WT neurons to enhance the proliferation index of DIPG cells and that effect to be abolished when co-cultured with Cav3.2KO neurons. To deduce whether the effect is based on direct connection of neurotransmitter release we will collect conditioned media from WT and Cav3.2KO neurons and apply the conditioned media to DIPG cells and measure the proliferation index. We anticipate the conditioned media from WT neurons will enhance the proliferation index of DIPG cells and the conditioned media from Cav3.2KO neurons will have a minor effect on the proliferation index. Additionally we will assess what neurotransmitters are being released in the conditioned media by performing ELISAs for neurotransmitters as Glutamate, GABA and acetylcholine which all exhibit tumor promoting properties[36, 39, 43]. Additionally, we will assess the conditioned media for paracrine factors such as neuroligin-3 (NLGN3) and brain-derived neurotrophic factor (BDNF) which have been shown to be secreted from neurons and promote DIPG growth[44, 45, 47]. We expect the Cav3.2KO neurons to have lower levels of some neurotransmitter or neurotropic signals. We will then assess synaptic connections in WT and Cav3.2KO co-cultures with DIPG cells. Neurons will be identified utilizing neurofilament, presynaptic neuronal connections will be identified using synapsin and post-synaptic connections in the tumor will be identified using PSD95. We will quantify the % colocalization of Synapsin-PSD95 between WT and Cav3.2KO neurons and DIPG cells. We anticipate seeing a decrease

in neuronal-DIPG connections in Cav3.2KO co-cultures compared to Wild type co-cultures.

Additional alternative approaches would be to perform spatial transcriptomics on tumors from WT and Cav3.2KO mice. We would follow a similar timeline utilized for the single-cell RNA-sequencing. We will utilize the 10X Visium HD Spatial Gene expression platform for the sequencing. We will perform H&E staining as well immunofluorescence staining with neurons labeled with Neurofilament, tumor labeled with GFP, astrocytes labeled with GFAP, microglia labeled with Iba1 which will be utilized to integrate cell types with the expression data utilizing CODEX[189]. We will focus on the interaction of neuron and tumor cells to identify differences between WT and Cav3.2KO. Additionally, we could examine the effect Cav3.2KO has on other cells in the microenvironment utilizing the markers for all the corresponding cell types.

4.3.0 Summary and Conclusions

There remains a need for better understanding of brain tumors as well as identification of new therapeutic targets. The work in this thesis demonstrates the tumor intrinsic and microenvironmental role of T-type calcium channels in glioblastoma. This work represented the first characterization of microenvironmental T-type calcium channels specifically neuronal Cav3.2 in promoting GBM growth and progression through regulation of neuronal and glial processes. This work provides a framework for examining other potential targets within the tumor microenvironment that are contributing to brain tumor growth. Additionally the therapeutic targeting of T-type calcium channels in glioblastoma in combination with standard of care provides compelling evidence for clinical trials in newly diagnosed GBM patients.

The characterization of T-type calcium channels in medulloblastoma opens a new class of targets for examination with standard of care. The T-type calcium channels exhibit elevated expression across the various subtypes of MB which will open up examination of the different mechanisms they drive in each of the subtypes of MB. The efficacy of mibefradil in the in vivo medulloblastoma model demonstrates a viable therapeutic option for future preclinical studies in the different subtypes. Medulloblastoma has a good prognosis but one of the major issues is the permanent neurological deficits patients experience the rest of their life pointing towards the need for new therapeutics that will exhibit lower negative side effects. Additionally, the potential combination of mibefradil with standard of care could potentially result in lowering the doses of standard of care hopefully lowering the negative side effects of the therapeutics.

The preliminary data generated from this thesis demonstrates the viability of targeting of T-type calcium channels in brain tumors, opening the exploration of T-type calcium channels in other brain tumors. The proposed aims would represent the first characterization of T-type calcium channels in diffuse intrinsic pontine gliomas. DIPG tumors are unfortunately inoperable and have a dismal life expectancy, requiring further elucidation of the mechanism of the tumors as well as the identification of new therapeutic targets. The examination of T-type calcium channels in DIPG will elucidate the contribution of T-type calcium channels in the tumor as well as the contribution from the tumor microenvironment. The cancer neuroscience field has demonstrated that the role of the tumor microenvironment contributes significantly to tumor progression. This is a relatively new field, so the elucidation of the microenvironmental contributions of T-type calcium channels can be pivotal in providing fundamental mechanistic knowledge in DIPG tumor biology. The characterization of T-type calcium channels would potentially open new therapeutic options for patients to receive with standard of care.

The characterization of T-type calcium channels in the microenvironment with tissue specific knockouts in neurons and OPCs will provide mechanisms into the contributions how neurons and OPCs are promoting GBM progression. One of the major reasons why most personalized therapies have failed in GBM is the tumor heterogeneity. One of the major contributing factors to the GBM tumor heterogeneity is the interaction with the other cell types within the tumor microenvironment. The tissue-specific knockout of T-type calcium channels in neurons and OPCs will help elucidate the distinct contributions of each cell type to GBM progression, growth, and cell state. This approach may provide valuable insights into the underlying mechanisms driving tumor-microenvironment interactions and identify potential therapeutic targets. Lastly, the synthetic lethal CRISPR screens will identify therapeutic targets that can be combined with T-type calcium channel inhibitors, paving the way for novel drug combination strategies. By uncovering vulnerabilities both within tumor cells and the surrounding microenvironment, these findings will inform critical preclinical studies with the ultimate goal of advancing optimized treatment regimens into clinical trials.

Collectively, this work provides a comprehensive foundation for understanding the role of T-type calcium channels in brain tumors and their microenvironment, offering new avenues for therapeutic intervention that could ultimately improve patient outcomes through more effective and less toxic treatment strategies.

References

1. Stupp, R., et al., *Radiotherapy plus concomitant and adjuvant temozolomide for glioblastoma.* N Engl J Med, 2005. **352**(10): p. 987-96.
2. Northcott, P.A., et al., *The whole-genome landscape of medulloblastoma subtypes.* Nature, 2017. **547**(7663): p. 311-317.
3. Taylor, K.R., et al., *Recurrent activating ACVR1 mutations in diffuse intrinsic pontine glioma.* Nature genetics, 2014. **46**(5): p. 457-461.
4. Ostrom, Q.T., et al., *CBTRUS Statistical Report: Primary brain and other central nervous system tumors diagnosed in the United States in 2010-2014.* Neuro Oncol, 2017. **19**(suppl_5): p. v1-v88.
5. Board, P.A.T.E. *PDQ Adult Central Nervous System Tumors Treatment*. 2018.
6. Wen, P.Y. and D.A. Reardon, *Neuro-oncology in 2015: Progress in glioma diagnosis, classification and treatment.* Nat Rev Neurol, 2016. **12**(2): p. 69-70.
7. Wen, P.Y. and S. Kesari, *Malignant gliomas in adults.* N Engl J Med, 2008. **359**(5): p. 492-507.
8. Hegi, M.E., et al., *MGMT gene silencing and benefit from temozolomide in glioblastoma.* N Engl J Med, 2005. **352**(10): p. 997-1003.
9. Galli, R., et al., *Isolation and characterization of tumorigenic, stem-like neural precursors from human glioblastoma.* Cancer Res, 2004. **64**(19): p. 7011-21.
10. Singh, S.K., et al., *Identification of human brain tumour initiating cells.* Nature, 2004. **432**(7015): p. 396-401.
11. Lathia, J.D., et al., *Cancer stem cells in glioblastoma.* Genes Dev, 2015. **29**(12): p. 1203-17.
12. Bao, S., et al., *Glioma stem cells promote radioresistance by preferential activation of the DNA damage response.* Nature, 2006. **444**(7120): p. 756-60.
13. Cancer Genome Atlas Research, N., *Comprehensive genomic characterization defines human glioblastoma genes and core pathways.* Nature, 2008. **455**(7216): p. 1061-8.
14. Brennan, C.W., et al., *The somatic genomic landscape of glioblastoma.* Cell, 2013. **155**(2): p. 462-77.
15. Zhang, Y., et al., *The p53 Pathway in Glioblastoma.* Cancers (Basel), 2018. **10**(9).
16. Zhang, Y., Y. Xiong, and W.G. Yarbrough, *ARF promotes MDM2 degradation and stabilizes p53: ARF-INK4a locus deletion impairs both the Rb and p53 tumor suppression pathways.* Cell, 1998. **92**(6): p. 725-34.
17. Westphal, M., C.L. Maire, and K. Lamszus, *EGFR as a Target for Glioblastoma Treatment: An Unfulfilled Promise.* CNS Drugs, 2017. **31**(9): p. 723-735.
18. Xu, H., et al., *Epidermal growth factor receptor in glioblastoma.* Oncol Lett, 2017. **14**(1): p. 512-516.
19. Zhao, H.F., et al., *Recent advances in the use of PI3K inhibitors for glioblastoma multiforme: current preclinical and clinical development.* Mol Cancer, 2017. **16**(1): p. 100.

20. Wang, Q., et al., *Tumor evolution of glioma-intrinsic gene expression subtypes associates with immunological changes in the microenvironment.* Cancer cell, 2017. **32**(1): p. 42-56. e6.
21. Neftel, C., et al., *An integrative model of cellular states, plasticity, and genetics for glioblastoma.* Cell, 2019. **178**(4): p. 835-849. e21.
22. Leone, A., et al., *Transfection of human mn23-H1 into the human MDA-MB-435 breast carcinoma cell line: Effects on tumor metastatic potential, colonization and enzymatic activity.* Oncogene, 1993. **8**: p. 2325-2333.
23. Ward, E., et al., *Childhood and adolescent cancer statistics, 2014.* CA Cancer J Clin, 2014. **64**(2): p. 83-103.
24. Ostrom, Q.T., et al., *CBTRUS Statistical Report: Pediatric Brain Tumor Foundation Childhood and Adolescent Primary Brain and Other Central Nervous System Tumors Diagnosed in the United States in 2014-2018.* Neuro Oncol, 2022. **24**(Suppl 3): p. iii1-iii38.
25. Cotter, J.A. and C. Hawkins, *Medulloblastoma: WHO 2021 and beyond.* Pediatric and Developmental Pathology, 2022. **25**(1): p. 23-33.
26. Louis, D.N., et al., *The 2016 World Health Organization classification of tumors of the central nervous system: a summary.* Acta neuropathologica, 2016. **131**: p. 803-820.
27. Northcott, P.A., et al., *Medulloblastomics: the end of the beginning.* Nature Reviews Cancer, 2012. **12**(12): p. 818-834.
28. Taylor, M.D., et al., *Molecular subgroups of medulloblastoma: the current consensus.* Acta neuropathologica, 2012. **123**: p. 465-472.
29. Rausch, T., et al., *Genome sequencing of pediatric medulloblastoma links catastrophic DNA rearrangements with TP53 mutations.* Cell, 2012. **148**(1): p. 59-71.
30. Khuong-Quang, D.-A., et al., *K27M mutation in histone H3. 3 defines clinically and biologically distinct subgroups of pediatric diffuse intrinsic pontine gliomas.* Acta neuropathologica, 2012. **124**: p. 439-447.
31. Cohen, K.J., N. Jabado, and J. Grill, *Diffuse intrinsic pontine gliomas—current management and new biologic insights. Is there a glimmer of hope?* Neuro-oncology, 2017. **19**(8): p. 1025-1034.
32. Price, M., et al., *CBTRUS Statistical Report: American Brain Tumor Association & NCI Neuro-Oncology Branch Adolescent and Young Adult Primary Brain and Other Central Nervous System Tumors Diagnosed in the United States in 2016–2020.* Neuro-oncology, 2024. **26**(Supplement_3): p. iii1-iii53.
33. Mount, C.W., et al., *Potent antitumor efficacy of anti-GD2 CAR T cells in H3-K27M+ diffuse midline gliomas.* Nature medicine, 2018. **24**(5): p. 572-579.
34. Majzner, R.G., et al., *GD2-CAR T cell therapy for H3K27M-mutated diffuse midline gliomas.* Nature, 2022. **603**(7903): p. 934-941.
35. Monje, M., et al., *Intravenous and intracranial GD2-CAR T cells for H3K27M+ diffuse midline gliomas.* Nature, 2024: p. 1-8.
36. Venkatesh, H.S., et al., *Electrical and synaptic integration of glioma into neural circuits.* Nature, 2019. **573**(7775): p. 539-545.

37. Venkataramani, V., et al., *Glutamatergic synaptic input to glioma cells drives brain tumour progression.* Nature, 2019. **573**(7775): p. 532-538.
38. Zeng, Q., et al., *Synaptic proximity enables NMDAR signalling to promote brain metastasis.* Nature, 2019. **573**(7775): p. 526-531.
39. Barron, T., et al., *GABAergic neuron-to-glioma synapses in diffuse midline gliomas.* bioRxiv, 2022: p. 2022.11. 08.515720.
40. Huang-Hobbs, E., et al., *Remote neuronal activity drives glioma progression through SEMA4F.* Nature, 2023. **619**(7971): p. 844-850.
41. Tetzlaff, S.K., et al., *Characterizing and targeting glioblastoma neuron-tumor networks with retrograde tracing.* Cell, 2024.
42. Sun, Y., et al., *Brain-wide neuronal circuit connectome of human glioblastoma.* bioRxiv, 2024: p. 2024.03. 01.583047.
43. Drexler, R., et al., *Cholinergic Neuronal Activity Promotes Diffuse Midline Glioma Growth through Muscarinic Signaling.* bioRxiv, 2024.
44. Venkatesh, H.S., et al., *Neuronal activity promotes glioma growth through neuroligin-3 secretion.* Cell, 2015. **161**(4): p. 803-816.
45. Venkatesh, H.S., et al., *Targeting neuronal activity-regulated neuroligin-3 dependency in high-grade glioma.* Nature, 2017. **549**(7673): p. 533-537.
46. Pardridge, W.M., Y.S. Kang, and J.L. Buciak, *Transport of human recombinant brain-derived neurotrophic factor (Bdnf) through the rat blood-brain barrier in vivo using vector-mediated peptide drug delivery.* Pharmaceutical Res, 1994. **11**(5): p. 738-746.
47. Taylor, K.R., et al., *Glioma synapses recruit mechanisms of adaptive plasticity.* Nature, 2023. **623**(7986): p. 366-374.
48. Buckingham, S.C., et al., *Glutamate release by primary brain tumors induces epileptic activity.* Nature medicine, 2011. **17**(10): p. 1269-1274.
49. Robert, S.M., et al., *SLC7A11 expression is associated with seizures and predicts poor survival in patients with malignant glioma.* Science translational medicine, 2015. **7**(289): p. 289ra86-289ra86.
50. Yu, K., et al., *PIK3CA variants selectively initiate brain hyperactivity during gliomagenesis.* Nature, 2020. **578**(7793): p. 166-171.
51. Campbell, S.L., S.C. Buckingham, and H. Sontheimer, *Human glioma cells induce hyperexcitability in cortical networks.* Epilepsia, 2012. **53**(8): p. 1360-1370.
52. Campbell, S.L., et al., *GABAergic disinhibition and impaired KCC2 cotransporter activity underlie tumor-associated epilepsy.* Glia, 2015. **63**(1): p. 23-36.
53. Zamponi, G.W., et al., *The Physiology, Pathology, and Pharmacology of Voltage-Gated Calcium Channels and Their Future Therapeutic Potential.* Pharmacol Rev, 2015. **67**(4): p. 821-70.
54. Dolphin, A.C., *Voltage-gated calcium channels and their auxiliary subunits: physiology and pathophysiology and pharmacology.* J Physiol, 2016. **594**(19): p. 5369-90.
55. Calhoun, J.D., et al., *Cacna1g is a genetic modifier of epilepsy in a mouse model of Dravet syndrome.* Epilepsia, 2017. **58**(8): p. e111-e115.

56. Perez-Reyes, E., et al., *Molecular characterization of a neuronal low-voltage-activated T-type calcium channel.* Nature, 1998. **391**(6670): p. 896-900.
57. Talley, E.M., et al., *Differential distribution of three members of a gene family encoding low voltage-activated (T-type) calcium channels.* Journal of Neuroscience, 1999. **19**(6): p. 1895-1911.
58. Leresche, N. and R.C. Lambert, *T-type calcium channels in synaptic plasticity.* Channels, 2017. **11**(2): p. 121-139.
59. Crunelli, V., et al., *The 'window'T-type calcium current in brain dynamics of different behavioural states.* The Journal of physiology, 2005. **562**(1): p. 121-129.
60. Huguenard, J., *Low-threshold calcium currents in central nervous system neurons.* Annual review of physiology, 1996. **58**: p. 329-348.
61. Perez-Reyes, E., *Molecular physiology of low-voltage-activated t-type calcium channels.* Physiological reviews, 2003. **83**(1): p. 117-161.
62. Cain, S.M. and T.P. Snutch, *T-type calcium channels in burst-firing, network synchrony, and epilepsy.* Biochimica et Biophysica Acta (BBA)-Biomembranes, 2013. **1828**(7): p. 1572-1578.
63. Suzuki, S. and M.A. Rogawski, *T-type calcium channels mediate the transition between tonic and phasic firing in thalamic neurons.* Proceedings of the National Academy of Sciences, 1989. **86**(18): p. 7228-7232.
64. Dreyfus, F.M., et al., *Selective T-type calcium channel block in thalamic neurons reveals channel redundancy and physiological impact of ITwindow.* Journal of Neuroscience, 2010. **30**(1): p. 99-109.
65. Wang, G., et al., *CaV3. 2 calcium channels control NMDA receptor-mediated transmission: a new mechanism for absence epilepsy.* Genes & development, 2015. **29**(14): p. 1535-1551.
66. Lambert, R.C., et al., *The many faces of T-type calcium channels.* Pflügers Archiv-European Journal of Physiology, 2014. **466**: p. 415-423.
67. Destexhe, A., et al., *Dendritic low-threshold calcium currents in thalamic relay cells.* Journal of Neuroscience, 1998. **18**(10): p. 3574-3588.
68. Huguenard, J.R. and D.A. McCormick, *Thalamic synchrony and dynamic regulation of global forebrain oscillations.* Trends in neurosciences, 2007. **30**(7): p. 350-356.
69. Sallan, M.C., et al., *T-type Ca(2+) Channels: T for Targetable.* Cancer Res, 2018. **78**(3): p. 603-609.
70. Antal, L. and M. Martin-Caraballo, *T-type Calcium Channels in Cancer.* Cancers (Basel), 2019. **11**(2).
71. Zhang, Y., et al., *Targetable T-type Calcium Channels Drive Glioblastoma.* Cancer Res, 2017. **77**(13): p. 3479-3490.
72. Valerie, N.C., et al., *Inhibition of T-type calcium channels disrupts Akt signaling and promotes apoptosis in glioblastoma cells.* Biochem Pharmacol, 2013. **85**(7): p. 888-97.
73. Zhang, Y., et al., *Inhibition of T-type Ca(2)(+) channels by endostatin attenuates human glioblastoma cell proliferation and migration.* Br J Pharmacol, 2012. **166**(4): p. 1247-60.

74. Niklasson, M., et al., *Membrane-Depolarizing Channel Blockers Induce Selective Glioma Cell Death by Impairing Nutrient Transport and Unfolded Protein/Amino Acid Responses.* Cancer Res, 2017. **77**(7): p. 1741-1752.
75. Latour, I., et al., *Expression of T-type calcium channel splice variants in human glioma.* Glia, 2004. **48**(2): p. 112-9.
76. Martin, R.L., et al., *Mibefradil block of cloned T-type calcium channels.* J Pharmacol Exp Ther, 2000. **295**(1): p. 302-8.
77. Mullins, M.E., et al., *Life-threatening interaction of mibefradil and beta-blockers with dihydropyridine calcium channel blockers.* JAMA, 1998. **280**(2): p. 157-8.
78. Keir, S.T., et al., *Mibefradil, a novel therapy for glioblastoma multiforme: cell cycle synchronization and interlaced therapy in a murine model.* J Neurooncol, 2013. **111**(2): p. 97-102.
79. Sheehan, J.P., et al., *Inhibition of glioblastoma and enhancement of survival via the use of mibefradil in conjunction with radiosurgery.* J Neurosurg, 2013. **118**(4): p. 830-7.
80. Panner, A., et al., *Variation of T-type calcium channel protein expression affects cell division of cultured tumor cells.* Cell Calcium, 2005. **37**(2): p. 105-19.
81. Krouse, A.J., et al., *Repurposing and Rescuing of Mibefradil, an Antihypertensive, for Cancer: A Case Study.* Assay Drug Dev Technol, 2015. **13**(10): p. 650-3.
82. Holdhoff, M., et al., *Timed sequential therapy of the selective T-type calcium channel blocker mibefradil and temozolomide in patients with recurrent high-grade gliomas.* Neuro Oncol, 2017. **19**(6): p. 845-852.
83. Lester-Coll, N.H., et al., *Mibefradil dihydrochoride with hypofractionated radiation for recurrent glioblastoma: A phase I dose expansion trial.* Journal of Clinical Oncology, 2018. **36**(15_suppl): p. e14046-e14046.
84. Akbani, R., et al., *Realizing the promise of reverse phase protein arrays for clinical, translational, and basic research: a workshop report: the RPPA (Reverse Phase Protein Array) society.* Mol Cell Proteomics, 2014. **13**(7): p. 1625-43.
85. Cui, C., et al., *Targeting calcium signaling in cancer therapy.* Acta Pharm Sin B, 2017. **7**(1): p. 3-17.
86. Clapham, D.E., *Calcium signaling.* Cell, 2007. **131**(6): p. 1047-58.
87. Monteith, G.R., N. Prevarskaya, and S.J. Roberts-Thomson, *The calcium-cancer signalling nexus.* Nat Rev Cancer, 2017. **17**(6): p. 367-380.
88. Allbritton, N.L., T. Meyer, and L. Stryer, *Range of messenger action of calcium ion and inositol 1,4,5-trisphosphate.* Science, 1992. **258**(5089): p. 1812-5.
89. Brink, F., *The role of calcium ions in neural processes.* Pharmacol Rev, 1954. **6**(3): p. 243-98.
90. Brini, M. and E. Carafoli, *Calcium signalling: a historical account, recent developments and future perspectives.* Cell Mol Life Sci, 2000. **57**(3): p. 354-70.
91. Rasmussen, H. and J.E. Rasmussen, *Calcium as intracellular messenger: from simplicity to complexity.* Curr Top Cell Regul, 1990. **31**: p. 1-109.
92. Silver, R.B., *Imaging structured space-time patterns of Ca2+ signals: essential information for decisions in cell division.* FASEB J, 1999. **13 Suppl 2**: p. S209-15.

93. Deliot, N. and B. Constantin, *Plasma membrane calcium channels in cancer: Alterations and consequences for cell proliferation and migration.* Biochim Biophys Acta, 2015. **1848**(10 Pt B): p. 2512-22.
94. Roderick, H.L. and S.J. Cook, *Ca2+ signalling checkpoints in cancer: remodelling Ca2+ for cancer cell proliferation and survival.* Nat Rev Cancer, 2008. **8**(5): p. 361-75.
95. Prevarskaya, N., et al., *Remodelling of Ca2+ transport in cancer: how it contributes to cancer hallmarks?* Philos Trans R Soc Lond B Biol Sci, 2014. **369**(1638): p. 20130097.
96. See, V., et al., *Calcium-dependent regulation of the cell cycle via a novel MAPK--NF-kappaB pathway in Swiss 3T3 cells.* J Cell Biol, 2004. **166**(5): p. 661-72.
97. Wen, P.Y. and D.A. Reardon, *Progress in glioma diagnosis, classification and treatment.* Nature Reviews Neurology, 2016. **12**(2): p. 69-70.
98. Louis, D.N., et al., *The 2021 WHO classification of tumors of the central nervous system: a summary.* Neuro-oncology, 2021. **23**(8): p. 1231-1251.
99. Pan, Y., et al., *NF1 mutation drives neuronal activity-dependent initiation of optic glioma.* Nature, 2021. **594**(7862): p. 277-282.
100. Krishna, S., et al., *Glioblastoma remodelling of human neural circuits decreases survival.* Nature, 2023. **617**(7961): p. 599-607.
101. Anastasaki, C., et al., *Neuronal hyperexcitability drives central and peripheral nervous system tumor progression in models of neurofibromatosis-1.* Nature communications, 2022. **13**(1): p. 2785.
102. Anastasaki, C., et al., *NF1 mutation-driven neuronal hyperexcitability sets a threshold for tumorigenesis and therapeutic targeting of murine optic glioma.* Neuro-oncology, 2024: p. noae054.
103. Venkataramani, V., et al., *Glioblastoma hijacks neuronal mechanisms for brain invasion.* Cell, 2022. **185**(16): p. 2899-2917. e31.
104. Drexler, R., et al., *A prognostic neural epigenetic signature in high-grade glioma.* Nature Medicine, 2024: p. 1-14.
105. Cribbs, L.L., et al., *Molecular cloning and functional expression of Cav3. 1c, a T-type calcium channel from human brain.* FEBS letters, 2000. **466**(1): p. 54-58.
106. Papazoglou, A., et al., *Gender specific hippocampal whole genome transcriptome data from mice lacking the Cav2. 3 R-type or Cav3. 2 T-type voltage-gated calcium channel.* Data in brief, 2017. **12**: p. 81-86.
107. Bernal Sierra, Y.A., et al., *Genetic tracing of Cav3. 2 T-type calcium channel expression in the peripheral nervous system.* Frontiers in molecular neuroscience, 2017. **10**: p. 70.
108. Aguado, C., et al., *Ontogenic changes and differential localization of T-type Ca2+ channel subunits Cav3. 1 and Cav3. 2 in mouse hippocampus and cerebellum.* Frontiers in neuroanatomy, 2016. **10**: p. 83.
109. François, A., et al., *The low-threshold calcium channel Cav3. 2 determines low-threshold mechanoreceptor function.* Cell reports, 2015. **10**(3): p. 370-382.

110. Gangarossa, G., et al., *T-type calcium channel Cav3. 2 deficient mice show elevated anxiety, impaired memory and reduced sensitivity to psychostimulants.* Frontiers in Behavioral Neuroscience, 2014. **8**: p. 92.
111. Becker, A.J., et al., *Transcriptional upregulation of Cav3. 2 mediates epileptogenesis in the pilocarpine model of epilepsy.* Journal of Neuroscience, 2008. **28**(49): p. 13341-13353.
112. Powell, K.L., et al., *A Cav3. 2 T-type calcium channel point mutation has splice-variant-specific effects on function and segregates with seizure expression in a polygenic rat model of absence epilepsy.* Journal of Neuroscience, 2009. **29**(2): p. 371-380.
113. Cai, S., et al., *Targeting T-type/CaV3. 2 channels for chronic pain.* Translational Research, 2021. **234**: p. 20-30.
114. Zhang, Y., et al., *Targetable T-type calcium channels drive glioblastoma.* Cancer research, 2017. **77**(13): p. 3479-3490.
115. Visa, A., et al., *T-Type Cav3. 1 channels mediate progression and chemotherapeutic resistance in glioblastoma.* Cancer research, 2019. **79**(8): p. 1857-1868.
116. Sheehan, J.P., et al., *Inhibition of glioblastoma and enhancement of survival via the use of mibefradil in conjunction with radiosurgery.* Journal of neurosurgery, 2013. **118**(4): p. 830-837.
117. Paradkar, S., et al., *Creation of a new class of radiosensitizers for glioblastoma based on the mibefradil pharmacophore.* Oncotarget, 2021. **12**(9): p. 891.
118. Huang, Y., et al., *Oligodendrocyte Progenitor Cells Promote Neovascularization in Glioma by Disrupting the Blood–Brain Barrier.* Cancer Research, 2014. **74**(4): p. 1011-1021.
119. Hambardzumyan, D., et al., *Modeling adult gliomas using RCAS/t-va technology.* Translational oncology, 2009. **2**(2): p. 89-IN6.
120. Li, P., et al., *A population of Nestin-expressing progenitors in the cerebellum exhibits increased tumorigenicity.* Nature neuroscience, 2013. **16**(12): p. 1737-1744.
121. Ostrom, Q.T., et al., *CBTRUS statistical report: primary brain and other central nervous system tumors diagnosed in the United States in 2010–2014.* Neuro-oncology, 2017. **19**(suppl_5): p. v1-v88.
122. Ravi, V.M., et al., *Spatially resolved multi-omics deciphers bidirectional tumor-host interdependence in glioblastoma.* Cancer cell, 2022. **40**(6): p. 639-655. e13.
123. Tarhan, L., et al., *Single-cell Portal: an interactive home for single-cell genomics data.* bioRxiv, 2023: p. 2023.07.13.548886.
124. Richards, L.M., et al., *Gradient of developmental and injury response transcriptional states defines functional vulnerabilities underpinning glioblastoma heterogeneity.* Nature Cancer, 2021. **2**(2): p. 157-173.
125. Morabito, S., et al., *hdWGCNA identifies co-expression networks in high-dimensional transcriptomics data.* Cell reports methods, 2023. **3**(6).
126. Mishra, S.K. and K. Hermsmeyer, *Selective inhibition of T-type Ca2+ channels by Ro 40-5967.* Circulation research, 1994. **75**(1): p. 144-148.

127. Mullaney, K.J., et al., *The role of -SH groups in methylmercuric chloride-induced D-aspartate and rubidium release from rat primary astrocyte cultures.* Brain Res, 1994. **641**(1): p. 1-9.
128. Jung, E., et al., *Tumor cell plasticity, heterogeneity, and resistance in crucial microenvironmental niches in glioma.* Nature communications, 2021. **12**(1): p. 1014.
129. Weil, S., et al., *Tumor microtubes convey resistance to surgical lesions and chemotherapy in gliomas.* Neuro-oncology, 2017. **19**(10): p. 1316-1326.
130. Pozniak, C.D., et al., *Sox10 directs neural stem cells toward the oligodendrocyte lineage by decreasing Suppressor of Fused expression.* Proceedings of the National Academy of Sciences, 2010. **107**(50): p. 21795-21800.
131. Stolt, C.C., et al., *Terminal differentiation of myelin-forming oligodendrocytes depends on the transcription factor Sox10.* Genes & development, 2002. **16**(2): p. 165-170.
132. Glasgow, S.M., et al., *Mutual antagonism between Sox10 and NFIA regulates diversification of glial lineages and glioma subtypes.* Nature neuroscience, 2014. **17**(10): p. 1322-1329.
133. Ferletta, M., et al., *Sox10 has a broad expression pattern in gliomas and enhances platelet-derived growth factor-B–induced gliomagenesis.* Molecular Cancer Research, 2007. **5**(9): p. 891-897.
134. Wu, Y., et al., *Glioblastoma epigenome profiling identifies SOX10 as a master regulator of molecular tumour subtype.* Nature communications, 2020. **11**(1): p. 6434.
135. Blanchart, A., et al., *Endogenous GABAA receptor activity suppresses glioma growth.* Oncogene, 2017. **36**(6): p. 777-786.
136. Holdhoff, M., et al., *Timed sequential therapy of the selective T-type calcium channel blocker mibefradil and temozolomide in patients with recurrent high-grade gliomas.* Neuro-oncology, 2017. **19**(6): p. 845-852.
137. Lester-Coll, N.H., et al., *Mibefradil dihydrochoride with hypofractionated radiation for recurrent glioblastoma: A phase I dose expansion trial*. 2018, American Society of Clinical Oncology.
138. Juraschka, K. and M.D. Taylor, *Medulloblastoma in the age of molecular subgroups: a review: JNSPG 75th Anniversary Invited Review Article.* Journal of Neurosurgery: Pediatrics, 2019. **24**(4): p. 353-363.
139. Eberhart, C.G., et al., *Histopathologic grading of medulloblastomas: a Pediatric Oncology Group study.* Cancer, 2002. **94**(2): p. 552-560.
140. Taylor, R.E., et al., *Results of a randomized study of preradiation chemotherapy versus radiotherapy alone for nonmetastatic medulloblastoma: The International Society of Paediatric Oncology/United Kingdom Children's Cancer Study Group PNET-3 Study.* Journal of Clinical Oncology, 2003. **21**(8): p. 1581-1591.
141. Thompson, E.M., et al., *Prognostic value of medulloblastoma extent of resection after accounting for molecular subgroup: a retrospective integrated clinical and molecular analysis.* The lancet oncology, 2016. **17**(4): p. 484-495.

142. Michalski, J.M., et al., *Children's oncology group phase III trial of reduced-dose and reduced-volume radiotherapy with chemotherapy for newly diagnosed average-risk medulloblastoma.* Journal of Clinical Oncology, 2021. **39**(24): p. 2685-2697.
143. Monteith, G.R., N. Prevarskaya, and S.J. Roberts-Thomson, *The calcium–cancer signalling nexus.* Nature Reviews Cancer, 2017. **17**(6): p. 373-380.
144. Déliot, N. and B. Constantin, *Plasma membrane calcium channels in cancer: Alterations and consequences for cell proliferation and migration.* Biochimica et Biophysica Acta (BBA)-Biomembranes, 2015. **1848**(10): p. 2512-2522.
145. Taylor, J.T., et al., *Selective blockade of T-type Ca2+ channels suppresses human breast cancer cell proliferation.* Cancer letters, 2008. **267**(1): p. 116-124.
146. Dube, C.J., et al., *Microenvironment T-Type calcium channels regulate neuronal and glial processes to promote glioblastoma growth.* bioRxiv, 2024: p. 2024.08. 22.609229.
147. Dziegielewska, B., et al., *T-type Ca2+ channel inhibition induces p53-dependent cell growth arrest and apoptosis through activation of p38-MAPK in colon cancer cells.* Molecular Cancer Research, 2014. **12**(3): p. 348-358.
148. Shapiro, J.A., et al., *OpenPBTA: The Open Pediatric Brain Tumor Atlas.* Cell genomics, 2023. **3**(7).
149. Cerami, E., et al., *The cBio cancer genomics portal: an open platform for exploring multidimensional cancer genomics data.* Cancer discovery, 2012. **2**(5): p. 401-404.
150. Riemondy, K.A., et al., *Neoplastic and immune single-cell transcriptomics define subgroup-specific intra-tumoral heterogeneity of childhood medulloblastoma.* Neuro-oncology, 2022. **24**(2): p. 273-286.
151. Li, Y., et al., *Functional and molecular interactions between the HGF/c-Met pathway and c-Myc in large-cell medulloblastoma.* Laboratory investigation, 2008. **88**(2): p. 98-111.
152. Guessous, F., et al., *Cooperation between c-Met and focal adhesion kinase family members in medulloblastoma and implications for therapy.* Molecular Cancer Therapeutics, 2012. **11**(2): p. 288-297.
153. Brightman, M. and Y. Kadota, *Nonpermeable and permeable vessels of the brain.* NIDA Res Monogr, 1992. **120**: p. 87-107.
154. Einspahr, J.G., et al., *Functional protein pathway activation mapping of the progression of normal skin to squamous cell carcinoma.* Cancer prevention research, 2012. **5**(3): p. 403-413.
155. Pierobon, M., et al., *Reverse-phase protein microarrays.* Molecular Profiling: Methods and Protocols, 2012: p. 215-235.
156. Paweletz, C.P., et al., *Reverse phase protein microarrays which capture disease progression show activation of pro-survival pathways at the cancer invasion front.* Oncogene, 2001. **20**(16): p. 1981-1989.
157. Li, Y., et al., *Interactions between PTEN and the c-Met pathway in glioblastoma and implications for therapy.* Molecular cancer therapeutics, 2009. **8**(2): p. 376-385.

158. Sedeeq, M., et al., *T-type calcium channel inhibitors induce apoptosis in medulloblastoma cells associated with altered metabolic activity.* Molecular neurobiology, 2022. **59**(5): p. 2932-2945.
159. Szlachta, K., et al., *CRISPR knockout screening identifies combinatorial drug targets in pancreatic cancer and models cellular drug response.* Nat Commun, 2018. **9**(1): p. 4275.
160. Li, W., et al., *MAGeCK enables robust identification of essential genes from genome-scale CRISPR/Cas9 knockout screens.* Genome Biol, 2014. **15**(12): p. 554.
161. Lothian, C. and U. Lendahl, *An evolutionarily conserved region in the second intron of the human nestin gene directs gene expression to CNS progenitor cells and to early neural crest cells.* Eur J Neurosci, 1997. **9**(3): p. 452-62.
162. Marino, S., et al., *Induction of medulloblastomas in p53-null mutant mice by somatic inactivation of Rb in the external granular layer cells of the cerebellum.* Genes Dev, 2000. **14**(8): p. 994-1004.
163. Tronche, F., et al., *Disruption of the glucocorticoid receptor gene in the nervous system results in reduced anxiety.* Nat Genet, 1999. **23**(1): p. 99-103.
164. Varghese, R.S., et al., *Protein network construction using reverse phase protein array data.* Methods, 2017. **124**: p. 89-99.
165. Baldelli, E., et al., *Reverse Phase Protein Microarrays.* Methods Mol Biol, 2017. **1606**: p. 149-169.
166. Pierobon, M., et al., *Reverse-phase protein microarrays.* Methods Mol Biol, 2012. **823**: p. 215-35.
167. Wilson, B., L.A. Liotta, and E. Petricoin, 3rd, *Monitoring proteins and protein networks using reverse phase protein arrays.* Dis Markers, 2010. **28**(4): p. 225-32.
168. Yao, M., et al., *Astrocytic trans-differentiation completes a multicellular paracrine feedback loop required for medulloblastoma tumor growth.* Cell, 2020. **180**(3): p. 502-520. e19.
169. Gibson, P., et al., *Subtypes of medulloblastoma have distinct developmental origins.* Nature, 2010. **468**(7327): p. 1095-1099.
170. Swartling, F.J., et al., *Pleiotropic role for MYCN in medulloblastoma.* Genes & development, 2010. **24**(10): p. 1059-1072.
171. Genovesi, L.A., et al., *Sleeping Beauty mutagenesis in a mouse medulloblastoma model defines networks that discriminate between human molecular subgroups.* Proceedings of the National Academy of Sciences, 2013. **110**(46): p. E4325-E4334.
172. Filbin, M.G., et al., *Developmental and oncogenic programs in H3K27M gliomas dissected by single-cell RNA-seq.* Science, 2018. **360**(6386): p. 331-335.
173. Schwab, M.H., et al., *Neuronal basic helix-loop-helix proteins (NEX and BETA2/Neuro D) regulate terminal granule cell differentiation in the hippocampus.* J Neurosci, 2000. **20**(10): p. 3714-24.
174. Francois, A., et al., *The Low-Threshold Calcium Channel Cav3.2 Determines Low-Threshold Mechanoreceptor Function.* Cell Rep, 2015. **10**(3): p. 370-382.
175. Audesirk, G., *Electrophysiology of lead intoxication: Effects on voltage-sensitive ion channels.* Neurotoxicology, 1993. **14**(2-3): p. 137-148.

176. Aggarwal, A., et al., *Glutamate indicators with improved activation kinetics and localization for imaging synaptic transmission.* Nature methods, 2023. **20**(6): p. 925-934.
177. Fulton, D., et al., *Regulation of L-type Ca++ currents and process morphology in white matter oligodendrocyte precursor cells by golli-myelin proteins.* Glia, 2010. **58**(11): p. 1292-1303.
178. Bergles, D.E., et al., *Glutamatergic synapses on oligodendrocyte precursor cells in the hippocampus.* Nature, 2000. **405**(6783): p. 187-191.
179. Hide, T., et al., *Oligodendrocyte progenitor cells and macrophages/microglia produce glioma stem cell niches at the tumor border.* EBioMedicine, 2018. **30**: p. 94-104.
180. Liu, C., et al., *Mosaic analysis with double markers reveals tumor cell of origin in glioma.* Cell, 2011. **146**(2): p. 209-221.
181. Nagaraja, S., et al., *Histone variant and cell context determine H3K27M reprogramming of the enhancer landscape and oncogenic state.* Molecular cell, 2019. **76**(6): p. 965-980. e12.
182. Holland, E.C., et al., *Modeling mutations in the G1 arrest pathway in human gliomas: overexpression of CDK4 but not loss of INK4a-ARF induces hyperploidy in cultured mouse astrocytes.* Genes Dev, 1998. **12**(23): p. 3644-9.
183. Holland, E.C., et al., *A constitutively active epidermal growth factor receptor cooperates with disruption of G1 cell-cycle arrest pathways to induce glioma-like lesions in mice.* Genes Dev, 1998. **12**(23): p. 3675-85.
184. Hambardzumyan, D., et al., *Modeling Adult Gliomas Using RCAS/t-va Technology.* Transl Oncol, 2009. **2**(2): p. 89-95.
185. Ross, J.L., et al., *Microglia and monocyte-derived macrophages drive progression of pediatric high-grade gliomas and are transcriptionally shaped by histone mutations.* Immunity, 2024. **57**(11): p. 2669-2687. e6.
186. Marks, N., et al., *Activation of caspase-3 and apoptosis in cerebellar granule cells.* J Neurosci Res, 1998. **52**: p. 334-341.
187. Liao, Y.-F., et al., *Involvement of the Cav3. 2 T-type calcium channel in thalamic neuron discharge patterns.* Molecular pain, 2011. **7**: p. 1744-8069-7-43.
188. Çarçak, N., et al., *Cav3. 2 T-type calcium channel mutation influences kindling-induced thalamic neuronal firing patterns in Genetic Absence Epilepsy Rats From Strasbourg.* Epilepsia, 2019. **60**(7): p. 1378-1386.
189. Greenwald, A.C., et al., *Integrative spatial analysis reveals a multi-layered organization of glioblastoma.* Cell, 2024. **187**(10): p. 2485-2501. e26.